Ecological and evolutionary dynamics of influenza viruses

by

Sarah E. Cobey

A dissertation submitted in partial fulfillment
of the requirements for the degree of
Doctor of Philosophy
(Ecology and Evolutionary Biology)
in The University of Michigan
2009

Doctoral committee:

Professor Mercedes Pascual, Chair
Professor Mark L. Wilson
Assistant Professor Aaron A. King
David P. Mindell, California Academy of Sciences

Acknowledgements

I have been extremely fortunate to conduct research with generous and highly skilled colleagues and mentors. I would particularly like to thank my dissertation committee: Aaron King, Mark Wilson, David Mindell, and my advisor, Mercedes Pascual. Their suggestions and instruction have fundamentally shaped and improved the chapters here. They have similarly influenced my approach to research, and I am grateful for their prodding questions and feedback over the past few years.

The greatest privilege has been the opportunity to watch and learn how science gets done by one of the most inspiring people in the field, Mercedes. I have felt very fortunate to work with someone who radiates such a potent combination of enthusiasm, professionalism, creativity, and talent. I am deeply grateful for her strong support and critical encouragement. I also specially thank Katia Koelle for her relentless yet prudent optimism and curiosity. By example and kind invitations, Mercedes and Katia have drawn me closer to all there is to love about scientific research. I would not have found my way as quickly (or had as much fun) without them.

Many thanks are appropriate for specific chapters. Mercedes originally posed the idea of investigating the effect of a tradeoff in receptor preference on the evolution of host range (chapter 2). She also forged the collaboration with Ulf Dieckmann, who taught me the underpinnings of adaptive dynamics and helped develop the specific questions addressed in the paper. Casey Schneider-Mizell gave useful advice on the technical details of the project. Additional helpful comments were received from Sarah Feldt, Diego Ruiz Moreno, Sergey Kryazhimsky, Katia, Jan Jaap Poos, Åke Brännström, Andreas Gros, and two anonymous reviewers. Mercedes' support for the collaboration came from a Centennial Fellowship from the James S. McDonnell Foundation and Ulf's from the Vienna Science and Technology Fund, WWTF. I received funding from the U.S. National Committee for IIASA and a Rackham Travel Research Grant.

Chapter 3 was inspired by collaboration with Katia, Mercedes, and Bryan Grenfell on a model of epochal evolution of influenza. Jianzhi Zhang provided perspective on the modified branch-site test of positive selection. Bryan suggested that I look at changes in glycosylation sites in the hemagglutinin protein. I particularly thank Sergei Kosakovsky Pond and his then supervisor, Simon Frost, for agreeing to investigate a new method for inferring episodic selection on phylogenies. Though this approach eventually proved intractable, the collaboration was useful for stimulating thinking. I thank Sergei for maintaining the message boards for their software, and for being open to spontaneous technical and philosophical discussions about methods.

The primary question in chapter 4—whether there is cross-immunity between different subtypes and types of influenza—was addressed by Lyudmila Karpova in her dissertation and later in an article she published. It was extraordinarily gracious of her and her supervisor, Ivan Marinich, to share the bulk of their data with us for free. Mercedes provided critical support in getting the collaboration off the ground and also helped to obtain further data. Additional financial support was provided by a Block Grant from the Department of Ecology and Evolutionary Biology. Aaron has provided extensive and patient mentoring in developing and fitting the model; it has been a pleasure to muse and learn to troubleshoot problems with him. Advice from Ed Ionides, Karina Laneri, and Anindya Bhadra helped to refine the model and the heuristics used for fitting. Mark, Sheng Li, and Bryan have also made excellent suggestions that will guide the development of the project.

Inspiration to explore the consequences of a multidegenerate genotype-phenotype map (chapter 5) arose directly from the many-to-one genotype-phenotype map underlying the model developed with Katia, Mercedes, and Bryan. Mercedes provided essential input on the technical aspects of this chapter. I also thank Sunetra Gupta for pointing me to relevant literature and Derek Smith for discussing some of the biological assumptions of the model.

I am also grateful for having been surrounded by gracious and skilled labmates: Katia, Diego, David Alonso, Christopher Warren, Stefano Allesina, Luis Fernando Chaves, Andres Baeza, Ed Baskerville, Yael Artzy, Karina, and Trevor Bedford.

Numerous discussions with Diego, Casey, Jon Zelner, and other members of the Complex Systems Advanced Academic Workshop (CSAAW) about technical and abstract matters alike made completing this work much easier and more fun. Administrators of the EEB department, including Julia Eussen, Jane Sullivan, Sonja Botes, Gail Sullivan, Kaye Hill, Susan Stark, Christy Byks-Jazayeri, Diana Hirsch, Nancy Smith, and Amber Stadler have made arranging research, travel, and collaborations easier at innumerable junctions.

I would also like to acknowledge core financial support. Where not otherwise noted, my research was funded by a Graduate Research Fellowship from the National Science Foundation, a graduate student research assistantship from Mercedes (from the McDonnell Foundation), and the EEB department.

When I first became interested in scientific research as a career, I remember being struck by the inordinate congeniality of the biologists I worked with. Unfortunately, nationality was a confounding factor at the time (though I still owe deep gratitude to Andy Dobson, my undergraduate advisor, and Peter Daszak, who both encouraged me in my first research projects). Having met and made friends with scores more scientists over the past few years, I'm delighted to realize that spirited inquiry, friendliness, and intellectual generosity are the norm. This is wonderful news in a field that focuses on ethically troubling consumer-resource interactions and potentially overwhelming or chaotic rates of change. I am excited about our work ahead.

Contents

List of Figures

List of Tables

Chapter 1

Introduction

Evolutionary biology considers which forms of life are possible and which of those forms is likely to appear and spread. Ecology tries to explain the dynamics and diversity of populations, typically assuming a fixed number of forms. On a fundamental level, they describe similar processes: two superficially polar examples are the neutral theories of evolution (Kimura 1983) and ecology (Hubbell 1997), which both account for the diversity of forms at the levels of genotypes and phenotypes, respectively. They differ in that the neutral theory of evolution assumes new forms arise by a constant rate of mutation, and the neutral theory of ecology assumes they appear by a constant rate of immigration. In these simple models, all extant forms are governed by identical and constant birth-death processes.

Ecological and evolutionary processes often occur at very different temporal scales, and it is not surprising that much progress has been made in each field by assuming the absence of noteworthy dynamics in the other. Limits to this separation of time scales can appear as rates of competition and phenotypic change converge. Ecological processes are, relatively speaking, fast: probably all life history strategies require intraspecific or interspecific interactions, which can occur repeatedly in a single generation. Convergence thus often arises as the units of selection increase their rates of mutation, whose effects can be complemented by recombination, horizontal gene transfer, and transformation. Another necessary component is a mapping between genotype and phenotype that allows rapid changes in genotype to be visible to selection. The robustness or genetic potential of genotype-phenotype maps can evolve adaptively in response to mutation rates and external pressures (Wagner 2007). The strength and speed of selection can be further augmented by large population sizes. Together, these factors

can permit a rapid evolutionary responsiveness to ecological change. Changes in phenotypes can then change the terms of the ecological interactions.

Host-pathogen systems provide some of the most exciting cases of the convergence of evolutionary and ecological time scales. RNA viruses have the highest known mutation rates (Drake et al. 1998). Horizontal gene transfer and transformation allow bacteria to evolve literally within generations. Large population sizes are a distinction of small (e.g., unicellular or viral) organisms. What makes these systems particularly interesting relative to other microbial interactions are the multiple time scales of host evolution. On the shortest time scale—potentially on the order of several viral generations—is the phenotypically plastic response of hosts with adaptive immunity. Within hosts, immune cells and pathogens can undergo both consumer-resource dynamics and adaptive evolution (Mclean et al. 1991; Nowak et al. 1991; Perelson 2002). On a slightly longer time scale, pathogen evolution occurs against a backdrop of changing frequencies of susceptible, infected, and recovered hosts. Finally, hosts evolve improved immune defenses against pathogens over generations, and pathogens can further adapt to host populations.

The best understood host-pathogen systems are unsurprisingly those where at least one time scale can be dropped. Major insights have been gained from ecological models that combine traditional disease dynamics with spatial structure (Keeling et al. 2001), transmission networks (Lloyd-Smith et al. 2005), competition among multiple strains (Koelle et al. 2006; Nagao & Koelle 2008; Rohani et al. 2003), multiple hosts (Keeling et al. 2001; Schenzle 1984), and seasonal (Keeling & Grenfell 2002) and climatic forcing (Koelle et al. 2005; Pascual et al. 2006; Pascual et al. 2000). These approaches have worked for pathogens such as measles and cholera, which, despite their high intrinsic mutation rates, have relatively static phenotypes. Similarly, pathogen evolution is best understood when ecological feedback is restricted. Traditional tests of positive selection, for example, report long-term averages and ignore contributions of population dynamics (Suzuki 2006). The evolution of virulence has also classically been interpreted as independent from disease dynamics (Anderson & May 1982; Herre 1993) [but see Dwyer et al. (1990)].

For pathogens with high mutation rates, flexible genotype-phenotype maps, and rapidly changing ecologies, these models can be less useful. A recent wave of research attempts to integrate evolutionary and ecological theory and observations more finely under a framework labeled "phylodynamics" (Grenfell et al. 2004). Integrations include null models of strain evolution under SIR interactions (Gordo et al. 2009), strain evolution in transmission networks (Buckee et al. 2004), the stochastic dynamics of adaptation and invasion (Andre & Day 2005; Antia et al. 2003), the evolution of antiviral resistance during pandemics (Lipsitch et al. 2007), and inference of transmission rates and population size using coalescent theory (Biek et al. 2006; Pybus et al. 2001). No specific approach or set of assumptions dominates, beyond some integration of time scales; phylodynamic models clearly inherit their structure from traditional models in ecology or evolution and borrow as necessary from the other field. As the density of these models increases, a challenge will be to find ways to statistically validate them using both epidemiological and genetic observations (Cobey & Koelle 2008).

This dissertation is a series of investigations into the major ecological and evolutionary dynamics of one of the most enigmatic pathogens, influenza. Influenza undergoes rapid genetic and phenotypic evolution and infects multiple host species whose ecologies are in rapid flux. What follows is an overview of the virus's natural history and a description of the hypotheses tested in this dissertation.

Natural history of influenza

Structure and antigenicity

The genome of influenza consists of eight RNA segments, each 850 to 2300 bases, which code for ten proteins. Two of these proteins, hemagglutinin (HA) and neuraminidase (NA) are abundant on the virus's surface, with approximately four HA for every NA. Within influenza A, there are sixteen general forms of HA and nine forms of NA. Combinations of HA and NA identify subtypes, e.g., H3N2. Amino acid sequences of HA differ up to 20% within subtypes and 30-70% between them (Skehel & Wiley 2000). Influenza B does not have subtypes.

Hemagglutinin and neuraminidase are the primary determinants of antigenicity. Antibody-binding sites of some subtypes of HA and NA have been described by X-ray crystallography and electron micrographs of monoclonal antibody escape mutants (Bizebard et al. 1995; Fleury et al. 1999; Knossow et al. 2002). These sites are grouped into antibody-binding regions, or epitopes, on the globular head of hemagglutinin (HA1). In the 1980s, five epitopes (A-E) were identified on H3N2, but their relevance for contemporary strains in humans is unclear. HA1 of the H1N1 subtype has four or five recognized epitopes (Caton et al. 1982; Gerhard et al. 1981), and the N2 NA has at least two (Gulati et al. 2002). Different subtypes can share epitopes (Ekiert et al. 2009; Okuno et al. 1993; Smirnov et al. 1999; Yoshida et al. 2009).

Antibodies neutralize influenza viruses through steric inhibition of receptor binding or membrane fusion rather than inducing conformational change in HA. The receptor-binding site is a highly conserved pocket at the top of the HA1 (in H3N2, the site falls near epitopes A and B) and shows little variation among subtypes (Skehel & Wiley 2000). Antibodies can neutralize viruses by blocking the receptor-binding site directly (Bizebard et al. 1995) or by binding to an epitope some distance away (Fleury et al. 1999). Antibodies to the same epitope can compete or interact synergistically in neutralization (Brown et al. 1990; Sanna et al. 2000).

Immunity

Hosts resist infection through humoral immunity, cellular immunity, and innate immunity. The impact of each kind of immunity, especially to competitive dynamics among strains, is an open question.

Healthy mammals infected with influenza develop several kinds of antibody responses. In the serum, initial infection provokes the production of antigen-specific immunoglobulin M (IgM), by clonal selection of mature B cells. After several weeks, IgM matures to IgG, which is more specific and forms the basis of long-lasting immunity (Yu et al. 2008). IgG can also confer maternal immunity via transplacental transfer (Puck et al. 1980; Reuman et al. 1987). Mucosal immunity and maternal antibodies secreted in breast milk are manifested by IgA (Renegar et al. 2004; Sweet et al. 1987).

Antibodies are probably the largest contributors to strain-specific immunity and cross-immunity within subtypes; they also may play a role in heterosubtypic immunity. Most antibodies in sera of infected or vaccinated humans target HA1 (Sato et al. 2004; Yu et al. 2008), though some individuals can also mount responses to NA (Cox & Brokstad 1999; Monto & Kendal 1973). All mammals investigated demonstrate antibodies to nucleoprotein (NP) (Cox & Brokstad 1999; Deboer et al. 1990). Antibody responses can be monoclonal (antibodies to one epitope are present in antisera) or polyclonal (antibodies to multiple epitopes are present); responses in natural host populations tend to be polyclonal, but they vary in depth and specificity.

Cellular immunity can significantly attenuate pathology and speed viral clearance, though it appears to play a lesser role in preventing infection [Liang et al. (1994) and review in Thomas et al. (2006)]. T-cells only attack presenting cells, and thus they usually lag behind IgM (in a primary response) or IgG (in a secondary response) in appearance and proliferation during infection. Mice challenged with a virus containing the internal proteins of human H1N1 produced CD8+ T-cells specific to all six internal proteins, though T-cells specific to epitopes on polymerase (PA) and NP predominated and could be detected ≥570 days after initial infection. Secondary responses tended to be dominated by NP (Belz et al. 2000; Marshall et al. 2001). CD4+ T-cells bolster CD8+ and B cell responses and appear requisite for T-cell memory (Belz et al. 2002).

Studies on human immunity generally do not separate the effects of innate, cellular, and humoral immunity. They do, however, suggest there can be attenuation of symptoms during secondary infections, depending on strains' antigenic relatedness (measured by hemagglutination inhibition, or HA relatedness) (Gill & Murphy 1977; Sonoguchi et al. 1985). It is possible that the strength of cross-immunity between strains changes with time since the first infection. One small study observed several cases of rapid reinfection with a heterologous subtype, sometimes within days of clearing the first subtype, and the secondary infection was no more likely to be asymptomatic than the first (Frank et al. 1983). In contrast, students at high schools experiencing concurrent epidemics of H3N2 and H1N1 were less likely to suffer multiple infections than students at schools with sequential epidemics (Sonoguchi et al. 1986).

Evolution

Influenza viruses evolve by point mutations, reassortment of whole gene segments, and less frequently by recombination (Boni et al. 2008; Hirst et al. 2004; Suarez et al. 2004).

Point mutations are influenza's most frequent means of escaping immune surveillance, and they are also a means to modulate virulence, develop drug resistance, and adapt to new hosts or tissue types. Monoclonal antibody escape mutants can arise in vitro every 10^4 to 10^6 viruses (Webster & Laver 1980). They commonly avoid recognition through conformational changes, which tend to affect only the local structure within the surrounding epitope (Knossow et al. 1984). Hemagglutinin may be particularly tolerant of such changes. In H3N2, epitope A mostly consists of a loop extending from the rest of the molecule, and epitopes B and C are bulges (Wiley et al. 1981). While amino acids at certain positions, such as loops, might have a dramatically greater influence than others on antibody recognition, the location of influential positions can change over time (Nakajima et al. 2005). As for other pathogens, tertiary protein structure greatly complicates predictions of the locations of antibody epitopes (Korber et al. 2006).

Influenza viruses can also potentially escape immune surveillance through the addition of glycosylation sites [Asn-X-Thr/Ser, where X is any amino acid except proline or potentially aspartic acid (Gallagher et al. 1992)]. In avian influenza viruses, the main role of glycosylation appears to be as a mediator of the relative binding affinities of HA and NA (Wagner et al. 2000). However, host cell carbohydrates could potentially bind to these sites also to form a "glycan shield" to antibodies. Glycosylation might be a major mechanism of antibody escape by HIV (Wei et al. 2003). The number of potential glycosylation sites on HA1 of H3N2 has increased from two to six or seven since the subtype emerged in humans (Abe et al. 2004). Glycosylation might thus be an especially rapid effecter of antigenic change in some influenza viruses in some hosts (Schulze 1997), though it is not well tolerated by all subtypes of HA (Tsuchiya et al. 2002).

The accumulation of point mutations in response to immune pressure has been labeled "antigenic drift" (Webster et al. 1992), and it underlies the characteristic phylogeny of H3N2 HA1 in human viruses: genetic distance steadily increases from the founding strain, and no strain persists more than a few years (Fitch et al. 1991). Recently

it has been shown that these strains in human H3N2 form antigenic clusters defined by cross-reactivity patterns. Only one cluster appears to dominate at any time (Smith et al. 2004). Extended coexistence of lineages appears more common in H1N1 and influenza B (Chen & Holmes 2008; Nelson et al. 2008b).

In contrast to antigenic drift, "antigenic shift" by reassortment—the reshuffling of HA and NA types—was once thought to be strictly associated with pandemics (Webster et al. 1992). There is growing evidence that reassortment might be as common in humans (Chen & Holmes 2008; Holmes et al. 2005; Lindstrom et al. 2004; Nelson et al. 2008a; Nelson et al. 2008b) as in other hosts (Hatchette et al. 2004; Webby et al. 2004), with the epidemic potential of the reassortant likely depending on the extent of preexisting immunity to its HA and NA (Monto & Kendal 1973). Reassortment might also lead to partial immune escape by changing other antigenic determinants, such as T-cell epitopes on internal genes.

Ecology

Influenza in humans is highly seasonal in temperate regions, with a three- to four-month epidemic period in winter and few cases in the summer (Cox & Subbarao 2000). Prevalence shows no clear periodicity in the tropics (Chow et al. 2006; Viboud et al. 2006a). The mechanisms behind influenza's seasonality are not understood (Lipsitch & Viboud 2009). Major hypotheses include increases in host susceptibility due to seasonal vitamin D deficiency (Cannell et al. 2006) and changes in viral transmissibility driven by humidity and temperature (Lowen et al. 2007; Schaffer et al. 1976; Shaman & Kohn 2009).

Pandemic and interpandemic influenza A (H3N2) strains circulate globally over short time periods, while H1N1 and influenza B viruses show more spatial structure and less rapid mixing (Finkelman et al. 2007). H3N2 outbreaks have high spatial synchrony (Bonabeau et al. 1998; Greene et al. 2006; Viboud et al. 2006b), and phylogenetic studies of strains circulating in France (Lavenu et al. 2006), Japan (Nakajima et al. 1991), New York (Nelson et al. 2006), and the continental United States (Nelson et al. 2008a) demonstrate that multiple lineages seed annual epidemics in each community. Swabs

from air travelers support the hypothesis that there is interhemispheric transport of strains throughout the year (Sato et al. 2000). A recent model proposes that a network of populations in East and Southeast Asia supports year-round transmission of H3N2, with antigenically novel variants arising from this network and spreading throughout the world (Russell et al. 2008).

In humans, incidence is usually inferred from deaths to pneumonia and influenza. Until recently, few countries tracked deaths or infections by type and subtype. Observations from WHO collaborating labs reporting to the CDC suggest that seasons dominated by H3N2 have relatively low incidence of H1N1 and/or influenza B and vice-versa (Finkelman et al. 2007; Greene et al. 2006; Thompson et al. 2003). Estimates of annual incidence range from 5-20% in interpandemic years and 40-50% during pandemics (Cox & Subbarao 2000). Contact with young children is a significant risk factor for infection (Gubareva et al. 2002; Viboud et al. 2004), and vaccination of young children can dramatically reduce incidence in older contact children and adults (Hurwitz et al. 2000; Monto et al. 1970).

Many other species can be infected with influenza viruses. Multiple subtypes of influenza A are endemic in swine, domestic poultry, and horses. Influenza A is seasonal in many aquatic birds, which are its natural hosts (Halvorson et al. 1983). Repeated transmission between wild birds and domestic poultry (Alexander 2000; Munster et al. 2005; Zhou et al. 1999), birds and swine (Ludwig et al. 1994; Webby et al. 2004), domestic poultry and humans (Bridges et al. 2002; Lin et al. 2000; Olofsson et al. 2005), and swine and humans (Claas et al. 1994; Gregory et al. 2001; Myers et al. 2006; Olsen et al. 2000; Ottis et al. 1982; Peiris et al. 2001) occurs in many parts of the developed and developing world where the populations cohabitate. Influenza B has only been found in humans and seals (Webster et al. 1992).

Overview of dissertation

The dynamics of influenza are poorly understood because of limited surveillance, uncertainty about the nature and strength of hosts' immune responses, the pathogen's rapid evolution, and the breadth of factors that appear relevant to its ecology. This

dissertation presents explanations of how the diversity of influenza viruses is regulated by a combination of ecological and evolutionary mechanisms. Chapters 2 and 3 examine the dynamics of influenza viruses in humans: Chapter 2 explores molecular evidence for a theory of H3N2 evolution in humans, and chapter 3 attempts to resolve the fundamental epidemiological differences between H3N2, H1N1, and influenza B. Chapter 4 presents a theoretical model, motivated by recent observations of influenza and other pathogens, of how strains might compete when their phenotypes are perceived differently by different hosts. Chapter 5 investigates how host ecology could shape the long term evolution of influenza viruses' host range.

Chapter 2. Episodic positive selection in H3N2

Several hypotheses have been proposed to explain why, given influenza's high mutation rate and strong selection pressures from immune surveillance, the genetic diversity of influenza strains remains bounded. One of the more contentious hypotheses proposes that H3N2 undergoes "epochal evolution": most mutations are phenotypically neutral, but some occasionally have large effects on phenotype. Any novel phenotype has a selective advantage, since it partially escapes immune surveillance. It might also competitively exclude the resident phenotype. With certain assumptions about the nature of the genotype-phenotype map of HA, this process can generate cyclical patterns of genetic diversity over time that coincide with the replacement dynamics of major antigenic phenotypes. In chapter 3, I present independent evidence for episodically strong and otherwise weak, continuous positive selection in the HA of H3N2. I also test the hypothesis that the punctuated changes in antigenicity are driven by the addition of potential glycosylation sites near HA epitopes rather than epistatic point mutations. Finally, I consider the relative strength of selection in influenza's other genes and suggest where deviations from epochal evolution might have occurred.

Chapter 3. Cross-immunity and the dynamics of influenza A and B in humans

Influenza A (H3N2 and H1N1) and B all show interannual variability in their attack rates and positive selection in their HA. An intriguing question is whether the dynamics of

H1N1 and B might also be driven by epochal evolution or whether there might instead or in addition be competition between types or subtypes. Competition at these levels is suggested by historical patterns of subtype replacement, phase displacement between H3N2 and (as a set) B and H1N1, and heterosubtypic cross-immunity demonstrated in challenge experiments in nonhuman hosts.

In this chapter, I describe novel observations from St. Petersburg, Russia, of influenza's hospitalizations by subtype over several decades. I propose that major patterns can be explained by differences in the epidemiological and evolutionary rates of each type and subtype. Using a recently developed method of nonlinear dynamical inference, I also statistically evaluate the potential for heterotypic and heterosubtypic immunity over this time period.

Chapter 4. Strain competition under a multidegenerate genotype-phenotype map

An implicit assumption in models of strain competition is a one-to-one or many-to-one mapping between genotype and phenotype. Empirical evidence shows that such an assumption is not always biologically accurate. The phenotypes of pathogens that are mainly targeted by cellular immunity, for example, will be defined by recognition by host MHC alleles; two strains might thus be competitors in some hosts but not others. There is also evidence that hosts often mount heterogeneous antibody responses to pathogens such as influenza and HIV. In the same vein, strains that differ in a few but not all of their epitopes may thus be perceived as identical in some hosts but not others.

Rather than a one-to-one or many-to-one genotype-to-phenotype mapping, heterogeneity in host immunity implies that a single genotype can be perceived as several different phenotypes by hosts with identical infection histories. This chapter shows how including a multidegenerate genotype-phenotype map affects a traditional model of strain competition, and specifically how the diversity of strains can be influenced not only by the strength of cross-immunity but also by the diversity of host responses. Parameterizing such models will be increasingly tractable in the future as data accumulate on the genetic composition of host populations, immunodominance of various epitopes, and breadth of immune repertoires.

Chapter 5. Evolution of influenza's host range

Recent research tends to focus on specific mutations that might be required for avian viruses, such as H5N1, to adapt to humans. This chapter takes a broader perspective, asking instead how host range should evolve given a basic set of ecological and evolutionary assumptions. Molecular work reveals that influenza viruses face tradeoffs in their ability to infect different host species. This chapter focuses on one such tradeoff, the virus's preference for one of two possible forms of hosts' sialic acid receptor. Influenza's reservoir, waterfowl, has one form of this receptor, humans have another, and two potential "intermediate hosts"—chickens and pigs—have both forms of the receptor. This analysis uses the approach of adaptive dynamics to investigate how different ecologies influence the evolution of viruses' preference for one or the other form of the sialic acid receptor.

For a broad range of ecologies, specialists to each receptor type can easily coexist. Interestingly, ecological differences have a greater effect than tradeoff strength on the evolution of host range. Analysis of a neutral ecological case suggests these results are extensible to other pathogens facing similar tradeoffs.

Together, these chapters test hypotheses of how influenza's diversity might be regulated over different time scales and host populations. The first and last chapters focus on evolutionary dynamics and the middle two on ecological processes; the third and fourth are generalizable across host species, while the first and second focus specifically on evolution in humans. In addition, every chapter presents different methods for integrating ecological and evolutionary hypotheses. The results here should contribute to our understanding of not only influenza but also other host-pathogen systems whose dynamics are enriched by the interplay of ecology and evolution.

References

Abe, Y., Takashita, E., Sugawara, K., Matsuzaki, Y., Muraki, Y. & Hongo, S. 2004 Effect of the addition of oligosaccharides on the biological activities and antigenicity of influenza A/H3N2 virus hemagglutinin. *Journal of Virology* **78**, 9605-9611.

Alexander, D. J. 2000 A review of avian influenza in different bird species. *Veterinary Microbiology* **74**, 3-13.

Anderson, R. M. & May, R. M. 1982 Coevolution of Hosts and Parasites. *Parasitology* **85**, 411-426.

Andre, J. B. & Day, T. 2005 The effect of disease life history on the evolutionary emergence of novel pathogens. *Proceedings of the Royal Society B-Biological Sciences* **272**, 1949-1956.

Antia, R., Regoes, R. R., Koella, J. C. & Bergstrom, C. T. 2003 The role of evolution in the emergence of infectious diseases. *Nature* **426**, 658-661.

Belz, G. T., Wodarz, D., Diaz, G., Nowak, M. A. & Doherty, P. C. 2002 Compromised influenza virus-specific CD8(+)-T-Cell memory in CD4(+)-T-cell-deficient mice. *Journal of Virology* **76**, 12388-12393.

Belz, G. T., Xie, W. D., Altman, J. D. & Doherty, P. C. 2000 A previously unrecognized H-2D(b)-restricted peptide prominent in the primary influenza A virus-specific CD8(+) T-cell response is much less apparent following secondary challenge. *Journal of Virology* **74**, 3486-3493.

Biek, R., Drummond, A. J. & Poss, M. 2006 A virus reveals population structure and recent demographic history of its carnivore host. *Science* **311**, 538-541.

Bizebard, T., Gigant, B., Rigolet, P., Rasmussen, B., Diat, O., Bosecke, P., Wharton, S. a., Skehel, J. J. & Knossow, M. 1995 Structure of Influenza-Virus Hemagglutinin Complexed with a Neutralizing Antibody. *Nature* **376**, 92-94.

Bonabeau, E., Toubiana, L. & Flahault, A. 1998 Evidence for global mixing in real influenza epidemics. *Journal of Physics A-Mathematical and General* **31**, L361-L365.

Boni, M. F., Zhou, Y., Taubenberger, J. K. & Holmes, E. C. 2008 Homologous recombination is very rare or absent in human influenza A virus. *Journal of Virology* **82**, 4807-4811.

Bridges, C. B., Lim, W., Hu-Primmer, J., Sims, L., Fukuda, K., Mak, K. H., Rowe, T., Thompson, W. W., Conn, L., Lu, X. H., Cox, N. J. & Katz, J. M. 2002 Risk of influenza A (H5N1) infection among poultry workers, Hong Kong, 1997-1998. *Journal of Infectious Diseases* **185**, 1005-1010.

Brown, L. E., Murray, J. M., White, D. O. & Jackson, D. C. 1990 An Analysis of the Properties of Monoclonal-Antibodies Directed to Epitopes on Influenza-Virus Hemagglutinin. *Archives of Virology* **114**, 1-26.

Buckee, C. O., Koelle, K., Mustard, M. J. & Gupta, S. 2004 The effects of host contact network structure on pathogen diversity and strain structure. *Proceedings of the National Academy of Sciences of the United States of America* **101**, 10839-10844.

Cannell, J. J., Vieth, R., Umhau, J. C., Holick, M. F., Grant, W. B., Madronich, S., Garland, C. F. & Giovannucci, E. 2006 Epidemic influenza and vitamin D. *Epidemiology and Infection* **134**, 1129-1140.

Caton, A. J., Brownlee, G. G., Yewdell, J. W. & Gerhard, W. 1982 The antigenic structure of the influenza virus A/PR/8/34 hemagglutinin (H1 subtype). *Cell* **31**, 417-427.

Chen, R. B. & Holmes, E. C. 2008 The evolutionary dynamics of human influenza B virus. *Journal of Molecular Evolution* **66**, 655-663.

Chow, a., Ma, S., Ling, A. E. & Chew, S. K. 2006 Influenza-associated deaths in tropical Singapore. *Emerging Infectious Diseases* **12**, 114-121.

Claas, E. C. J., Kawaoka, Y., Dejong, J. C., Masurel, N. & Webster, R. G. 1994 Infection of Children with Avian-Human Reassortant Influenza-Virus from Pigs in Europe. *Virology* **204**, 453-457.

Cobey, S. & Koelle, K. 2008 Capturing escape in infectious disease dynamics. *Trends in Ecology & Evolution* **23**, 572-577.

Cox, N. J. & Subbarao, K. 2000 Global epidemiology of influenza: Past and present. *Annual Review of Medicine* **51**, 407-421.

Cox, R. J. & Brokstad, K. A. 1999 The postvaccination antibody response to influenza virus proteins. *Apmis* **107**, 289-296.

Deboer, G. F., Back, W. & Osterhaus, a. D. M. E. 1990 An Elisa for Detection of Antibodies against Influenza-a Nucleoprotein in Humans and Various Animal Species. *Archives of Virology* **115**, 47-61.

Drake, J. W., Charlesworth, B., Charlesworth, D. & Crow, J. F. 1998 Rates of spontaneous mutation. *Genetics* **148**, 1667-1686.

Dwyer, G., Levin, S. A. & Buttel, L. 1990 A Simulation-Model of the Population-Dynamics and Evolution of Myxomatosis. *Ecological Monographs* **60**, 423-447.

Ekiert, D. C., Bhabha, G., Elsliger, M. A., Friesen, R. H. E., Jongeneelen, M., Throsby, M., Goudsmit, J. & Wilson, I. A. 2009 Antibody Recognition of a Highly Conserved Influenza Virus Epitope. *Science* **324**, 246-251.

Finkelman, B. S., Viboud, C., Koelle, K., Ferrari, M. J., Bharti, N. & Grenfell, B. T. 2007 Global patterns in seasonal activity of influenza A/H3N2, A/H1N1, and B from 1997 to 2005: viral coexistence and latitudinal gradients. *PLoS One* **2**, e1296.

Fitch, W. M., Leiter, J. M. E., Li, X. & Palese, P. 1991 Positive Darwinian evolution in human influenza A viruses. *Proceedings of the National Academy of Sciences of the United States of America* **88**, 4270-4274.

Fleury, D., Barrere, B., Bizebard, T., Daniels, R. S., Skehel, J. J. & Knossow, M. 1999 A complex of influenza hemagglutinin with a neutralizing antibody that binds outside the virus receptor binding site. *Nature Structural Biology* **6**, 530-534.

Frank, A. L., Taber, L. H. & Wells, J. M. 1983 Individuals infected with two subtypes of influenza A virus in the same season. *The Journal of Infectious Diseases* **147**, 120-124.

Gallagher, P. J., Henneberry, J. M., Sambrook, J. F. & Gething, M. J. H. 1992 Glycosylation Requirements for Intracellular-Transport and Function of the Hemagglutinin of Influenza-Virus. *Journal of Virology* **66**, 7136-7145.

Gerhard, W., Yewdell, J., Frankel, M. E. & Webster, R. 1981 Antigenic Structure of Influenza-Virus Hemagglutinin Defined by Hybridoma Antibodies. *Nature* **290**, 713-717.

Gill, P. W. & Murphy, A. M. 1977 Naturally acquired immunity to influenza tpe A: a further prospective study. *Medical Journal of Australia* **2**, 761-765.

Gordo, I., Gomes, M. G. M., Reis, D. G. & Campos, P. R. A. 2009 Genetic diversity in the SIR model of pathogen evolution. *PLoS One* **4**, e4876.

Greene, S. K., Ionides, E. L. & Wilson, M. L. 2006 Patterns of influenza-associated mortality among US elderly by geographic region and virus subtype, 1968-1998. *American Journal of Epidemiology* **163**, 316-326.

Gregory, V., Lim, W., Cameron, K., Bennett, M., Marozin, S., Klimov, A., Hall, H., Cox, N., Hay, A. & Lin, Y. P. 2001 Infection of a child in Hong Kong by an influenza A H3N2 virus closely related to viruses circulating in European pigs. *Journal of General Virology* **82**, 1397-1406.

Grenfell, B. T., Pybus, O. G., Gog, J. R., Wood, J. L. N., Daly, J. M., Mumford, J. A. & Holmes, E. C. 2004 Unifying the epidemiological and evolutionary dynamics of pathogens. *Science* **303**, 327-332.

Gubareva, L. V., Novikov, D. V. & Hayden, F. G. 2002 Assessment of hemagglutinin sequence heterogeneity during influenza virus transmission in families. *The Journal of Infectious Diseases* **186**, 1575-1581.

Gulati, U., Hwang, C. C., Venkatramani, L., Gulati, S., Stray, S. J., Lee, J. T., Laver, W. G., Bochkarev, A., Zlotnick, A. & Air, G. M. 2002 Antibody epitopes on the neuraminidase of a recent H3N2 influenza virus (A/memphis/31/98). *Journal of Virology* **76**, 12274-12280.

Halvorson, D., Karunakaran, D., Senne, D., Kelleher, C., Bailey, C., Abraham, a., Hinshaw, V. & Newman, J. 1983 Epizootiology of Avian Influenza - Simultaneous Monitoring of Sentinel Ducks and Turkeys in Minnesota. *Avian Diseases* **27**, 77-85.

Hatchette, T. F., Walker, D., Johnson, C., Baker, A., Pryor, S. P. & Webster, R. G. 2004 Influenza A viruses in feral Canadian ducks: extensive reassortment in nature. *Journal of General Virology* **85**, 2327-2337.

Herre, E. A. 1993 Population-Structure and the Evolution of Virulence in Nematode Parasites of Fig Wasps. *Science* **259**, 1442-1445.

Hirst, M., Astell, C. R., Griffith, M., Coughlin, S. M., Moksa, M., Zeng, T., Smailus, D. E., Holt, R. A., Jones, S., Marra, M. A., Petric, M., Krajden, M., Lawrence, D., Mak, A., Chow, R., Skowronski, D. M., Tweed, S. A., Goh, S., Brunham, R. C., Robinson, J., Bowes, V., Sojonky, K., Byrne, S. K., Li, Y., Kobasa, D., Booth, T. & Paetzel, M. 2004 Novel avian influenza H7N3 strain outbreak, British Columbia. *Emerging Infectious Diseases* **10**, 2192-2195.

Holmes, E. C., Ghedin, E., Miller, N., Taylor, J., Bao, Y., St. George, K., Grenfell, B. T., Salzburg, S. L., Fraser, C. M., Lipman, D. J. & Taubenberger, J. K. 2005 Whole-genome analysis of human influenza A virus reveals multiple persistent lineages and reassortment among recent H3N2 viruses. *Public Library of Science* **3**, 1-10.

Hubbell, S. P. 1997 A unified theory of biogeography and relative species abundance and its application to tropical rain forests and coral reefs. *Coral Reefs* **16**, S9-S21.

Hurwitz, E. S., Haber, M., Chang, A., Shope, T., Teo, S., Ginsberg, M., Waecker, N. & Cox, N. J. 2000 Effectiveness of influenza vaccination of day care children in reducing influenza-related morbidity among household contacts. *Jama-Journal of the American Medical Association* **284**, 1677-1682.

Keeling, M. J. & Grenfell, B. T. 2002 Understanding the persistence of measles: reconciling theory, simulation and observation. *Proceedings of the Royal Society of London Series B-Biological Sciences* **269**, 335-343.

Keeling, M. J., Woolhouse, M. E. J., Shaw, D. J., Matthews, L., Chase-Topping, M., Haydon, D. T., Cornell, S. J., Kappey, J., Wilesmith, J. & Grenfell, B. T. 2001 Dynamics of the 2001 UK foot and mouth epidemic: Stochastic dispersal in a heterogeneous landscape. *Science* **294**, 813-817.

Kimura, M. 1983 *The Neutral Theory of Molecular Evolution*. Cambridge: Cambridge University Press.

Knossow, M., Daniels, R. S., Douglas, a. R., Skehel, J. J. & Wiley, D. C. 1984 3-Dimensional Structure of an Antigenic Mutant of the Influenza-Virus Hemagglutinin. *Nature* **311**, 678-680.

Knossow, M., Gaudier, M., Douglas, A., Barrere, B., Bizebard, T., Barbey, C., Gigant, B. & Skehelt, J. J. 2002 Mechanism of neutralization of influenza virus infectivity by antibodies. *Virology* **302**, 294-298.

Koelle, K., Pascual, M. & Yunus, M. 2006 Serotype cycles in cholera dynamics. *Proceedings of the Royal Society B-Biological Sciences* **273**, 2879-2886.

Koelle, K., Rodo, X., Pascual, M., Yunus, M. & Mostafa, G. 2005 Refractory periods and climate forcing in cholera dynamics. *Nature* **436**, 696-700.

Korber, B., LaBute, M. & Yusim, K. 2006 Immunoinformatics comes of age. *Plos Computational Biology* **2**, 0484-0492.

Lavenu, a., Leruez-Ville, M., Chaix, M. L., Boelle, P. Y., Rogez, S., Freymuth, F., Hay, A., Rouzioux, C. & Carrat, F. 2006 Detailed analysis of the genetic evolution of influenza virus during the course of an epidemic. *Epidemiology and Infection* **134**, 514-520.

Liang, S. H., Mozdzanowska, K., Palladino, G. & Gerhard, W. 1994 Heterosubtypic Immunity to Influenza Type-a Virus in Mice - Effector Mechanisms and Their Longevity. *Journal of Immunology* **152**, 1653-1661.

Lin, Y. P., Shaw, M., Gregory, V., Cameron, K., Lim, W., Klimov, A., Subbarao, K., Guan, Y., Krauss, S., Shortridge, K., Webster, R., Cox, N. & Hay, A. 2000 Avian-to-human transmission of H9N2 subtype influenza A viruses: Relationship between H9N2 and H5N1 human isolates. *Proceedings of the National Academy of Sciences of the United States of America* **97**, 9654-9658.

Lindstrom, S. E., Cox, N. J. & Klimov, A. 2004 Genetic analysis of human H2N2 and early H3N2 influenza viruses, 1957-1972: evidence for genetic divergence and multiple reassortment events. *Virology* **328**, 101-119.

Lipsitch, M., Cohen, T., Murray, M. & Levin, B. R. 2007 Antiviral resistance and the control of pandemic influenza. *Plos Medicine* **4**, 111-121.

Lipsitch, M. & Viboud, C. C. 2009 Influenza seasonality: Lifting the fog. *Proceedings of the National Academy of Sciences of the United States of America* **106**, 3645-3646.

Lloyd-Smith, J. O., Schreiber, S. J., Kopp, P. E. & Getz, W. M. 2005 Superspreading and the effect of individual variation on disease emergence. *Nature* **438**, 355-359.

Lowen, A. C., Mubareka, S., Steel, J. & Palese, P. 2007 Influenza virus transmission is dependent on relative humidity and temperature. *PLoS Pathogens* **3**, e151.

Ludwig, S., Haustein, a., Kaleta, E. F. & Scholtissek, C. 1994 Recent Influenza-a (H1N1) Infections of Pigs and Turkeys in Northern Europe. *Virology* **202**, 281-286.

Marshall, D. R., Turner, S. J., Belz, G. T., Wingo, S., Andreansky, S., Sangster, M. Y., Riberdy, J. M., Liu, T. B., Tan, M. & Doherty, P. C. 2001 Measuring the diaspora for virus-specific CD8(+) T cells. *Proceedings of the National Academy of Sciences of the United States of America* **98**, 6313-6318.

Mclean, A. R., Emery, V. C., Webster, A. & Griffiths, P. D. 1991 Population-Dynamics of Hiv within an Individual after Treatment with Zidovudine. *Aids* **5**, 485-489.

Monto, a. S., Davenpor.Fm, Napier, J. a. & Francis, T. 1970 Modification of an Outbreak of Influenza in Tecumseh, Michigan by Vaccination of Schoolchildren. *Journal of Infectious Diseases* **122**, 16-&.

Monto, A. S. & Kendal, A. P. 1973 Effect of Neuraminidase Antibody on Hong-Kong Influenza. *Lancet* **1**, 623-625.

Munster, V. J., Wallensten, A., Baas, C., Rimmelzwaan, G. F., Schutten, M., Olsen, B., Osterhaus, A. D. M. E. & Fouchier, R. A. M. 2005 Mallards and highly pathogenic avian influenza ancestral viruses, northern Europe. *Emerging Infectious Diseases* **11**, 1545-1551.

Myers, K. P., Olsen, C. W., Setterquist, S. F., Capuano, A. W., Donham, K. J., Thacker, E. L., Merchant, J. A. & Gray, G. C. 2006 Are swine workers in the United States at increased risk of infection with zoonotic influenza virus? *Clinical Infectious Diseases* **42**, 14-20.

Nagao, Y. & Koelle, K. 2008 Decreases in dengue transmission may act to increase the incidence of dengue hemorrhagic fever. *Proceedings of the National Academy of Sciences of the United States of America* **105**, 2238-2243.

Nakajima, K., Nobusawa, E., Nagy, A. & Nakajima, S. 2005 Accumulation of amino acid substitutions promotes irreversible structural changes in the hemagglutinin of human influenza AH3 virus during evolution. *Journal of Virology* **79**, 6472-6477.

Nakajima, S., Nakamura, K., Nishikawa, F. & Nakajima, K. 1991 Genetic-Relationship between the Ha Genes of Type-a Influenza-Viruses Isolated in Off-Seasons and Later Epidemic Seasons. *Epidemiology and Infection* **106**, 383-395.

Nelson, M. I., Edelman, L., Spiro, D. J., Boyne, A. R., Bera, J., Halpin, R., Ghedin, E., Miller, M. A., Simonsen, L., Viboud, C. & Holmes, E. C. 2008a Molecular epidemiology of A/H3N2 and A/H1N1 influenza virus during a single epidemic season in the United States. *PLoS Pathogens* **4**, e1000133.

Nelson, M. I., Simonsen, L., Viboud, C., Miller, M. A., Taylor, J., George, K. S., Griesemer, S. B., Ghedi, E., Sengamalay, N. A., Spiro, D. J., Volkov, I., Grenfell, B. T., Lipman, D. J., Taubenberger, J. K. & Holmes, E. C. 2006 Stochastic processes are key determinants of short-term evolution in influenza A virus. *PLoS Pathogens* **2**, e125.

Nelson, M. I., Viboud, C., Simonsen, L., Bennett, R. T., Griesemer, S. B., George, K. S., Taylor, J., Spiro, D. J., Sengamalay, N. A., Ghedin, E., Taubenberger, J. K. &

Holmes, E. C. 2008b Multiple reassortment events in the evolutionary history of H1N1 influenza A virus since 1918. *PLoS Pathogens* **4**, e1000012.

Nowak, M. A., Anderson, R. M., Mclean, A. R., Wolfs, T. F. W., Goudsmit, J. & May, R. M. 1991 Antigenic Diversity Thresholds and the Development of Aids. *Science* **254**, 963-969.

Okuno, Y., Isegawa, Y., Sasao, F. & Ueda, S. 1993 A Common Neutralizing Epitope Conserved between the Hemagglutinins of Influenza-a Virus H1 and H2 Strains. *Journal of Virology* **67**, 2552-2558.

Olofsson, S., Kumlin, U., Dimock, K. & Arnberg, N. 2005 Avian influenza and sialic acid receptors: more than meets the eye? *Lancet Infectious Diseases* **5**, 184-188.

Olsen, C. W., Carey, S., Hinshaw, L. & Karasin, A. I. 2000 Virologic and serologic surveillance for human, swine and avian influenza virus infections among pigs in the north-central United States. *Archives of Virology* **145**, 1399-1419.

Ottis, K., Sidoli, L., Bachmann, P. a., Webster, R. G. & Kaplan, M. M. 1982 Human Influenza-a Viruses in Pigs - Isolation of a H3N2-Strain Antigenically Related to a/England/42/72 and Evidence for Continuous Circulation of Human Viruses in the Pig-Population. *Archives of Virology* **73**, 103-108.

Pascual, M., Ahumada, J. A., Chaves, L. F., Rodo, X. & Bouma, M. 2006 Malaria resurgence in the East African highlands: Temperature trends revisited. *Proceedings of the National Academy of Sciences of the United States of America* **103**, 5829-5834.

Pascual, M., Rodo, X., Ellner, S. P., Colwell, R. & Bouma, M. J. 2000 Cholera dynamics and El Nino-Southern Oscillation. *Science* **289**, 1766-1769.

Peiris, J. S. M., Guan, Y., Markwell, D., Ghose, P., Webster, R. G. & Shortridge, K. F. 2001 Cocirculation of avian H9N2 and contemporary "human" H3N2 influenza A viruses in pigs in southeastern China: Potential for genetic reassortment? *Journal of Virology* **75**, 9679-9686.

Perelson, A. S. 2002 Modelling viral and immune system dynamics. *Nature Reviews Immunology* **2**, 28-36.

Puck, J. M., Glezen, W. P., Frank, A. L. & Six, H. R. 1980 Protection of Infants from Infection with Influenza-a Virus by Transplacentally Acquired Antibody. *Journal of Infectious Diseases* **142**, 844-849.

Pybus, O. G., Charleston, M. A., Gupta, S., Rambaut, A., Holmes, E. C. & Harvey, P. H. 2001 The epidemic behavior of the hepatitis C virus. *Science* **292**, 2323-2325.

Renegar, K. B., Small, P. A., Boykins, L. G. & Wright, P. F. 2004 Role of IgA versus IgG in the control of influenza viral infection in the murine respiratory tract. *Journal of Immunology* **173**, 1978-1986.

Reuman, P. D., Ayoub, E. M. & Small, P. A. 1987 Effect of Passive Maternal Antibody on Influenza Illness in Children - a Prospective-Study of Influenza-a in Mother-Infant Pairs. *Pediatric Infectious Disease Journal* **6**, 398-403.

Rohani, P., Green, C. J., Mantilla-Beniers, N. B. & Grenfell, B. T. 2003 Ecological interference between fatal diseases. *Nature* **422**, 885-888.

Russell, C. A., Jones, T. C., Barr, I. G., Cox, N. J., Garten, R. J., Gregory, V., Gust, I. D., Hampson, A. W., Hay, A. J., Hurt, A. C., de Jong, J. C., Kelso, A., Klimov, A. I., Kageyama, T., Komadina, N., Lapedes, A. S., Lin, Y. P., Mosterin, A., Obuchi, M., Odagiri, T., Osterhaus, A. D. M. E., Rimmelzwaan, G. F., Shaw, M. W.,

Skepner, E., Stohr, K., Tashiro, M., Fouchier, R. A. M. & Smith, D. J. 2008 The global circulation of seasonal influenza A (H3N2) viruses. *Science* **320**, 340-346.
Sanna, P. P., Ramiro-Ibanez, F. & De Logu, A. 2000 Synergistic interactions of antibodies in rate of virus neutralization. *Virology* **270**, 386-396.
Sato, K., Morishita, T., Nobusawa, E., Suzuki, Y., Miyazaki, Y., Fukui, Y., Suzuki, S. & Nakajima, K. 2000 Surveillance of influenza viruses isolated from travellers at Nagoya International Airport. *Epidemiology and Infection* **124**, 507-514.
Sato, K., Morishita, T., Nobusawa, E., Tonegawa, K., Sakae, K., Nakajima, S. & Nakajima, K. 2004 Amino-acid change on the antigenic region B1 of H3 haemagglutinin may be a trigger for the emergence of drift strain of influenza A virus. *Epidemiology and Infection* **132**, 399-406.
Schaffer, F. L., Soergel, M. E. & Straube, D. C. 1976 Survival of Airborne Influenza-Virus - Effects of Propagating Host, Relative Humidity, and Composition of Spray Fluids. *Archives of Virology* **51**, 263-273.
Schenzle, D. 1984 An age-structured model of pre- and post-vaccination measles transmission. *IMA J Math App Med Biol* **1**, 169-191.
Schulze, I. T. 1997 Effects of glycosylation on the properties and functions of influenza virus hemagglutinin. *Journal of Infectious Diseases* **176**, S24-S28.
Shaman, J. & Kohn, M. 2009 Absolute humidity modulates influenza survival, transmission, and seasonality. *Proceedings of the National Academy of Sciences of the United States of America* **106**, 3243-3248.
Skehel, J. J. & Wiley, D. C. 2000 Receptor binding and membrane fusion in virus entry: The influenza hemagglutinin. *Annual Review of Biochemistry* **69**, 531-569.
Smirnov, Y. a., Lipatov, A. S., Gitelman, A. K., Okuno, Y., Van Beek, R., Osterhaus, A. D. M. E. & Claas, E. C. J. 1999 An epitope shared by the hemagglutinins of H1, H2, H5, and H6 subtypes of influenza A virus. *Acta Virologica* **43**, 237-244.
Smith, D. J., Lapedes, A. S., de Jong, J. C., Bestebroer, T. M., Rimmelzwaan, G. F., Osterhaus, A. D. M. E. & Fouchier, R. A. M. 2004 Mapping the antigenic and genetic evolution of influenza virus. *Science* **305**, 371-376.
Sonoguchi, T., Naito, H., Hara, M., Takeuchi, Y. & Fukumi, H. 1985 Cross-Subtype Protection in Humans during Sequential, Overlapping, and or Concurrent Epidemics Caused by H3N2 and H1N1 Influenza-Viruses. *Journal of Infectious Diseases* **151**, 81-88.
Sonoguchi, T., Sakoh, M., Kunita, N., Satsuta, K., Noriki, H. & Fukumi, H. 1986 Reinfection with influenza A (H2N2, H3N2, and H1N1) viruses in soldiers and students in Japan. *The Journal of Infectious Diseases* **153**, 33-40.
Suarez, D. L., Senne, D. A., Banks, J., Brown, I. H., Essen, S. C., Lee, C. W., Manvell, R. J., Mathieu-Benson, C., Moreno, V., Pedersen, J. C., Panigrahy, B., Rojas, H., Spackman, E. & Alexander, D. J. 2004 Recombination resulting in virulence shift in avian influenza outbreak, Chile. *Emerging Infectious Diseases* **10**, 693-699.
Suzuki, Y. 2006 Natural selection on the influenza virus genome. *Molecular Biology and Evolution* **23**, 1902-1911.
Sweet, C., Jakeman, K. J. & Smith, H. 1987 Role of Milk-Derived Igg in Passive Maternal Protection of Neonatal Ferrets against Influenza. *Journal of General Virology* **68**, 2681-2686.

Thomas, P. G., Keating, R., Hulse-Post, D. J. & Doherty, P. C. 2006 Cell-mediated protection in influenza infection. *Emerging Infectious Diseases* **12**, 48-54.

Thompson, W. W., Shay, D. K., Weintraub, E., Brammer, L., Cox, N., Anderson, L. J. & Fukuda, K. 2003 Mortality associated with influenza and respiratory syncytial virus in the United States. *Jama-Journal of the American Medical Association* **289**, 179-186.

Tsuchiya, E., Sugawara, K., Hongo, S., Matsuzaki, Y., Muraki, Y., Li, Z. N. & Nakamura, K. 2002 Effect of addition of new oligosaccharide chains to the globular head of influenza A/H2N2 virus haemagglutinin on the intracellular transport and biological activities of the molecule. *Journal of General Virology* **83**, 1137-1146.

Viboud, C., Alonso, W. J. & Simonsen, L. 2006a Influenza in tropical regions. *Plos Medicine* **3**, 468-471.

Viboud, C., Bjornstad, O. N., Smith, D. L., Simonsen, L., Miller, M. A. & Grenfell, B. T. 2006b Synchrony, waves, and spatial hierarchies in the spread of influenza. *Science* **312**, 447-451.

Viboud, C., Boelle, P. Y., Cauchemez, S., Lavenu, A., Valleron, A. J., Flahault, A. & Carrat, F. 2004 Risk factors of influenza transmission in households. *British Journal of General Practice* **54**, 684-689.

Wagner, A. 2007 *Robustness and Evolvability in Living Systems*. Princeton Studies in Complexity. Princeton: Princeton University Press.

Wagner, R., Wolff, T., Herwig, A., Pleschka, S. & Klenk, H. D. 2000 Interdependence of hemagglutinin glycosylation and neuraminidase as regulators of influenza virus growth: a study by reverse genetics. *Journal of Virology* **74**, 6316-6323.

Webby, R. J., Rossow, K., Erickson, G., Sims, Y. & Webster, R. 2004 Multiple lineages of antigenically and genetically diverse influenza A virus co-circulate in the United States swine population. *Virus Research* **103**, 67-73.

Webster, R. G., Bean, W. J., Gorman, O. T., Chambers, T. M. & Kawaoka, Y. 1992 Evolution and Ecology of Influenza-A Viruses. *Microbiological Reviews* **56**, 152-179.

Webster, R. G. & Laver, W. G. 1980 Determination of the Number of Nonoverlapping Antigenic Areas on Hong-Kong (H3N2) Influenza-Virus Hemagglutinin with Monoclonal-Antibodies and the Selection of Variants with Potential Epidemiological Significance. *Virology* **104**, 139-148.

Wei, X. P., Decker, J. M., Wang, S. Y., Hui, H. X., Kappes, J. C., Wu, X. Y., Salazar-Gonzalez, J. F., Salazar, M. G., Kilby, J. M., Saag, M. S., Komarova, N. L., Nowak, M. A., Hahn, B. H., Kwong, P. D. & Shaw, G. M. 2003 Antibody neutralization and escape by HIV-1. *Nature* **422**, 307-312.

Wiley, D. C., Wilson, I. a. & Skehel, J. J. 1981 Structural Identification of the Antibody-Binding Sites of Hong-Kong Influenza Hemagglutinin and Their Involvement in Antigenic Variation. *Nature* **289**, 373-378.

Yoshida, T., Igarashi, M., Ozaki, H., Kishida, N., Tomabechi, D., Kida, H., Ito, K. & Takada, A. 2009 Cross-protective potential of a novel monoclonal antibody directed against antigenic site B of the hemagglutinin of influenza A viruses. *PLoS Pathogens* **5**, e10000350.

Yu, X. C., Tsibane, T., McGraw, P. A., House, F. S., Keefer, C. J., Hicar, M. D., Tumpey, T. M., Pappas, C., Perrone, L. A., Martinez, O., Stevens, J., Wilson, I. A., Aguilar, P. V., Altschuler, E. L., Basler, C. F. & Crowe, J. E. 2008 Neutralizing antibodies derived from the B cells of 1918 influenza pandemic survivors. *Nature* **455**, 532-536.

Zhou, N. N., Shortridge, K. F., Claas, E. C. J., Krauss, S. L. & Webster, R. G. 1999 Rapid evolution of H5N1 influenza viruses in chickens in Hong Kong. *Journal of Virology* **73**, 3366-3374.

Chapter 2

Episodic positive selection in influenza A (H3N2)

Introduction

The high burden of influenza in humans is a direct consequence of the virus's ability to escape preexisting immunity. Long-term immunity to influenza is mediated by antibodies, which confer lifelong protection to specific strains and partial cross-immunity to others (Gill & Murphy 1985; Yu et al. 2008). Most antibodies target influenza's surface proteins, especially its hemagglutinin (HA). The process by which influenza viruses escape recognition by prevailing antibodies through point mutations has been called "antigenic drift" (Webster et al. 1992).

Considering influenza's high mutation rate and the strong positive selection on HA, it is surprising that the genetic diversity of influenza viruses remains bounded rather than proliferating over time (Ferguson et al. 2003). Two kinds of hypotheses have been proposed to account for the restricted diversity. The first argues that pathogen diversity is restricted by a density-dependent process that causes an additional reduction in the number of susceptible hosts beyond the intrinsic dynamics of a seasonally-forced SIR model (Ferguson et al. 2003; Tria et al. 2005). This reduction has been ascribed to "generalized immunity," a hypothetical phenomenon that would protect a recently recovered individual from infection with any influenza strain for an approximately six-month period. Models that invoke generalized immunity have also incorporated other factors, such as heterogeneity in host transmission and variation in strain fitness, to explain dynamics. Notably, the concept of generalized immunity was motivated by computational simulations rather than laboratory experiment; empirical support for generalized immunity is modest. Enhanced cellular immunity following influenza infection in mice can confer partial protection to subsequent infections (Thomas et al.

2006), but there is still no evidence of broad, transient protection in humans. In fact, humans can be reinfected and infectious within days of clearing infections with another subtype (Frank et al. 1983).

Another hypothesis to explain the restricted diversity of HA over time is that individual mutations in HA, rather than always having small effects on antigenicity, can occasionally cause large changes in antigenic phenotype. If these changes are sufficiently abrupt, they can displace resident strains through cross-immunity. Selective sweeps have been proposed previously for H3N2 HA (Fitch et al. 1991) and H1N1 HA (Ina & Gojobori 1994), though the dynamics of the antigenic diversity of HA of any subtype has been characterized only recently (Smith et al. 2004). Remarkably, strains of H3N2 from 1968 to 2003 fall into eleven distinct antigenic clusters, inferred from cross-reactivities of antisera from ferrets challenged with these strains. Each cluster dominates within one or two years of its emergence and persists for roughly one to eight years before being displaced by a novel cluster. A longitudinal study of reinfection in humans suggests that cross-immunity may be as high as 95% within clusters and 60-84% between clusters (Gill & Murphy 1977).

These observations were synthesized in a model of "epochal evolution" for H3N2 (Koelle et al. 2006). In contrast to the assumptions of previous models, which postulate that genetic distance correlates linearly with antigenic distance (and therefore cross-immunity), the clusters support the assumption that the continuous genetic change observed in H3N2 HA can cause punctuated antigenic change. Most nucleotide and amino acid substitutions do not result in cluster transitions and therefore have negligible effect on antigenicity or fitness. The model proposes that the nonlinear mapping between genotype and phenotype can be approximated by evolution on connected neutral networks. A founding strain begins in a neutral network, i.e., a set of genotypes that are connected by single mutations and map to the same phenotype, and diffuses through high-dimensional genotype space via mutations until arriving at a node (sequence) belonging to an adjacent network. This new phenotype, which presumably has structurally significant amino acid substitutions in whichever epitopes are being targeted by the host population, has a larger supply of susceptibles than do strains in the old network. The model posits that the new network corresponds to one of two kinds of

phenotypic change: a mutation may either cause a slight change in antigenicity, corresponding to evolution within a cluster, or a major change, corresponding to the discovery of a new cluster. In the former case, cross-immunity between strains on adjacent networks remains high, and in the latter case, cross-immunity is lower. When a novel cluster arises, it can rapidly outcompete the resident cluster through cross-immunity, though clusters can also coexist.

The authors support their argument by showing in simulations that a neutral network model can reproduce both the characteristic phylogeny of HA and also the spikes in incidence that are associated with cluster transitions. Further, the authors predict, and confirm with sequence data and simulations, boom-and-bust cycles of strain diversity: diffusion in genotype space causes the average pairwise genetic distances of extant strains to increase as a cluster spreads. This diffusion in genotype space can be seen in the phylogenies of some clusters. For example, in clusters BE89 and BE92, multiple lineages persist from one year to the next. The trees of WU95 and SY97, in contrast, generally have unidirectional growth, which echoes the traditional descriptions of HA trees as a whole. This pattern could be due to sampling or genetic drift, perhaps augmented by off-season extinction, but it also suggests selective sweeps might occur within clusters. Similarly, the patterns in BE89 and BE92 could reflect neutral evolution or positive selection.

Selection within clusters might be a nontrivial component of influenza's evolutionary and ecological dynamics. It could suggest that influenza's fitness is modulated by more than escape from antibodies to HA, that ferrets are a poor model for human immunity, or that neutral networks are a poor representation for evolution within HA. There is additional indirect evidence that selection on HA occurs within clusters. Koelle et al. (2006) found that realistic cycles and increases in genetic diversity were not obtainable without the option of minor phenotypic changes within clusters. The incomplete cross-immunity demonstrated in longitudinal studies and frequent observations of antigenic drift in HA from season to season suggest this result is biologically plausible (Gill & Murphy 1977; Russell et al. 2008). However, it is also possible that within-cluster evolution is modulated by selection on T-cell epitopes on other genes, antibody epitopes on NA, or factors unrelated to immunity.

This chapter tests whether there is support for the idea that episodic positive selection in H3 HA is associated with the major antigenic clusters. I also examine evidence for weaker selection within clusters in HA. Finally, I weigh evidence for selection driven by other parts of the genome. I find weak within-cluster positive selection, driven by mutations at antibody-binding epitopes in HA and the addition of glycosylation sites. Positive selection also appears over long time scales in NA, NP, M2, and potentially several other proteins. The results suggest that immune escape, primarily from antibodies to HA, is the driving selective pressure on influenza. Other forms of immunity and other components of fitness probably contribute less to the dynamics. The results confirm that a model of strictly neutral evolution within clusters is inappropriate; positive selection operates continuously, though with varying intensity.

Positive selection on hemagglutinin

Multiple aspects of HA could be under selection, including the stability of secondary structures involved in transcription, usage bias of its codons, and the final structure of its protein. Changes in secondary structure are positively selected in avian H5N1 (Gultyaev et al. 2007), though no research appears to have been done on this topic in human influenza. Codon usage bias is a characteristic of many viruses. It is usually associated with adaptation to new host environments: At least in theory, viruses that adopt the codon bias of host cells have access to optimal tRNA frequencies, speeding translation (Ikemura 1981; Zuckerkandl & Pauling 1965). The increases in replication efficiency resulting from codon bias can have profound effects on viral fitness even when the amino acid structure is unchanged (Coleman et al. 2008). However, there is only a weak correlation between the genome-wide codon biases of influenza A and B viruses and their human and chicken hosts (Scapoli et al. 2007) and the bias appears to be under strong phylogenetic conservation (Zhou et al. 2005). Nonetheless, significant, positive correlations between these viruses and the genes expressed in host epithelial or gastrointestinal cells (in humans and birds, respectively) might exist and have yet to be investigated. Codon bias can also arise from mutational pressure. Codons in the epitopes of HA in human H3N2 show a bias toward substitutional changes relative to NA and NP,

potentially reflecting recent frequency dependent selection (Plotkin & Dushoff 2003). A whole-genome study of multiple influenza A subtypes found that codon bias appears mainly driven by GC composition, a marker of mutational bias (Zhou et al. 2005). Selection on synonymous codons is thus a potential factor in the long-term evolution of human influenza viruses, but it is an unlikely cause of strongly episodic selection.

The first part of this analysis tests for positive selection on the protein structure of HA. Traditional tests of positive selection on protein structure compare the relative frequencies of nonsynonymous (replacement) substitutions per nonsynonymous site to synonymous (silent) nucleotide substitutions per synonymous site. An excess of nonsynonymous substitutions is the hallmark of positive selection. In nucleotide substitution models, the nonsynonymous substitution rate is given by dN (in codon substitution models, β) and the synonymous rate by dS (α), with their ratio represented as dN/dS ($\beta/\alpha = \omega$); for convenience, I use them interchangeably in the text. Tests based on dN and dS have the advantage of not making specific assumptions about population dynamics during the period in which selection might have occurred (Kosakovsky Pond & Frost 2005b).

The relationship between dN and dS is the subject of the following investigations, which test for positive selection on the HA of putative cluster founders, within clusters, and in influenza's other genes. The investigations use a powerful approach for detecting selection in taxa with potentially weakly positive selection and relatively low divergence: Rather than fitting substitution rates on a site-by-site basis, they assume a distribution of discrete rate classes across sites (supplementary material). This approach, dubbed Random Effects Likelihood (REL), is thus able to detect significant weak selection across many sites where site-by-site inference (Fixed Effects Likelihood, FEL) would fail to find significant deviation from neutrality for each individual site. This approach is not without its weaknesses, however. Where possible, I complement results with those from the far more conservative site-by-site method. In both approaches, likelihood comparisons of fitted, unconstrained models to those in which dN is constrained to equal dS reveal whether positive selection is operating.

Selection on cluster founders

The antigenic clusters identified by Smith et al. (2004) are also clustered monophyletically, reflecting the common descent of strains assigned to a particular cluster. If selection on cluster founders were strong and positive, the dN/dS ratio of trunk branches connecting disparate phenotypes should be elevated compared to other branches, which represent evolution within clusters. In principle, of the within-cluster branches, the candidates most likely to be positively selected are those along the trunk: mutations on the trunk are specifically the ones most apt to be conserved in future lineages, and thus might have initially been positively selected.

Unfortunately, the low divergence of the HA phylogeny precludes meaningful calculations of dN and dS on individual branches. Instead, I test for a necessary, but not sufficient, pattern supporting the model of Koelle et al. (2006): significantly elevated dN/dS in some sites in the set of branches linking clusters (i.e., in putative cluster founders, as a group) and no elevation of dN/dS on the set of the other trunk branches. Episodic positive selection on HA would predict dN/dS > 1 in the first group. If evolution within clusters is neutral, dN/dS should be statistically indistinguishable from one in the second group. If there is still positive selection within clusters, the dN/dS of the second group should exceed one in some sites. We would expect it to be lower than that of the first group if the model of Koelle et al. (2006) is correct, i.e., if there is strong positive selection on cluster founders.

Comparisons of dN/dS among branch sets were made using the modified branch-site test of positive selection (Yang 1997; Yang & Nielsen 2002; Zhang et al. 2005). This method compares fitted dN/dS substitution rate categories in two sets of branches, the "foreground" and "background," which are determined a priori. One class of sites [class 0 in Yang & Nielsen (2002) and Zhang et al. (2005)] includes codons under negative selection and is fitted so that $0 < \omega_0 < 1$. Class 1 includes codons under neutral evolution and is set equal to one. Class 2a codons are under positive selection in the foreground (at rate ω_2) and purifying selection (ω_0) in the background; class 2b codons are under positive selection (ω_2) in the foreground and neutral evolution (ω_1) in the background. To

detect positive selection, the model in which ω_2 is fitted is compared by the likelihood ratio test to a model in which ω_2 is constrained to be one in the foreground branches.

In the first analysis, the foreground branches correspond to the cluster-substitution branches along the trunk, and the background branches are all other trunk branches. To construct the phylogeny, the TVM + Γ codon substitution model was chosen for the 253 antigenically typed HA sequences used in Smith et al. (2004). Available models were compared via AIC using MrAIC software (Nylander 2004). This codon substitution model was then used to infer the phylogeny by maximum likelihood in PHYML (Guindon & Gascuel 2003). The branch-site test of positive selection was executed in PAML version 3.15 using the codonml (a derivative of codeml) routine (Yang 1997).

When no site-by-site variation is allowed, the dN/dS ratio for the entire HA on the branches linking clusters is 0.38, reflecting the predominance of purifying selection to which HA as a whole is subjected. When categories ω_0, ω_1, and ω_2 are fitted, the cluster-transition branches show a class of sites with strong and significant positive selection ($\omega_2 \sim 8.6$) compared to the neutral model ($2\Delta L = 15.6$, $p < 0.01$; χ^2, d.f. = 1) (table 2.1). The six sites found under significant positive selection by Bayes empirical Bayes analysis (Yang et al. 2005) are all located within known antibody epitopes (table 2.2).

When the same models are fitted to the trunk branches corresponding to within-cluster evolution, reversing the foreground and background branches, the unconstrained model shows a ω that is elevated (approximately 2.2) but not significantly different from one ($2\Delta L = 1.36$, $p < 0.24$; χ^2, d.f. = 1) (table 2.1). Two of the three positively selected sites are in known epitopes (table 2.2).

The branch-site test of positive selection thus gives results consistent with episodic selection on the tertiary structure of HA, driven by antibody escape at known epitopes, and demarcated by the major phenotypes reported by Smith et al. (2004). It cannot, however, provide resolution at the level of individual cluster transitions, and thus it cannot exclude the hypothesis that some cluster transitions were not associated with positive selection on HA. It further assumes that sites remain in the same class, i.e., that selection pressures on them do not change over time. It also cannot exclude significant positive selection within clusters, not only because of the necessary aggregation of

branches and sites in this test but also because only branches along the trunk are considered. Positive diversifying selection, suggested in some of the phylogenies of individual clusters, could cause elevated dN/dS ratios along twig and tip branches. Low divergence again prohibits resolution of dN/dS for individual branches, and thus the next test of selection also relies on inference of rate classes.

Selection within clusters

A REL approach was used to test for positive selection within clusters (Kosakovsky Pond & Frost 2005a). REL as implemented in HyPhy (hereafter "REL") is a more general case of the branch-site test of positive selection and is similarly suited to detecting weak positive selection across an alignment (Kosakovsky Pond et al. 2005). The approach uses the codon substitution model of Muse and Gaut (1994). Parameters are then fitted, given a phylogeny (supplementary material). As in the branch-site test of positive selection, REL assumes a discrete distribution of rate classes, and the number of such classes is declared a priori. A major difference between the two models is that REL assumes both synonymous and nonsynonymous rates can vary, while the branch-site test assumes only variation in nonsynonymous rates.

REL was applied separately to the six most sampled clusters identified by Smith et al. (2004) (average number of samples per cluster = 28, range = 16-51), since results below these sample sizes are less reliable (Kosakovsky Pond & Frost 2005b). For each cluster, trees were built in the PHYML online server (Guindon & Gascuel 2003; Guindon et al. 2005) using the HKY substitution model (Hasegawa et al. 1985), a four-category gamma distribution of rate classes and an additional class of invariant sites. The REL models were then fitted, again assuming the HKY substitution model, in HyPhy. Models of increasing complexity were sequentially tested: the number of synonymous and nonsynonymous rate classes was incremented until there was no improvement in AIC. The maximum likelihoods of the unconstrained models were then compared to those of models in which the highest nonsynonymous substitution rate was constrained to equal the synonymous substitution rate (i.e., where no positive selection was allowed, and all other rate classes were fitted).

For each of the six clusters examined, a model that fit multiple dN and dS rate classes independently performed better than models with a single mean dN/dS (table 2.3). In every cluster, models that allowed positive selection outperformed models in which the highest rate class was constrained to one. The differences in performance were more dramatic in some clusters than others (e.g., BE92 v. BE89).

Every cluster had at least one site under positive selection; virtually all of these sites were located in known antibody epitopes, with the only two exceptions immediately adjacent to sites in epitopes (table 2.4). Only one of the sites under positive selection on the trunk in the branch-site test of positive selection was identified as positively selected in these clusters in the REL analysis (site 156, in epitope B, positively selected in SI87). This difference might arise from model misspecification by the branch-site test (e.g., in disallowing synonymous rate variation) or, more likely, long-term changes in selective pressures over the trunk that are not found in the short-term selective regimes of the clusters—a sign of epistasis (Koelle et al. 2006) or changes in the foci of antibody pressure. Two sites (226 in epitope D and 278 in epitope C) were under positive selection in more than one cluster. Direct estimation of rates at individual sites with FEL (supplementary material) failed to identify most of these sites as positively selected (table 2.S1). This is not surprising, considering the low divergence and small sample sizes of the clusters. However, each of the three sites found positively selected by FEL was also found selected by REL.

Glycosylation

During viral assembly, oligosaccharides present in the host cell can attach to the surface of viral proteins. N-linked sites that are potentially glycosylated (PNGS) during replication in vivo have the sequence Asn-X-Thr/Ser, where X is any amino acid except proline or potentially aspartic acid (Gallagher et al. 1992). Glycosylation is thought to play a major role in the function not only of influenza but also of HIV, Hendra, SARS-CoV, hepatitis C, and West Nile viruses (Vigerust et al. 2007). In HIV, the addition of PNGS has been associated with antibody escape (Wei et al. 2003; Zhou et al. 2007), though it does not necessarily correlate with the strength of neutralizing antibody

responses (Frost et al. 2005). There is similar diversity in the potential roles of glycosylation in HA of influenza. The addition of a glycosylation site in influenza B was associated with a decrease in the effectiveness of ferret antisera (Nakagawa et al. 2004). Experimental addition of a PNGS to HA was able to block antibody binding in the laboratory (Skehel et al. 1984); experimentally added sites have also been shown to disrupt transport activities, inhibit receptor binding, shield multiple epitopes simultaneously, and interfere with each other (Gallagher et al. 1992). There is evidence that glycosylation is an important factor in influenza's host-specific receptor binding abilities (Gambaryan et al. 1998). In avian influenza viruses, increases in the receptor binding strength of HA require compensation in the cleaving abilities of NA (Baigent & McCauley 2001; Wagner et al. 2000).

In human influenza viruses, however, most attention has been given to the hypothesis that PNGS in H3N2 HA are positively selected for immune escape. The number of PNGS in the HA of H3N2 has increased from six in 1968 to eleven in 2004. Abe et al. (2004) argue that several of the new PNGS appeared for the first time in major antigenic variants, and that glycosylation may thus play an important role in antigenic drift. Support for this position also comes from comparisons of H3 HA in different hosts and different HA types (Zhang et al. 2004). Avian H3 HA, which is probably under less positive selection, shows no increase in the number of PNGS over time. Human H1 HA, which is also probably under less intense selection, shows a slower, non-monotonic increase in sites with time.

Since PNGS are formed over short time scales by single amino acid substitutions, they are a clear case in which the dN/dS ratio can fail to detect major changes in structural phenotype that are positively selected. Notably, Smith et al. (2004) and Koelle et al. (2006) could not find any sites where substitutions were consistently predictive of transitions to new clusters; this pattern might appear if PNGS were precipitating major antigenic changes. To determine whether PNGS were associated with cluster transitions, PNGS were mapped to the phylogeny of HA (figure 2.2; table 2.5). The majority of PNGS appear on the trunk of the tree, suggesting they are positively selected upon appearance and then conserved. PNGS losses tend to occur on terminal branches. Remarkably, no PNGS additions or losses are associated with cluster transitions. It is thus

unlikely that they are associated with the major antigenic changes in HA. However, their placement suggests they improve the fitness of HA, perhaps by improving receptor binding or intracellular trafficking. Because of their potential interaction with NA, they also suggest that it might be important to consider the extent of possible influence of other genes on HA.

Positive selection on other genes

To determine whether other genes might be under positive selection and could precipitate partial or complete selective sweeps independently of antibody pressure on HA, REL analysis was performed on the rest of the influenza genome. To construct the most evenly sampled phylogeny, GenBank sequences were drawn primarily from Asia and chosen to span 1968 to the late 1990s (see supplementary material for accession numbers). Trees were built in the PHYML online server (Guindon & Gascuel 2003; Guindon et al. 2005) using the general time reversible substitution model, a four-category gamma distribution of rate classes and an additional class of invariant sites. The REL models were then fitted, again assuming a general reversible substitution model, with HyPhy software.

The best-fitting models for all genes except PB2 are those allowing positive selection in some sites (table 2.6). Considering both the size of the difference in AIC—that is, the ΔAIC between the constrained and unconstrained models—and the results of the empirical Bayes (table 2.7) and FEL analyses (table 2.S2), there is strong support for positive selection in HA, NA, NP, and M2, followed by a weaker signal in PA, PB1, M1, and NS1 and NS2. However, the FEL model, which is known to have an extremely small rate of false positives and high rate of false negatives for small data sets (Kosakovsky Pond & Frost 2005b), sometimes found stronger support (i.e., lower p values) for selection at particular sites relative to the REL models' Bayes factors. Rate "smoothing" is a known problem of REL models and can cause underestimation of positive selection when small numbers of sites are selected [Kosakovsky Pond & Frost (2005b) and Kosakovsky Pond, pers. comm.). Thus, this analysis might not be effective at ruling out strong positive selection on a few sites in any gene. With its temporal aggregation, it also fails if selective regimes change on individual sites over short periods of time.

Discussion

This study presents evidence consistent with episodic positive selection on the antigenic phenotypes defined by Smith et al. (2004). It also suggests that evolution within these phenotypes is not strictly neutral, in support of the model of Koelle et al. (2006). Potential sources of positive selection on HA within clusters include antibody-mediated selection in known epitopes and selection for PNGS. Since models of influenza's ecological and evolutionary dynamics tend to assume that strain-level selection can be approximated by selection on HA, other genes were examined for the presence of positively selected sites. Results suggest that positive selection is indeed strongest in HA, but it also likely shapes the evolution of NA, NP, and M2, and other proteins to a lesser extent.

Several competing perspectives have arisen on the precise tempo of positive selection in HA. Wolf et al. (2006) published analyses of H3N2 HA sequences collected over 1995 to 2005. Rather than inferring rates of dN and dS, they looked for and found a strong positive correlation between the number of nonsynonymous relative to synonymous substitutions in a lineage and the speed with which contemporary lineages went extinct. They found that the nonsynonymous substitutions tended to occur in HA's known B-cell epitopes, and that intervals between periods of rapid lineage turnover were characterized by a lower ratio of nonsynonymous to synonymous substitutions. They did not attempt to correlate periods of presumed antigenic turnover to the clusters identified by Smith et al. (2004), but their periods with high turnover appear to correspond to cluster emergence events (of WU95, SY97, and FU02); only one additional period of rapid lineage replacement (in SY97) was found. Notably, they did not otherwise find an excess of nonsynonymous substitutions during intervals of apparent stasis. Their findings are thus in keeping with the model of episodic positive selection, though they suggest mostly neutral evolution occurs between episodes of rapid displacement.

Two other studies use molecular evidence to argue instead for a model of continuous, positive, and effectively non-episodic selection on HA. Shih et al. (2007) plotted the frequency of amino acid fixation events in HA over time, using all H3N2 sequences available in GenBank. They found that most fixation events tended to occur

very rapidly and in most years, and that the majority of replacements were associated with known antigenic sites. Their analysis contains two flaws. First, the presence of several rapidly fixed sites within clusters is not inconsistent with a model of episodic positive selection; the model of Koelle et al. (2006) produces multiple fixation events in within clusters, despite the fact that cross-immunity within strains of the same cluster is high but imperfect (i.e., that positive selection is relatively weak)(figure 2.S1). Second, clusters do not emerge synchronously everywhere in the world, and inferring fixation rates from sequences aggregated over multiple locations and seasons (e.g., the latter half of the 2004-2005 season in the Northern hemisphere, the 2005 season in the Southern hemisphere, and the beginning of the 2005-2006 season in the northern hemisphere) creates an extended, artificial overlap between clusters that spreads the timing of fixation events; in any one location, fixation events are probably quite abrupt (K. Koelle, pers. comm.). Performing the same exercise with the data of Smith et al. (2004) gives the impression of much more continuous positive selection (K. Koelle, unpublished results).

A study by Suzuki (2008), which uses an approach similar to the first analysis presented here, also claims continuous, non-episodic positive selection. Suzuki partitioned branches into four groups, depending on whether they occurred on or off the trunk and whether they corresponded to within-cluster evolution or cluster transitions. He then used maximum parsimony analysis to infer whether positive selection occurred in branches in each category, focusing only on epitope sites (designated a priori). He found significant positive selection on the trunk branches, even when the cluster transitions were excluded, and neutral evolution in the epitopes off the trunk. It is not surprising that he did not find positive selection off the trunk, since his approach aggregates substitutions across sites within epitopes and could potentially mask the effects of positive selection at a few sites. His finding positive selection on the non-transition trunk branches conflicts with the analysis here, which found that sites in non-transition trunk branches were not significantly positively selected. The difference might be due to a failure in the fitting algorithm or differences in the underlying evolutionary models. It is curious that Wolf et al. (2006) also used codeml in PAML to infer dN/dS in the epitopes of all trunk branches from a 100-taxa subset of their sequences from 1995-2005 and failed to find significant positive selection. To resolve these ambiguities, it would be

helpful to fit models that allow for variation in synonymous as well as nonsynonymous substitution rates. This investigation would also be strengthened by the availability of more antigenically typed taxa. Despite large sequencing and antigenic typing efforts [e.g., Russell et al. (2008)], only the several hundred sequences published in Smith et al. (2004) are associated with publicly available antigenic information.

This analysis presents several new findings on selection in non-HA genes of influenza. In a genome-wide study of all H3N2 sequences in GenBank, Suzuki (2006) found significantly positively selected sites only in HA (two sites, positions 220 and 229), NA (one site, position 370), and NP (one site, position 131), despite the fact that at least 6% of the codons in every gene had $dN/dS > 1$ (but not significantly). His analysis relied on an extremely conservative site-by-site ancestral reconstruction of dN and dS using maximum parsimony. Bragstad et al. (2008) also reported no positively selected sites in the internal genes of H3N2 sequences collected in Denmark from 1999 to 2006 using a similarly conservative method. This study, in contrast, uses a more realistic model of sequence evolution and presents stronger evidence for long-term selection in genes outside HA. It also indicates (through ΔAIC of REL models and site-by-site methods) the relative strength and targets of selection. After HA, these results suggest NA might be under strongest selection pressure. One of its three positively selected sites occurred in a known B-cell epitope, and positively-selected site 120 is adjacent to site 119, which is associated with oseltamivir resistance (Abed et al. 2006). NP and M2 also appear positively selected. Several of their positively selected sites are in known T-cell epitopes, as are two sites in M2 [as identified in Suzuki et al. (2006)]. The major role of NP is genome encapsidation in preparation for RNA transcription; NP also interacts with RNA, viral RNA polymerase, and in close conjunction with M1 protein as well as host cell actin, nuclear RNA helicase, and other components (Portela & Digard 2002). Information on the roles of specific NP residues is scant. Suzuki (2006) reports that the position of 131 in NP is unknown; position 290 can serve as an antibody epitope in vitro (Varich & Kaverin 2004). Interestingly, many of the positively selected sites (NP positions 77, 98, and 136) in this study have continued to evolve more recently (Ghedin et al. 2005). M2 also fills functional and immunogenic roles. M2 forms the ion channel, which is the target of adamantane drugs; our data do not encompass the recent rise of adamantane

resistance, which is conferred by the S31N mutation (Nelson et al. 2009). The exposure of the protein to the surface of the virus allows it to be targeted by antibodies. All of 30 young adults tested in one study showed relatively high antibody titers to M proteins, and some showed faster and stronger antibody responses to M upon vaccination or challenge than to HA or NA (Khan et al. 1982). Recent clinical trials of a vaccine based on the M2 ectodomain have also demonstrated immunogenic epitopes (Schotsaert et al. 2009). A more comprehensive, recent analysis (Furuse et al. 2009) also finds positively selected sites in M2, including site 16 (located in the ectodomain) but not 81 (in the cytoplasmic domain). Since M1 and M2 share a 71-nucleotide reading frame, changes in M2 (e.g., at site 3) might necessitate compensatory mutations in M1. Immune-mediated selection on HA or M1 (through M2) might similarly drive compensatory changes in NP. It is also feasible that compensatory changes in genes might arise from functional changes in other genes with which they closely interact.

The patterns in glycosylation found in this study [also corroborated and published, after this analysis was performed, by Blackburne et al. (2008)] suggest that selection might occur via reassortment on whole genes or gene combinations. This hypothesis was not tested here, though some authors have argued (largely based on few examples, and for which counterexamples are available) that reassortment between HA and NA has preceded the emergence of major antigenic variants or especially successful strains (Chen & Holmes 2008; Nelson et al. 2008; Rambaut et al. 2008; Wolf et al. 2006). Hypothesis-driven exploration of specific interactions between genes, and between specific sites and functions (immunologic and non-immunologic), will help resolve the contribution of different genes to influenza's dynamics. This study suggests which genes outside HA most warrant investigation. Better resolution of antigenic and genetic data on HA and other genes in the next few years should allow a more quantitative understanding of influenza's evolutionary pressures and constraints.

Figure 2.1. Phylogeny of H3N2 HA showing antigenic clusters (colored tips) and (highlighted) cluster transition branches.

Figure 2.1

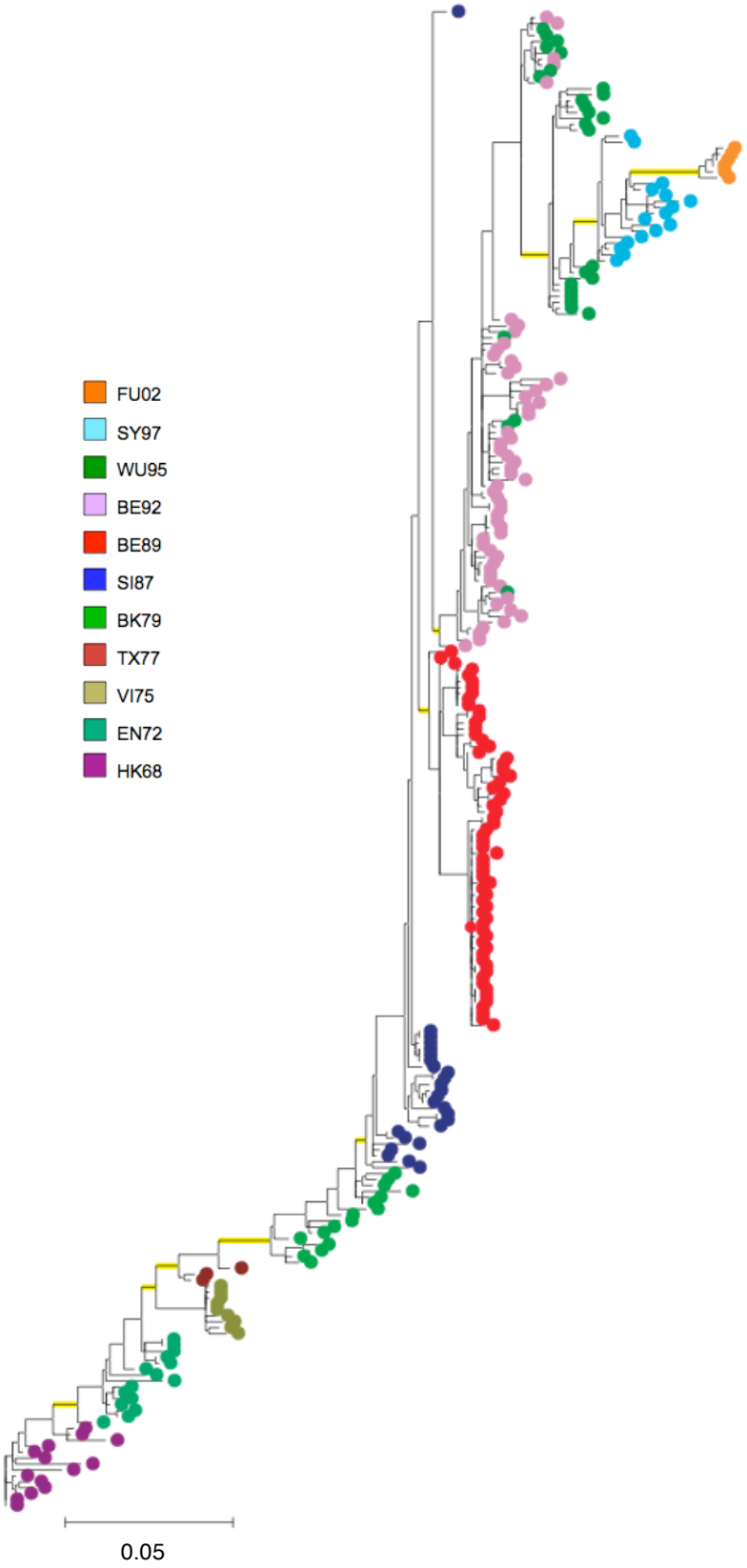

Figure 2.2. Phylogeny of H3N2 HA showing antigenic clusters (colored tips) and locations on branches where potential N-linked glycosylation sites (PNGS) were added (pink ×) and removed (light green ×).

Figure 2.2

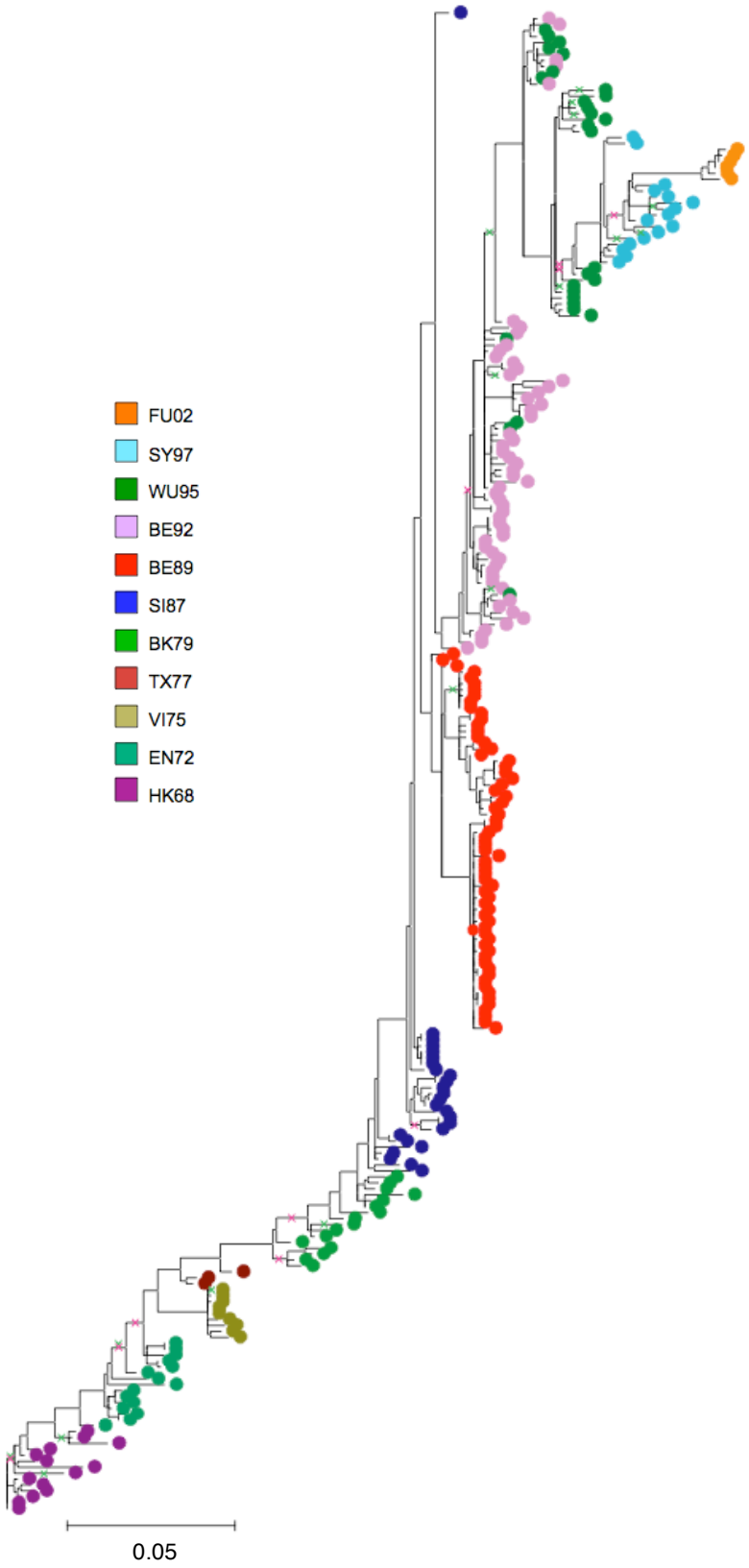

Table 2.1. Results of the modified branch-site test of positive selection. Site classes are described in the main text. The proportion of sites assigned to each class is listed in the first row under each model.

			Site class				log(L)
			0	1	2a	2b	
Foreground branches	Cluster transition	**Unconstrained model**					-7870
		Proportion	0.74	0.24	0.02	0.01	
		Background ω	0.10	1.00	0.10	1.00	
		Foreground ω	0.10	1.00	8.58	8.58	
		Neutral model					-7885
		Proportion	0.69	0.22	0.07	0.02	
		Background ω	0.10	1.00	0.10	1.00	
		Foreground ω	0.10	1.00	1.00	1.00	
	Non-transition trunk	**Unconstrained model**					-7880
		Proportion	0.75	0.25	0.00	0.00	
		Background ω	0.10	1.00	0.10	1.00	
		Foreground ω	0.10	1.00	2.24	2.24	
		Neutral model					-7879
		Proportion	0.72	0.24	0.03	0.01	
		Background ω	0.10	1.00	0.10	1.00	
		Foreground ω	0.10	1.00	1.00	1.00	

Table 2.2. Sites positively selected along the HA trunk. according to posterior probabilities (Pr) of Bayes empirical Bayes analysis in the branch-site test of positive selection.

		Site	Epitope	Pr
Foreground branches	Cluster transition	133	A	0.579
		155	B	1.000
		156	B	0.687
		189	B	0.803
		215	D	0.907
	Non-transition trunk	2		0.530
		63	E	0.635
		82	E	0.519

Table 2.3. Constrained and unconstrained REL models for the six best-sampled clusters. Column *n* gives the number of taxa available for the cluster. The non-positive discrete models are those that constrain $\beta \leq \alpha$, while the unconstrained models do not. The dual models allow rate variation in both β and α, as described in the text. Numbers under each model are AIC scores; the best-performing models are in bold. The ΔAIC column gives the difference between the AIC of the best-performing non-positive discrete and best-performing unconstrained model (consistently the dual model in each case).

		Non-positive discrete		**Unconstrained**		**Δ AIC**
Cluster	***n***	Constant	Dual	Constant	Dual	
BK79	16	4179.0	4136.4	4140.0	**4134.5**	1.9
SI87	20	4110.1	4071.1	4069.0	**4068.9**	2.1
BE89	37	4129.7	4100.8	4103.8	**4100.0**	0.8
BE92	51	5568.3	5492.4	5535.0	**5461.2**	31.3
WU95	28	4613.7	4574.8	4592.6	**4561.9**	12.9
SY97	16	3912.9	3909.9	3907.9	**3905.3**	4.7

Table 2.4. Sites positively selected by REL in the HA of the six best-sampled clusters. Sites adjacent but not directly in an epitope have the epitope listed in parenthesis. The last column lists the log of the Bayes Factor (BF) that $\beta > \alpha$ at that site. Sites positively selected with a BF between 20 and 50 are in italics; sites positively selected with BF >50 are in normal type.

Cluster	Site	Epitope	log(BF)
BK79	*137*	*A*	*3.07*
	213	D	8.14
SI87	156	B	6.87
	186	B	6.94
BE89	50	C	4.81
	78	E	7.52
	188	B	4.71
	193	B	4.74
	196	B	7.61
	278	C	4.74
BE92	*62*	*E*	*3.77*
	79	*(E)*	*3.73*
	96	D	6.45
	121	D	6.57
	124	A	6.24
	135	A	11.92
	138	A	6.40
	158	*B*	*3.51*
	201	D	9.17
	214	D	6.58
	216	*D*	*3.68*
	219	D	6.65
	226	D	29.01
	229	*D*	*3.67*
	248	*D*	*3.88*
	276	C	6.49
	278	*C*	*3.56*
WU95	226	D	7.99
SY97	144	A	6.58
	199	(B)	6.87

Table 2.5. Potential N-linked glycosylation sites (PNGS) in HA. B-cell epitopes are listed if any part of the PNGS overlaps them. The third column gives the cluster in which each PNGS arose and fixed, unless indicated otherwise in the notes.

Sites	Epitope	Cluster	Notes
8-10		-	Present except for small clade in HK68
22-24		-	Present throughout
38-40		-	Present throughout
45-47	C	SI87, BE89	Appears only in clades in SI87 and BE89
63-65	E	EN72	Present in HK68, lost, regained in EN72 and then fixed
81-83	E	HK68	Lost when PNGS at sites 63-65 added
122-124	A	WU95	Also present in branch of BK79
126-128	A/B	EN72	
133-135	A	WU95	
144-146	A	SY97	
165-167	B/D	-	Present except for small cllade in WU95 and VI75
246-248	D	BK79	
276-278	C	BE92	Added and lost within BE92
285-287		-	Present throughout

Table 2.6. Constrained and unconstrained REL models for all genes. Column *n* shows the number of taxa included for each gene. The non-positive discrete model constrains $\beta \leq \alpha$, while the unconstrained model does not. Numbers under each model are AIC scores; the best-performing models are in bold. The ΔAIC column gives the difference between the AIC of the best-performing non-positive discrete and best-performing unconstrained model. The last column indicates whether positively selected sites (PSS) were identified by empirical Bayes in REL with Bayes Factor >20 ("R", table 2.7) or with $p < 0.05$ by FEL ("F", table 2.S2). A dash means no positively selected sites were found for either method.

Protein	*n*	Non-positive	Unconstrained	ΔAIC	PSS
HA	213	16720.24	**16659.74**	60.5	R, F
NA	196	15781.63	**15728.47**	53.16	R, F
NP	95	12186.42	**12176.59**	9.83	R, F
PA	78	15255.04	**15254.21**	0.83	R
PB2	75	**16550.39**	16550.63	0.24	
PB1	78	14403.06	**14402.82**	0.24	-
M1	183	7221.37	**7220.38**	0.99	R
M2	183	3272.28	**3255.6**	16.68	R,F
NS1	80	5359.29	**5358.57**	0.72	-
NS2	80	2388.77	**2388.69**	0.08	-

Table 2.7. Sites positively selected by REL in all genes. The epitope column lists B-cell epitopes by their letter names and any known T-cell epitope (TCE), followed by the epitope's associated HLA allele [from Suzuki (2006)]. Sites adjacent but not directly in a B-cell epitope have the epitope listed in parenthesis. The last column lists the log of the Bayes Factor (BF) that $\beta > \alpha$ at that site. Sites positively selected with a BF between 20 and 50 are in italics; sites positively selected with BF >50 are in normal type. Epitopes followed by an apostrophe are those under possible selection in eggs.

Protein	Site	Epitope	log(BF)
HA	*133*	*A*	*3.26*
	135	*A; TCE (HLA-A*1101)*	*3.78*
	137	*A′; TCE (HLA-A*1101)*	*3.32*
	145	A	9.98
	159	*B′*	*3.40*
	193	*B′*	*3.31*
	199	*(B)′*	*3.57*
	201	*D*	*3.23*
	226	D'	17.91
	229	*D′*	*3.51*
	262	*E; TCE (HLA-DQA1*0102; HLA-DQB1*0602; HLA-*	*3.50*
	276	*C′*	*3.47*
NA	120		20.40
	267		4.41
	370	C	3.99
NP	18		4.10
	34		*3.21*
	50	*TCE (HLA-A*01)*	*3.13*
	64		*3.69*
	65		*3.62*
	77		4.32
	98	*TCE (HLA-A*6801)*	*3.52*
	127		*3.65*
	131		4.56
	136		*3.47*
	217		4.12
	290		4.09
	334		3.95
	375	TCE (HLA-DQA1*0501; HLA-DQB1*0201)	4.54
	421	*TCE (HLA-B*0702; HLA-B*3501)*	*3.71*
	450		4.38

Table 2.7 (continued)

Protein	Site	Epitope	log(BF)
PA	*65*		*3.60*
	263		*3.53*
	269		*3.24*
	272		*3.04*
	277		*3.28*
	348		*3.35*
	399		*3.18*
	404		*3.66*
	409		*3.03*
	618		*3.62*
	673		*3.65*
	688		*3.29*
	716		*3.23*
PB2	-	-	-
PB1	-	-	-
M1	3		3.98
	219		3.92
	235	*TCE (HLA-DQw3)*	*3.56*
M2	*3*		*3.71*
	11	*TCE (HLA-B*44)*	4.28
	13	*TCE (HLA-B*44)*	*3.31*
	14	*TCE (HLA-B*44)*	*3.21*
	16		4.28
	21		*3.25*
	52		4.00
	54		4.02
	77		*3.31*
	81	TCE (HLA-CW*0102)	3.94
	85	*TCE (HLA-CW*0102)*	*3.24*
NS1	-	-	-
NS2	-	-	-

Supplementary material

Description of REL and FEL models

The following description is a short summary of definitive presentations that can be found in Kosakovsky Pond & Frost (2005b) and Kosakovsky Pond et al. (in press).

Both models assume sites evolve according to an unobserved codon substitution rate matrix. The rate of substituting non-stop codon x with non-stop codon y ($x \neq y$) at site s under the MG94 and general reversible model is given by:

$$\text{MG94} \times \text{REV}_{x,y}(\mathrm{d}t) = \begin{cases} 0, & x \to y \text{ requires } \geq 2 \text{ nucleotide substitutions,} \\ \alpha_s R_{ij} \pi_{j_p} dt, & x \to y \text{ is a synonymous substitution of nucleotide } i \text{ with nucleotide } j, \\ \beta_s R_{ij} \pi_{j_p} dt, & x \to y \text{ is a nonsynonymous substitution of nucleotide } i \text{ with nucleotide } j. \end{cases} \quad (3.S1)$$

R_{ij} is the substitution rate of nucleotide i for nucleotide j, and π_{j_p} is the frequency of the target nucleotide j in codon position $p \in \{1, 2, 3\}$. The reversible model posits that $R_{ij} = R_{ji}$. Traditionally, R_{AG} is set equal to one, and the other rates are fitted. To save time, rates R_{ij} in codon models can be approximated by those from nucleotide substitution models, which account for target nucleotide frequencies π_j but (by definition) not codon positions p.

The model assumes that each site s has a specific rate of synonymous and nonsynonymous substitutions, α_s and β_s. FEL attempts to infer directly the individual rates, α_s and β_s, for each site. REL assumes a distribution of discrete rates $d \in \{1,\ldots, D\}$ in D categories, where D is fixed a priori. These rates, α_d and β_d, are found by maximizing the likelihood of the entire alignment, which is given by the product of individual site s likelihoods,

$$L(s) = \sum_{d=1}^{D} L(s \mid \alpha_s = \alpha_d, \beta_s = \beta_d)\, p^d \,. \qquad (3.S2)$$

In the branch-site test of positive selection, $\alpha_s = 1$ and $\beta_s = \omega_s$. In the unconstrained model, rate categories ω_d are fitted for foreground and background branches separately. In FEL and REL, both α and β can be allowed to vary. In the REL analysis here, rates were drawn from general discrete distributions and allowed to vary independently.

Fitting a model by REL or FEL in HyPhy traditionally begins with inferring nucleotide substitution rates R_{ij}, base frequencies π_j, and branch lengths from a given tree (which was itself constructed from a substitution model of some kind). A hybrid codon-nucleotide substitution model is then derived by assuming unchanged rates R_{ij} and proportional branch lengths; the latter will be used to scale α_s and β_s. Alternatively, a full codon model can be fit from a given tree.

Next, α_s and β_s (or α_d and β_d) are fit, assuming that each branch is an independent realization of the substitution process, though weighted by uncertainty in ancestral states. Positive selection in each model is revealed by demonstrating that the unconstrained model in which $\beta > \alpha$ outperforms the nested null hypothesis ($\alpha = \beta$) by the likelihood ratio test. Both the branch-site test of positive selection in PAML (Yang et al. 2005) and REL (Kosakovsky Pond & Frost 2005b) as implemented in HyPhy further attempt to classify sites by empirical Bayes analysis.

In the analysis here, full codon models with four discrete rate classes were used for most of the gene-level REL analyses (exceptions were PB1 and M, which did not appear able to converge on a codon model, and for which three discrete rate classes were fit). Full codon models were used in all the cluster analysis, and the number of rate classes was incremented until AIC ceased to improve; all clusters have two synonymous and two or three nonsynonymous classes.

GenBank accession numbers

HA: AY660991-AY661211, AF008665, AF008697, AF008711, , AF008725, AF008755, AF008769, AF008828, AF008867, AF008886, AF008888, AF008903, AF008905, AF092062, AF131997, AF180570, AF180602, AF180643, AF201874, AF368444, AF368446, D21173, D49961, ISDN38157, ISDNCDA001, ISDNENG72, ISDNHK71, ISDNTX77, ISDNVIC75, M16739, U08858, Z46405, Z46408, Z46413, Z46414

NA: AY210126, AY210129, AY210131, CY006685, U42631, CY007973, CY003554, CY006309, AY210134, AY210135, CY003530, AB124660, CY009006, CY006909, CY003498, CY006046, CY003730, AB124661, AB124663, CY006765, DQ508827, K01150, CY006101, CY006205, CY003490, CY006054, CY006757, CY006853, CY003738, CY003722, CY006317, CY006325, CY003746, CY008174, CY003522, CY003538, CY003506, CY003546, U42633, CY003514, DQ508835, U42635, U42636, U42770, U42771, U42772, U42773, CY003714, CY033608, U43427, CY036905, CY009014, CY006349, AF038260, U42777, U42778, U42779, U42780, U43419, U43422, U43426, CY006341, CY003754, CY007837, U71140, U71141, U71142, U71143, U51246, AF038261, AJ457945, AF038262, AF038263, AF038265, AF038264, EU857285, EU857289, EU857293, EU857295, EU857296, EU857298, EU857120, EU857126, EU857127, EU857130, EU857131, EU857169, EU857174, EU857175, EU857176, EU857172, EU857180, EU857181, EU857182, EU857183, EU857201, EU857202, EU857208, EU857212, EU857282, EU857283, EU857284, EU857286, EU857287, EF584349, EF584358, EF584359, AJ457939, EU857100, EU857101, EU857104, EU857105, EU857107, EU857108, EU857109, EU857110, EU857111, EU857112, EU857152, EU857153, EU857154, EU857155, EU857156, EU857157, EU857158, EU857159, EU857160, EU857161, EU857162, EU857163, EU857164, EU857165, EU857166, EU857167, EU857168, EU857303, EU857306, EF584371, AF382329, AF382330, AF382331, AF382332, AF386761, AF386763, AF386764, AJ293923, AJ457931, AJ457936, AJ457938, EU857096, EU857097, EU857098, EU857099, EU857113, EU857114, EU857115, EU857116, EU857117, EU857121, EU857128, EU857129, EU857132, EU857147, EU857148, EU857149, EU857246, EU857251, EU857252, EU857253, EU857254, EU857264, EU857266, EU857268, AJ457933, AJ457934, EU857170, EU857171, EU857173, EU857177, EU857178, EU857179, EU857185, EU857189, EU857203, EU857204, EU857205, EU857206, EU857207, EU857233, EU857234, EU857235, EU857236, EU857237, EU857238, EU857239, EU857240, EU857242, EU857243, EU857244, EU857317, DQ249253, EU857133, EU857134, EU857136, EU857144, EU857146, EU857188, EU857191, EU857193, EU857195, EU857196, EU857198, EU857199, EU857211, EU857213, EU857226, EU857229, EU857231, EU857260, EU857261, EU857262, EU857269, EU857312, EU857313, EU857314, U42776, DQ415341, DQ415342, DQ415343, AY589662, AY589663, AY589664, AY589666, AY589669, AY589670, AY589672, AY589673, AY589674, AY589676, AB281206, EU857321, EU857327, EU857345, AB433818, AB433819, EU857137, EU857138, EU857139, EU857192, EU857194, EU857197, EU857200, EU857214, EU857215, EU857216, EU857217, EU857218, EU857219, EU857220, EU857221, AB281193, AB281196, AB281198, EU857255,

EU857256, EU857257, EU857258, AB281201, AB281203, EU857270, EU857271, EU857300, EU857301, EU857331, EU857333

NP: AY210227, AY210230, AY210231, AY210232, CY006686, CY007974, CY009359, CY009639, D00051, AY210234, AY210236, AY210238, CY003555, CY006310, L07344, CY003531, CY009007, CY006910, CY003499, CY006047, CY003731, L07358, L07359, CY006766, DQ508826, CY006102, CY006206, CY003491, L07361, CY006055, CY006758, CY006854, CY006318, CY003739, CY003723, M22577, CY003747, CY006326, CY008175, CY003523, CY003507, CY003539, DQ508850, L07366, L07367, CY003547, CY003515, CY035201, DQ508834, L07372, L07373, L07374, L07353, L07354, L07357, CY035209, CY035217, CY036834, CY035225, CY035233, CY033609, CY003715, AF038254, CY009015, CY036906, CY006350, U71144, CY007838, CY003755, CY006342, AY936880, AF038255, AB019358, AB019361, U71145, U71146, U71147, CY038506, AF038256, AF038257, AF038258, AF038259, AF255748, AF255749, AF483604, AJ458277, CY036850, AB019359, AB019360, AJ293924, AJ458276, DQ487330, EU097851, EU097845, EU097846

PA: AY210199, AY210202, AY210203, CY006688, CY007976, CY009361, CY009641, DQ508928, AY210205, AY210206, AX350188, CY003557, CY006312, CY003533, CY009009, CY006912, CY003501, CY003733, CY006049, CY006768, DQ508824, CY006104, CY006208, CY003493, CY006057, CY006760, CY003725, CY006856, CY006320, CY003741, CY003749, CY006328, CY008177, CY003541, CY003509, CY003525, DQ508848, CY003549, CY003517, CY035203, DQ508832, CY035211, CY035219, CY035227, CY035235, CY033611, CY003717, AF037424, CY006352, CY036908, U71136, CY006344, AF037425, U71137, U71138, U71139, CY038508, AF037426, AF037427, AF037428, AF037429, AF257197, AF257198, AF483603, CY036852, AJ293922, DQ487327, EU097809, EU097820, EU097821, DQ415308, DQ415309, DQ415310, EU097815, EU097816, EU097818, EU097819, CY037348

PB2: AY210144, AY210146, AY210148, CY006690, AX350184, AY210149, AY210150, CY003559, CY006314, CY007978, CY009363, CY009643, DQ508926, M91712, CY003535, CY009011, CY003503, CY006914, CY003735, CY006051, CY006770, DQ508822, CY003495, CY006106, CY006210, CY006059, CY006762, CY003727, CY003743, CY006322, CY006858, CY003751, CY006330, CY008179, CY003511, CY003527, CY003543, DQ508846, CY003551, CY003519, CY035205, DQ508830, CY035213, CY035221, CY036838, CY035229, CY035237, CY003719, CY033613, AF037412, CY006354, CY036910, CY006346, U71132, AF037413, U71133, U71134, U71135, CY038510, AF037414, AF037415, AF037416, AF037417, AF258841, AF258842, AF483602, CY036854, AJ293920, DQ486029, DQ415286, DQ415287, DQ415288, AB443559, AB443560, CY037350

PB1: AF037418, AF037419, AF037420, AF037421, AF037422, AF037423, AF258822, AF258823, AF483601, AX350186, AY210279, AY210281, AY210282, AY210283, AY210284, CY003494, CY003502, CY003510, CY003518, CY003526, CY003534,

CY003542, CY003550, CY003558, CY003718, CY003726, CY003734, CY003742, CY003750, CY006050, CY006058, CY006105, CY006209, CY006313, CY006321, CY006329, CY006337, CY006345, CY006689, CY006761, CY006769, CY006857, CY006913, CY007977, CY008178, CY009010, CY009362, CY009642, CY033612, CY035204, CY035212, CY035220, CY035228, CY035236, CY036837, CY036853, CY036909, CY037349, CY038509, DQ415297, DQ415298, DQ415299, DQ487328, DQ508823, DQ508831, DQ508847, DQ508927, EU097778, EU097779, EU097780, EU097781, EU097782, EU097783, EU097800, U71128, U71129, U71130, U71131

M: AY210260, AY210263, AY210265, CY006684, CY006308, AY210267, AY210270, CY003553, CY007972, CY009005, CY003529, CY003497, CY006908, CY006045, CY003729, CY006764, K01140, DQ508828, CY006100, CY006204, CY003489, CY006053, CY006756, CY003721, CY006852, CY006316, CY003737, CY003745, CY006324, CY008173, CY003537, CY003505, CY003521, CY003545, CY003513, AF401293, L18999, DQ508836, CY033607, CY003713, CY006348, CY036904, CY009013, U65561, U65562, U65563, U65564, U65566, U65567, CY006332, CY006340, CY003753, AJ458339, U65573, U65574, U65576, U65577, U65568, U65569, U65565, AF038271, AF038272, AF038273, AF255369, EU597867, EU597868, EU597871, EU597873, EU597874, EU597876, EU597878, EU597879, EU597885, EU597887, EU597888, EU597890, EU597891, EU597897, EU597898, EU597899, EU597901, EU597904, EU597908, EU597909, EU597910, EU597912, EU597913, EU597914, EU597915, EU597919, EU597920, EU597921, EU597922, EU597924, EU597925, EU597926, AJ458305, AJ293925, AF386765, AF386767, AF386770, AF386771, EU597927, EU597928, EU597929, EU597932, EU597935, EU597938, EU597939, EU597940, EU597944, EU597945, EU597946, EU597947, EU597950, EU597951, EU597952, EU597953, EU597954, EU597955, EU597957, EU597958, EU597959, EU597964, EU597967, EU597969, EU597970, EU597971, EU597972, EU597973, EU597974, EU597978, EU597980, EU597986, EU597987, EU597988, EU597989, EU597990, EU597991, EU597992, EU597993, EU597995, EU597996, EU597998, EU597999, EU598002, EU598009, EU598010, EU598012, EU598013, EU598014, DQ249266, DQ415352, DQ415353, EU598016, EU598017, EU598018, EU598019, EU598021, EU598023, EU598024, EU598025, EU598031, EU598032, EU598033, EU598034, EU598035, EU598036, EU598038, EU598039, EU598040, EU598041, EU598042, EU598044, EU598045, AB281207, AB433834, AB433835, AB281194, AB281197, AB281199, AB281204, DQ849010

NS: AY210306, AY210307, AY210310, AY210311, CY006687, AY210312, AY210314, AY210315, CY003556, CY006311, CY007975, CY009360, CY009640, DQ508933, V01102, CY003532, CY009008, CY003500, CY006911, CY003732, CY006048, CY006767, DQ508829, CY003492, CY006207, CY006056, CY006759, CY003724, CY003740, CY006319, CY006855, CY003748, CY006327, CY008176, CY003508, CY003524, CY003540, DQ508853, CY003516, CY035202, DQ508837, CY035210, CY035218, CY035226, CY035234, CY036835, CY003716, CY033610, CY006351, CY009016, CY036907, CY003756, CY006335, CY006343, CY007839, U65670, AF038275, CY038507, U65671, U65672, U65673, U65674, AF038276, AF038277, AF038278, AF038279, AF256182, AF256183, CY036851, AJ293941,

AM502801, DQ487332, AB434123, AB434124, AM502797, CY037347, DQ415363, DQ415364, DQ415365, EF675055

Table 2.S1. Sites positively selected by FEL in HA clusters. A dash indicates no sites were found.

Cluster	Site	Epitope	p-value
BK79	-	-	-
SI87	186	B	0.09
BE89	-	-	-
BE92	138	A	0.09
	226	D	<0.01
WU95	-	-	-
SY97	-	-	-

Table 2.S2. Sites positively selected by FEL in all genes. A dash indicates no sites were found.

Protein	Site	p-value
HA	133	0.04
	135	0.01
	137	0.03
	145	0.02
	159	0.03
	226	<0.01
	262	0.05
NA	43	0.04
	120	<0.001
	370	0.01
NP	131	<0.01
	290	0.02
PA	-	-
PB2	-	-
PB1	-	-
M1	-	-
M2	16	0.02
	81	0.05
NS1	-	-
NS2	-	-

Figure 2.S1. Amino acid fixation events in a simulated and a real cluster. Top image shows simulated sequence evolution, and bottom shows replacements in the BE92 cluster. Colors indicate different amino acids; rows are sites. White areas show where no single amino acid is fixed at that site. The cluster was simulated from the model of Koelle et al. (2006) with the default parameters. Yellow circles show replacement events.

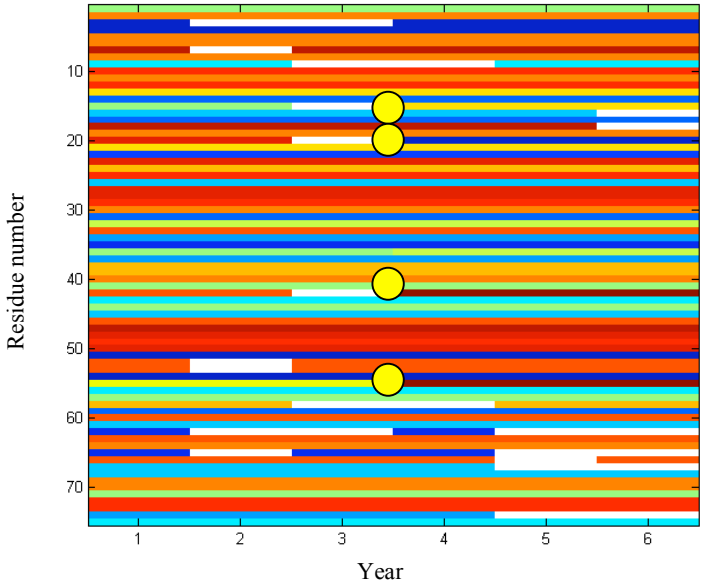

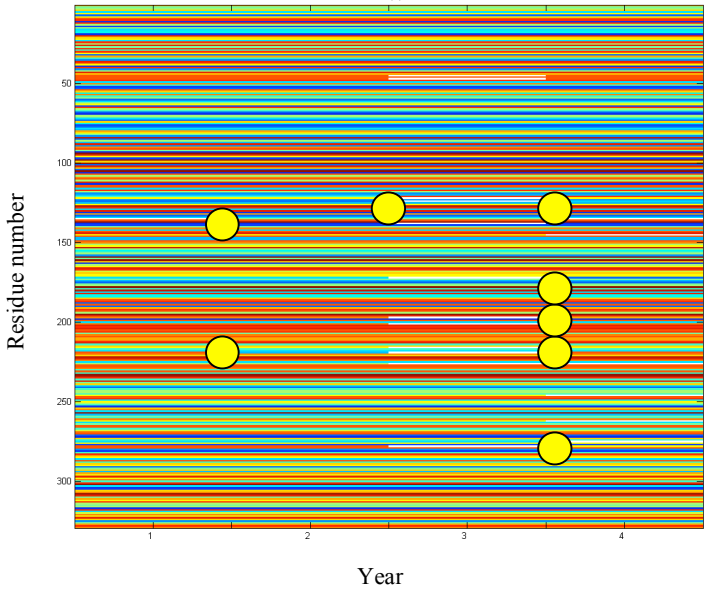

References

Abe, Y., Takashita, E., Sugawara, K., Matsuzaki, Y., Muraki, Y. & Hongo, S. 2004 Effect of the addition of oligosaccharides on the biological activities and antigenicity of influenza A/H3N2 virus hemagglutinin. *Journal of Virology* **78**, 9605-9611.

Abed, Y., Baz, M. & Boivin, G. 2006 Impact of neuraminidase mutations conferring influenza resistance to neuraminidase inhibitors in the N1 and N2 genetic backgrounds. *Antiviral Therapy* **11**, 971-976.

Baigent, S. J. & McCauley, J. W. 2001 Glycosylation of haemagglutinin and stalk-length of neuraminidase combine to regulate the growth of avian influenza viruses in tissue culture. *Virus Research* **79**, 177-185.

Blackburne, B. P., Hay, A. J. & Goldstein, R. A. 2008 Changing selective pressure during antigenic changes in human influenza H3. *PLoS Pathogens* **4**, e1000058.

Bragstad, K., Nielsen, L. & Fomsgaard, A. 2008 The evolution of human influenza A viruses 1999 to 2006: A complete genome study. *Virology Journal* **5**, 40.

Chen, R. B. & Holmes, E. C. 2008 The evolutionary dynamics of human influenza B virus. *Journal of Molecular Evolution* **66**, 655-663.

Coleman, J. R., Papamichail, D., Skiena, S., Futcher, B., Wimmer, E. & Mueller, S. 2008 Virus attenuation by genome-scale changes in codon pair bias. *Science* **320**, 1784-1787.

Ferguson, N. M., Galvani, A. P. & Bush, R. M. 2003 Ecological and immunological determinants of influenza evolution. *Nature* **422**, 428-433.

Fitch, W. M., Leiter, J. M. E., Li, X. & Palese, P. 1991 Positive Darwinian evolution in human influenza A viruses. *Proceedings of the National Academy of Sciences of the United States of America* **88**, 4270-4274.

Frank, A. L., Taber, L. H. & Wells, J. M. 1983 Individuals infected with two subtypes of influenza A virus in the same season. *The Journal of Infectious Diseases* **147**, 120-124.

Frost, S. D. W., Wrin, T., Smith, D. M., Pond, S. L. K., Liu, Y., Paxinos, E., Chappey, C., Galovich, J., Beauchaine, J., Petropoulos, C. J., Little, S. J. & Richman, D. D. 2005 Neutralizing antibody responses drive the evolution of human immunodeficiency virus type 1 envelope during recent HIV infection. *Proceedings of the National Academy of Sciences of the United States of America* **102**, 18514-18519.

Furuse, Y., Suzuki, A., Kamigaki, T. & Oshitani, H. 2009 Evolution of the M genes of the influenza A virus in different host species: large-scale sequence analysis. *Virology Journal* **6**.

Gallagher, P. J., Henneberry, J. M., Sambrook, J. F. & Gething, M. J. H. 1992 Glycosylation Requirements for Intracellular-Transport and Function of the Hemagglutinin of Influenza-Virus. *Journal of Virology* **66**, 7136-7145.

Gambaryan, A. S., Marinina, V. P., Tuzikov, A. B., Bovin, N. V., Rudneva, I. A., Sinitsyn, B. V., Shilov, A. A. & Matrosovich, M. N. 1998 Effects of host-dependent glycosylation of hemagglutinin on receptor-binding properties of H1N1 human influenza A virus grown in MDCK cells and in embryonated eggs. *Virology* **247**, 170-177.

Ghedin, E., Sengamalay, N. A., Shumway, M., Zaborsky, J., Feldblyum, T., Subbu, V., Spiro, D. J., Sitz, J., Koo, H., Bolotov, P., Dernovoy, D., Tatusova, T., Bao, Y., St. George, K., Taylor, J., Lipman, D. J., Fraser, C. M., Taubenberger, J. K. & Salzburg, S. L. 2005 Large-scale sequencing of human influenza reveals the dynamic nature of viral genome evolution. *Nature* **437**, 1162-1166.

Gill, P. W. & Murphy, A. M. 1977 Naturally acquired immunity to influenza tpe A: a further prospective study. *Medical Journal of Australia* **2**, 761-765.

Gill, P. W. & Murphy, A. M. 1985 Naturally Acquired-Immunity to Influenza Type-a - Lessons from 2 Coexisting Subtypes. *Medical Journal of Australia* **142**, 94-98.

Guindon, S. & Gascuel, O. 2003 A simple, fast, and accurate algorithm to estimate large phylogenies by maximum likelihood. *Systematic Biology* **52**, 696-704.

Guindon, S., Lethiec, F., Duroux, P. & Gascuel, O. 2005 PHYML Online - a web server for fast maximum likelihood-based phylogenetic inference. *Nucleic Acids Research* **33**, W557-W559.

Gultyaev, A. P., Heus, H. A. & Olsthoorn, R. C. L. 2007 An RNA conformational shift in recent H5N1 influenza A viruses. *Bioinformatics* **23**, 272-276.

Hasegawa, M., Kishino, H. & Yano, T. A. 1985 Dating of the Human Ape Splitting by a Molecular Clock of Mitochondrial-DNA. *Journal of Molecular Evolution* **22**, 160-174.

Ikemura, T. 1981 Choice of Synonymous Codon Is Constrained by the Availability of Transfer-Rnas. *Japanese Journal of Genetics* **56**, 533-555.

Ina, Y. & Gojobori, T. 1994 Statistical analysis of nucleotide sequences of the hemagglutinin gene of human influenza A viruses. *Proceedings of the National Academy of Sciences of the United States of America* **91**, 8388-8392.

Khan, M. W., Bucher, D. J., Koul, A. K., Kalish, G., Smith, H. & Kilbourne, E. D. 1982 Detection of antibodies to influenza virus M protein by an enzyme-linked immunosorbent assay. *Journal of Clinical Microbiology* **16**, 813-820.

Koelle, K., Cobey, S., Grenfell, B. & Pascual, M. 2006 Epochal evolution shapes the phylodynamics of interpandemic influenza. *Science* **314**, 1898-1903.

Kosakovsky Pond, S. L. & Frost, S. D. W. 2005a Datamonkey: rapid detection of selective pressure on individual sites of codon alignments. *Bioinformatics* **21**, 2531-2533.

Kosakovsky Pond, S. L. & Frost, S. D. W. 2005b Not so different after all: A comparison of methods for detecting amino acid sites under selection. *Molecular Biology and Evolution* **22**, 1208-1222.

Kosakovsky Pond, S. L., Frost, S. D. W. & Muse, S. V. 2005 HyPhy: hypothesis testing using phylogenies. *Bioinformatics* **21**, 676-679.

Kosakovsky Pond, S. L., Poon, A. F. & Frost, S. D. W. In press Estimating selection pressures on alignments of coding sequences. In *The Phylogenetic Handbook: A Practical Approach to DNA and Protein Phylogeny* (ed. M. Salemi & A.-M. Vandamme): Cambridge University Press.

Muse, S. V. & Gaut, B. S. 1994 A Likelihood Approach for Comparing Synonymous and Nonsynonymous Nucleotide Substitution Rates, with Application to the Chloroplast Genome. *Molecular Biology and Evolution* **11**, 715-724.

Nakagawa, N., Kubota, R., Maeda, A. & Okuno, Y. 2004 Influenza B virus Victoria group with a new glycosylation site was epidemic in Japan in the 2002-2003 season. *Journal of Clinical Microbiology* **42**, 3295-3297.

Nelson, M. I., Simonsen, L., Viboud, C., Miller, M. A. & Holmes, E. C. 2009 The origin and global emergence of adamantane resistant A/H3N2 influenza viruses. *Virology* **388**, 270-278.

Nelson, M. I., Viboud, C., Simonsen, L., Bennett, R. T., Griesemer, S. B., George, K. S., Taylor, J., Spiro, D. J., Sengamalay, N. A., Ghedin, E., Taubenberger, J. K. & Holmes, E. C. 2008 Multiple reassortment events in the evolutionary history of H1N1 influenza A virus since 1918. *PLoS Pathogens* **4**, e1000012.

Nylander, J. A. A. 2004 MrAIC.pl: Evolutionary Biology Centre, Uppsala University.

Plotkin, J. B. & Dushoff, J. 2003 Codon bias and frequency-dependent selection on the hemagglutinin epitopes of influenza A virus. *Proceedings of the National Academy of Sciences of the United States of America* **100**, 7152-7157.

Portela, A. & Digard, P. 2002 The influenza virus nucleoprotein: a multifunctional RNA-binding protein pivotal to virus replication. *Journal of General Virology* **83**, 723-734.

Rambaut, A., Pybus, O. G., Nelson, M. I., Viboud, C., Taubenberger, J. K. & Holmes, E. C. 2008 The genomic and epidemiological dynamics of human influenza A virus. *Nature* **453**, 615-620.

Russell, C. A., Jones, T. C., Barr, I. G., Cox, N. J., Garten, R. J., Gregory, V., Gust, I. D., Hampson, A. W., Hay, A. J., Hurt, A. C., de Jong, J. C., Kelso, A., Klimov, A. I., Kageyama, T., Komadina, N., Lapedes, A. S., Lin, Y. P., Mosterin, A., Obuchi, M., Odagiri, T., Osterhaus, A. D. M. E., Rimmelzwaan, G. F., Shaw, M. W., Skepner, E., Stohr, K., Tashiro, M., Fouchier, R. A. M. & Smith, D. J. 2008 The global circulation of seasonal influenza A (H3N2) viruses. *Science* **320**, 340-346.

Scapoli, C., De Lorenzi, S., Salvatorelli, G. & Barrai, I. 2007 Amino acid and codon use: in two influenza viruses and three hosts. *Medecine Et Maladies Infectieuses* **37**, 337-342.

Schotsaert, M., De Filette, M., Fiers, W. & Saelens, X. 2009 Universal M2 ectodomain-based influenza A vaccines: preclinical and clinical developments. *Expert Review of Vaccines* **8**, 499-508.

Shih, A. C. C., Hsiao, T. C., Ho, M. S. & Li, W. H. 2007 Simultaneous amino acid substitutions at antigenic sites drive influenza A hemagglutinin evolution. *Proceedings of the National Academy of Sciences of the United States of America* **104**, 6283-6288.

Skehel, J. J., Stevens, D. J., Daniels, R. S., Douglas, A. R., Knossow, M., Wilson, I. A. & Wiley, D. C. 1984 A Carbohydrate Side-Chain on Hemagglutinins of Hong-Kong Influenza-Viruses Inhibits Recognition by a Monoclonal-Antibody. *Proceedings of the National Academy of Sciences of the United States of America-Biological Sciences* **81**, 1779-1783.

Smith, D. J., Lapedes, A. S., de Jong, J. C., Bestebroer, T. M., Rimmelzwaan, G. F., Osterhaus, A. D. M. E. & Fouchier, R. A. M. 2004 Mapping the antigenic and genetic evolution of influenza virus. *Science* **305**, 371-376.

Suzuki, Y. 2006 Natural selection on the influenza virus genome. *Molecular Biology and Evolution* **23**, 1902-1911.

Suzuki, Y. 2008 Positive selection operates continuously on hemagglutinin during evolution of H3N2 human influenza A virus. *Gene* **427**, 111-116.
Thomas, P. G., Keating, R., Hulse-Post, D. J. & Doherty, P. C. 2006 Cell-mediated protection in influenza infection. *Emerging Infectious Diseases* **12**, 48-54.
Tria, F., Lassig, M., Peliti, L. & Franz, S. 2005 A minimal stochastic model for influenza evolution. *Journal of Statistical Mechanics-Theory and Experiment*, P07008.
Varich, N. L. & Kaverin, N. V. 2004 Antigenically relevant amino acid positions as revealed by reactions of monoclonal antibodies with the nucleoproteins of closely related influenza A virus strains. *Archives of Virology* **149**, 2271-2276.
Wagner, R., Wolff, T., Herwig, A., Pleschka, S. & Klenk, H. D. 2000 Interdependence of hemagglutinin glycosylation and neuraminidase as regulators of influenza virus growth: a study by reverse genetics. *Journal of Virology* **74**, 6316-6323.
Webster, R. G., Bean, W. J., Gorman, O. T., Chambers, T. M. & Kawaoka, Y. 1992 Evolution and Ecology of Influenza-A Viruses. *Microbiological Reviews* **56**, 152-179.
Wei, X. P., Decker, J. M., Wang, S. Y., Hui, H. X., Kappes, J. C., Wu, X. Y., Salazar-Gonzalez, J. F., Salazar, M. G., Kilby, J. M., Saag, M. S., Komarova, N. L., Nowak, M. A., Hahn, B. H., Kwong, P. D. & Shaw, G. M. 2003 Antibody neutralization and escape by HIV-1. *Nature* **422**, 307-312.
Wolf, Y. I., Viboud, C., Holmes, E. C., Koonin, E. V. & Lipman, D. J. 2006 Long intervals of stasis punctuated by bursts of positive selection in the seasonal evolution of influenza A virus. *Biology Direct* **1**, -.
Yang, Z. 1997 PAML: a program package for phylogenetic analysis by maximum likelihood. *Computer Applications in BioSciences* **13**, 555-556.
Yang, Z. H. & Nielsen, R. 2002 Codon-substitution models for detecting molecular adaptation at individual sites along specific lineages. *Molecular Biology and Evolution* **19**, 908-917.
Yang, Z. H., Wong, W. S. W. & Nielsen, R. 2005 Bayes empirical Bayes inference of amino acid sites under positive selection. *Molecular Biology and Evolution* **22**, 1107-1118.
Yu, X. C., Tsibane, T., McGraw, P. A., House, F. S., Keefer, C. J., Hicar, M. D., Tumpey, T. M., Pappas, C., Perrone, L. A., Martinez, O., Stevens, J., Wilson, I. A., Aguilar, P. V., Altschuler, E. L., Basler, C. F. & Crowe, J. E. 2008 Neutralizing antibodies derived from the B cells of 1918 influenza pandemic survivors. *Nature* **455**, 532-536.
Zhang, J. Z., Nielsen, R. & Yang, Z. H. 2005 Evaluation of an improved branch-site likelihood method for detecting positive selection at the molecular level. *Molecular Biology and Evolution* **22**, 2472-2479.
Zhang, M., Gaschen, B., Blay, W., Foley, B., Haigwood, N., Kuiken, C. & Korber, B. 2004 Tracking global patterns of N-linked glycosylation site variatio in highly variable viral glycoproteins: HIV, SIV, and HCV envelopes and influenza hemagglutinin. *Glycobiology* **14**, 1229-1246.
Zhou, T., Gu, W. J., Ma, J. M., Sun, X. & Lu, Z. H. 2005 Analysis of synonymous codon usage in H5N1 virus and other influenza A viruses. *Biosystems* **81**, 77-86.
Zhou, T. Q., Xu, L., Dey, B., Hessell, A. J., Van Ryk, D., Xiang, S. H., Yang, X. Z., Zhang, M. Y., Zwick, M. B., Arthos, J., Burton, D. R., Dimitrov, D. S., Sodroski,

J., Wyatt, R., Nabel, G. J. & Kwong, P. D. 2007 Structural definition of a conserved neutralization epitope on HIV-1 gp120. *Nature* **445**, 732-737.
Zuckerkandl, E. & Pauling, L. 1965 Molecules as Documents of Evolutionary History. *Journal of Theoretical Biology* **8**, 357-366.

Chapter 3

Cross-immunity and the dynamics of influenza A and B humans

Introduction

The threat of influenza to human health arises not only from the virus's complex ecological and evolutionary dynamics but also the relative obscurity with which it moves through human populations. Over long time scales, the diversity of influenza viruses is shaped by transmission with other host species (Webster et al. 1992), and over short time scales by patterns of global circulation (Rambaut et al. 2008; Russell et al. 2008). In both situations, competition between strains for susceptible hosts regulates influenza diversity. The primary driver of its evolution appears to be escape from host antibodies, but the tempo of this escape, the ultimate constraints on antigenic shapes available, and the contributions of different genes to fitness are not clear. The biggest obstacle to testing hypotheses about influenza remains the fact that the vast majority of its population dynamics are recorded indirectly. One result is that the epidemiological community still has little ability to predict the consequences of introducing H5N1 or an antigenically novel strain of H1N1 into the human population, much less what type or subtype may predominate in the next season.

We present here novel analysis of the most accurate and lengthy observations to date of influenza's three major phenotypes—influenza B and influenza A, which includes subtypes H3N2 and H1N1—collected over two decades from the population of present-day St. Petersburg, Russia (figure 3.1a). We use these observations to fit simple epidemiological models to each of the three strains, yielding information about the strains' different reproductive rates and the rates of antigenic evolution. An important question is whether variation in strain prevalence from year to year arises from strain-

specific dynamics alone or whether subtypes or types are also in competition with each other. Interference between H3N2 and B has been suggested previously from observations of alternating dominance between seasons (Ferguson et al. 2003). Heterosubtypic cross-immunity within influenza A is suggested by historical patterns of subtype replacement in humans (Earn et al. 2002; Epstein 2006; Ferguson et al. 2003; Monto & Kendal 1973) and laboratory and challenge experiments in animals (Benton et al. 2001; Boon et al. 2004; Heinen et al. 2001; Kurimura et al. 1973; Liang et al. 1994; Smirnov et al. 1999; Van Reeth et al. 2004). Our results suggest cross-immunity between H3N2 and influenza B and possibly other pairs. There might be some potential for predictability in influenza's dynamics from season to season at the level of types or subtypes.

Methods

Data

We analyzed monthly counts of serologically confirmed cases of influenza A H3N2 and H1N1 and influenza B among patients hospitalized for advanced respiratory disease in St. Petersburg, Russia (then Leningrad, USSR). Data were aggregated from adult and children's hospitals by the Research Institute of Influenza in St. Petersburg and have been described previously (Karpova et al. 2006). The hospitals' policy throughout this period was to attempt to obtain paired serological samples from all patients. The first sample was obtained upon admission and the second upon discharge. A confirmed case of a strain was defined as a fourfold or greater increase in antibody titer to that strain. Though data exist through 2004, we restrict our observations to avoid unknown but potentially dramatic changes in host behavior and sampling methods that may have accompanied the fall of the Soviet Union in December 1991. We analyze only the subset spanning January 1969 to June of 1991, though data are missing for 1971. Our model is ultimately fit to 757 observations (259 for H3N2, 259 for B, and 163 for H1N1) at 259 unique times.

Model

Our fitted model has two components: a process model and a measurement model. The process model is a mechanistic representation of the underlying disease dynamics. The measurement model describes how observations are generated from the dynamics. After describing both components in detail below, we outline the procedure used to fit the full model.

Process model

The disease dynamics are represented by a set of coupled stochastic differential equations. We track the number of hosts susceptible (*S*), infected (*I*), and recovered (*R*) to each strain *i*, where $i \in \{\text{H3N2, B, H1N1}\}$.

$$\frac{dS_i}{dt} = B(t)N + \gamma_i R_i - \frac{S_i}{N}\sum_j \sigma_{ij}\left[\beta_j(t)\xi_j(t)I_j + m\right] - D(t)S_i \tag{4.1a}$$

$$\frac{dI_{i,1}}{dt} = \frac{S_i}{N}\left[\beta_i(t)\xi_i(t)I_i + m\right] - \nu_i I_{i,1} - D(t)I_{i,1} \tag{4.1b}$$

$$\frac{dI_{i,2}}{dt} = \nu_i I_{i,1} - \nu_i I_{i,2} - D(t)I_{i,2} \tag{4.1c}$$

…

$$\frac{dR_i}{dt} = \nu_i I_{i,4} + \frac{S_i}{N}\sum_{j\neq i} \sigma_{ij}\left[\beta_j(t)\xi_j(t)I_j + m\right] - \gamma_i R_i - D(t)R_i \tag{4.1d}$$

$$\beta_i(t) = \beta_i\left[1 + \varepsilon\cos(2\pi t)\right] \tag{4.1e}$$

$$S_i + I_i + R_i = N \tag{4.1f}$$

The number of individuals susceptible to strain *i* increases with births and loss of immunity and decreases with deaths and infections; the infections may be with strain *i* or other strains *j* that share some cross-immunity with *i.* Monthly per capita birth and death rates, $B(t)$ and $D(t)$, were inferred from splines fitted to annual data for the city of St.

Petersburg (Karpova 2004)(figure 3.1b). The rate of loss of immunity, γ_i, is strain-specific and constant in time.

The rate at which individuals susceptible to *i* acquire infection with *i* depends on strain-specific, seasonally varying transmission rate, $\beta_i(t)$ (equation 4.1e), to which we add a strain-specific gamma noise term, $\xi_i(t) = \xi_i / \Delta t$, to capture stochastic changes in antigenicity,

$$\xi_i \sim \Gamma(\text{shape} = \Delta t/\phi_i \text{ , scale} = \phi_i). \qquad (4.3)$$

Since confirmed influenza cases in St. Petersburg consistently peak in winter, we force $\beta_i(t)$ with a sinusoidal function whose maxima are fixed on January 1 and whose amplitude, ε, is shared by all strains. Finally, we allow a small, constant rate of immigration *m* that ensures frequent reseeding of locally extinct strains. We set this rate to be approximately 8.3 y^{-1}, meaning a susceptible, on average, contacts an infected person from outside St. Petersburg once every eight years.

Individuals susceptible to *i* can also leave the susceptible class from infection with related strain *j*. The infection rate with strain *j* is analogous to infection with strain *i*, except that rather than becoming infectious with strain *j* (which does happen, but is tracked by dS_j/dt and dI_j/dt) individuals can become immune to *i*. The status-based approach assumes that cross-immunity is polarizing (Gog & Swinton 2002): Rather than all individuals infected with strain *j* developing a slight reduction in susceptibility to *i*, some fraction σ_{ij} of individuals infected with *j* become completely immune to *i* (i.e., transition directly from S_i to R_i) while the others remain susceptible to *i*. In this model, cross-immunity is symmetric, $\sigma_{ij} = \sigma_{ji}$.

Individuals infected with strain *i* transition sequentially and at a constant, strain-specific rate ν_i through four compartments, $I_{i,1} \ldots I_{i,4}$. (We use I_i to refer to the sum of all individuals across these compartments.) The total rate of recovery is thus given by $\nu_i/4$. Using multiple compartments allows a more realistic duration of infection; the single-compartment model ($I_i = I_{i,1}$) gives an exponential distribution of waiting times, whereas

the four-compartment model yields a four-category gamma distribution that better matches empirical observations (Carrat et al. 2008).

The transitions between states are modeled stochastically as whole numbers of individuals. The model thus incorporates demographic stochasticity and allows for local extinctions. Simulations occur in discrete time with a step size of one day.

Measurement model

If all infections resulted in perfectly observed hospitalizations, simulated monthly cases for each strain i would equal the total number of $S_i \rightarrow I_{i,1}$ transitions of that month, C_i. The observed cases in the data are confirmed new hospitalizations with each strain i. We thus introduce a strain-specific hospitalization rate, h_i. We assume the number of observed cases is drawn from a negative binomial distribution with mean $h_i C_i$ and a strain-specific dispersion parameter, d_i. The simulated observations, Y_i, are thus given by

$$Y_i \sim \text{negative binomial}(h_i C_i, d_i). \tag{4.4}$$

Since the negative binomial distribution can be derived from a Poisson distribution with nonstationary mean, it is well-suited for data in which sampling effort or virulence may have changed over time, but in which more complicated functions might lead to overfitting.

Fitting algorithm and heuristics

To fit the parameters, we use a flexible method for maximum likelihood estimation of partially observed, nonlinear dynamical systems (Ionides et al. 2006). The method iteratively filters a particle population over the set of observations. Each particle represents a possible numerical solution (i.e., set of parameter values, including initial values of the state variables) to the model. With a sufficiently large particle population and appropriate exploration and cooling parameters, this method has been shown

theoretically to converge on the MLE (Ionides et al. 2006). In practice, it has yielded plausible results for a single-strain system (King et al. 2008).

In applying this method, we make minimal assumptions about our parameters. In addition to the known birth and death rates and the fixed immigration rate m, we force $I_{H1N1} = 0$ at the beginning of the simulation (January, 1969) and introduce it through immigration in October of 1977. We also begin the simulation with total population size $N = 3{,}859{,}358$, obtained from Soviet census data. Between 1969 and 1977, individuals that start the simulation recovered to H1N1 do not lose their immunity, except through death. This assumption is in keeping with the observations that H1N1 was extinct in humans between 1957 and 1977, that the 1977 strain showed minimal genetic distinction from a strain in 1950 (Scholtissek et al. 1978), and that people are capable of maintaining strong neutralizing antibody responses to H1N1 strains decades after exposure (Kendal et al. 1979; Yu et al. 2008).

Results

Assuming no cross-immunity between the strains yields a R_0 of 8.6 for H3N2, 3.4 for influenza B, and 9.4 for H1N1 (table 3.1). The seasonal forcing ε is approximately 0.13, and thus the R_0 of all strains exceeds one throughout the year. Hosts' durations of immunity are shortest in B (~1.25 years) and longer in H3N2 and H1N1 (~3 years). Hospitalization rates per infected are greatest in H3N2 ($h_{\mathrm{H3N2}} = 1.3 \cdot 10^{-3}$) and approximately half as large in B and H1N1, and the inferred distributions are overdispersed ($2.6 < d_i < 4.0$). Immunity levels in 1969 were highest to H1N1, next highest to H3N2, and third highest to influenza B.

The model with cross-immunity had significantly higher likelihood (table 3.1). The best fit reported cross-immunity of roughly 0.76 between H3N2 and influenza B and cross-immunities of 0.36 between H3N2 and H1N1 and 0.39 between B and H1N1. Compared to the null model, values of R_0 were generally lower (4.1 for H3N2, 5.2 for B, and 6.5 for H1N1) and hospitalization rates were higher ($0.49 \cdot 10^{-3} – 2.5 \cdot 10^{-3}$) and generally less overdispersed ($2.3 < d_i < 6.1$). The durations of immunity were shorter, roughly 1.6 to 2 years, and not correlated in an obvious way to R_0. Initial values of the

state variables were similar to the null model's for H3N2 and H1N1, though initial immunity levels were higher for influenza B. The seasonal forcing parameter ε was almost identical to that of the null model. In most simulations with the fitted parameters, H1N1 was unable to invade or appeared after the 1977-1978 season (figure 3.2).

Discussion

We analyzed time series of serologically confirmed hospitalizations in St. Petersburg, Russia, over two decades to obtain basic information about the epidemiologic rates of influenza A H3N2, H1N1, and influenza B. We also sought to determine whether there was dynamical evidence of cross-immunity between types or subtypes. When we fit a model that assumes all strains have independent dynamics, except for shared seasonal forcing and a very low immigration rate, the results yield high values of R_0 and low rates of antigenic evolution in H1N1 and H3N2 and a much lower R_0 and higher rate of antigenic evolution in influenza B. This result suggests identifiability problems between a strain's R_0 and its rate of antigenic evolution. The model without cross-immunity outperformed the model with cross-immunity, inferring lower values of R_0 and smaller differences among the strains. Simulations from this model frequently do not allow invasion by H1N1, however. Its performance nonetheless suggests some basis for believing some degree of cross-immunity is likely, especially between H3N2 and B, but more investigation is necessary.

The model without cross-immunity is consistent with other estimates of hospitalization and mutation rates, though its predictions for R_0 are slightly high. Typical hospitalization rates for the general population in the U.S. have been estimated at 108 per 100,000 among children less than five years old and 20 per 100,000 person-years for children between 2 and 5 years old [reviewed in Fiore et al. (2008)]. With a 10% annual attack rate (Cauchemez et al. 2008), the per-case hospitalization rate would be on the order of 10^{-3} for the general population. The differences inferred in hospitalization rates between strains echo differences in observed mortality rates, which are generally lower for H1N1 and B than H3N2 (Fiore et al. 2008). Mutation and substitution rates are higher in influenza A than B viruses (Nobusawa & Sato 2006), and antigenic evolution is faster

in H3N2 than H1N1 (Rambaut et al. 2008). Epidemic- and season-specific reproductive numbers are more commonly estimated than direct estimates of R_0, and the majority suggest a seasonal reproductive number between 1 and 2 (table 3.S1). Direct estimates of the R_0 of H1N1 (Mills et al. 2004) and H3N2 (Gani et al. 2005) are lower than those reported here. The reproductive number of influenza B does not appear to have been estimated before. Time series of deaths to influenza-like illness from before 1957 suggest that the R_0 of influenza B is on par with that of H1N1 [e.g., Viboud et al. (2006b)].

Though this model may be considered large for containing 24 parameters (including initial values), it makes simplifying assumptions that might be important for understanding the dynamics of seasonal influenza. Probably the most important of these assumptions involve the nature of antigenic evolution and the effects of host age. Abrupt changes in antigenicity that cause spikes in incidence have been observed in H3N2 (Greene et al. 2006; Smith et al. 2004) and attributed to epochal evolution (Koelle et al. 2006). It is not clear, however, clear whether antigenic innovations should be represented by stochastic fluctuations in the rate of loss of immunity instead of the rate of transmission. A serial SIR formulation that represents the major antigenic variants within each subtype independently may be more appropriate (Koelle et al. 2009).

The data also reveal striking patterns in attack rates of each type and subtype by age (figure 3.S1), suggesting that an age-structured model might be useful in disentangling parameters. H3N2 and B show years of alternating dominance in adults, but years in which H3N2 dominates in adults also show inordinate spikes in prevalence in infants and young children. In contrast, the prevalence of B in infants and young children shows less intraannual and interannual variability, whereas older children show interannual oscillations similar to adults. H1N1, unlike H3N2 and B, does not show substantial variation in prevalence from year to year, and it is rarely the most common strain among ILI hospitalizations in any season.

These trends have not yet been quantitatively analyzed with more complex models. Nonetheless, our results so far suggest a (still highly speculative) qualitative explanation. Abrupt antigenic changes should be associated with a sudden loss of immunity independent of host age (Cobey & Koelle 2008). Punctuated antigenic

innovations in H3N2 could thus explain why spikes in prevalence appear simultaneously in all age classes, including infants (whose maternal antibodies to H3N2 will also fail). Some combination of more gradual antigenic change and potentially reduced R_0 of influenza B and H1N1 account for the higher average age of infection and the lack of synchronous spikes across age classes. Years in which influenza B dominates in adults thus would not result from significant antigenic change in B (which would cause a large outbreak in children) but from transiently reduced competition with H3N2. Others have suggested that competition could account for recent variation in dominance between H3N2 and H1N1 (Ferguson et al. 2003; Rambaut et al. 2008; Wolf et al. 2006).

This model makes assumptions about cross-immunity that are not necessarily justified or relevant to current dynamics. We assume that cross-immunity between heterologous types or subtypes is symmetric, though there is evidence that cross-immunity between strains of a single subtype can be asymmetric (Underwood 1980). Future work could include fitting a model for each directed pairwise interaction. Since strain-specific antibodies are the main selective pressure driving the evolution of H3N2 and presumably B (Chen & Holmes 2008; Shen et al. 2009) and H1N1 (Raymond et al. 1983) [but see Nelson et al. (2008) and Chen & Holmes (2008) for evidence that selection on whole reassorted genomes may be important], our model also assumes permanent strain-specific immunity. However, others have suggested the possibility of transient, strain-transcending immunity, which might be mediated by cellular immunity (Ferguson et al. 2003). The strength, specificity, and kinetics of T-cell responses are not well understood, but this might be an alternative or additional mechanism through which cross-immunity acts. We might also expect cross-immunity to change over longer time scales: strains that do not share common epitopes should have a selective advantage over those that do. Thus, cross-immunity might have existed between H3N2 and B in the 1970s but not in the 1980s or presently.

The complexity of the dynamics that can be generated by an interacting three-strain, seasonally forced disease is formidable. Because even an single, seasonally forced SIRS model can generate chaos, and the starting conditions in 1969 are not well known, the conclusions that can be inferred from a single time series are inherently limited. Supplementing this analysis with time series from other locations, information on hosts'

immune statuses, quantitative measures of antigenic change, and especially specific hypotheses about possible mechanisms of cross-immunity should lead to the development of predictive models and better insights for managing influenza.

Figure 3.1. Hospitalizations with serologically confirmed influenza and interpolated birth and death rates.

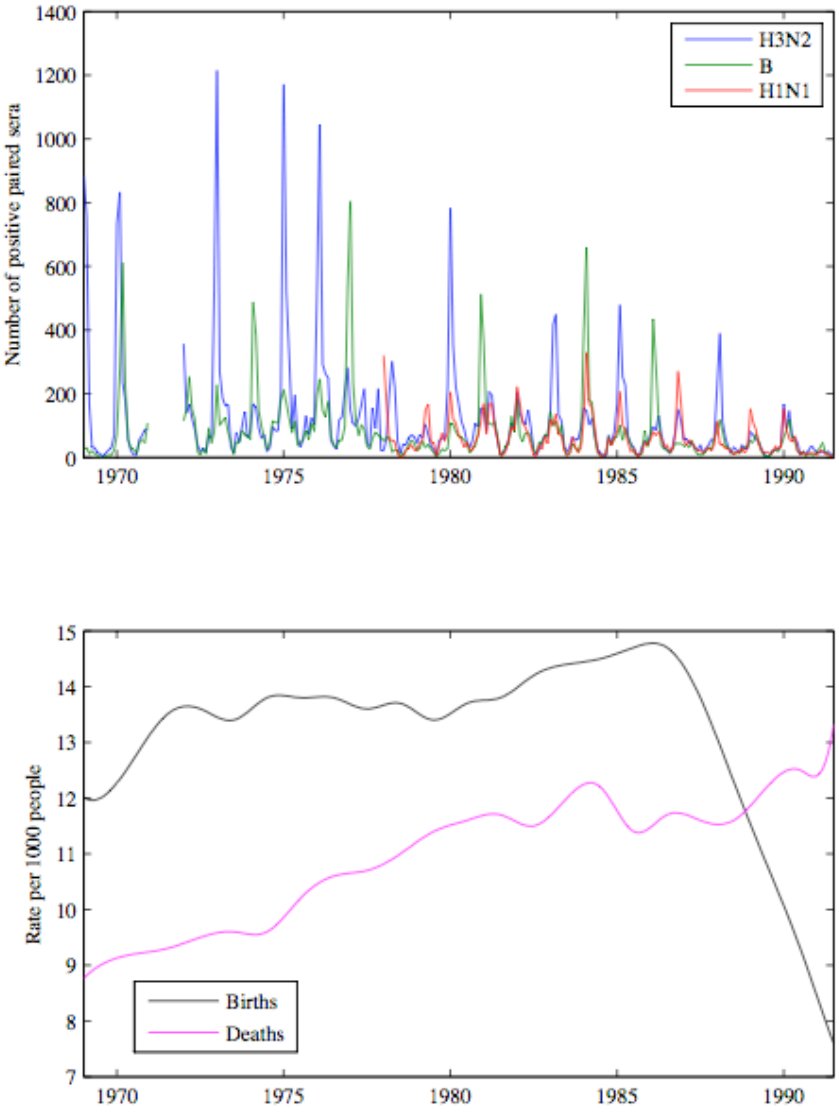

Figure 3.2. Simulated time series from the fit of the model with cross-immunity. In this simulation, H1N1 invades a season later than in the observed time series.

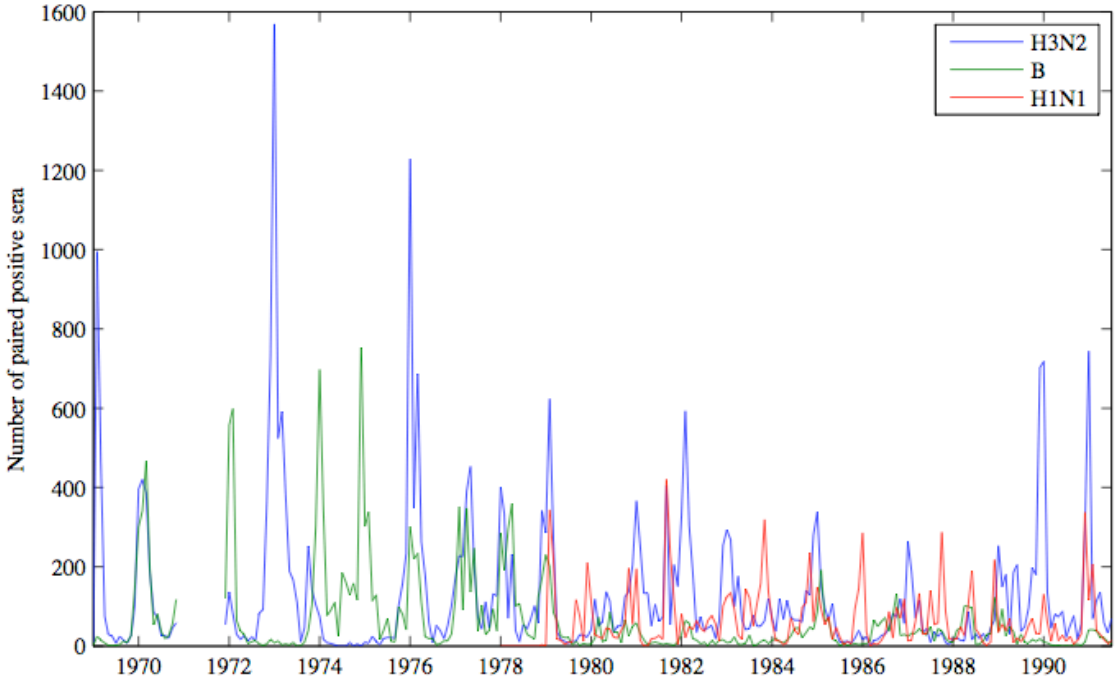

Table 3.1. Fitted parameters in models with and without cross-immunity.

	No cross-immunity	Cross-immunity
Log likelihood		
ε	0.13	0.14
$\sigma_{H3N2,B}$	-	0.75
$\sigma_{H3N2,H1N1}$	-	0.36
$\sigma_{B,H1N1}$	-	0.39
H3N2		
R_0	8.6	4.1
γ	0.32 y^{-1}	0.61 y^{-1}
ϕ	0.15	0.068
h	$1.3 \cdot 10^{-3}$ y^{-1}	$2.5 \cdot 10^{-3}$ y^{-1}
d	3.2	5.3
S(0)/N(0)	0.12	0.17
I(0)/N(0)	0.20	0.13
R(0)/N(0)	0.68	0.60
B		
R_0	3.4	5.2
γ	0.79 y^{-1}	0.48 y^{-1}
ϕ	0.055	0.090
h	$0.49 \cdot 10^{-3}$ y^{-1}	$1.6 \cdot 10^{-3}$ y^{-1}
d	2.6	6.1
S(0)/N(0)	0.17	0.09
I(0)/N(0)	0.17	0.04
R(0)/N(0)	0.66	0.87
H1N1		
R_0	9.4	6.5
γ	0.29 y^{-1}	0.58 y^{-1}
ϕ	0.20	0.098
h	$0.74 \cdot 10^{-3}$ y^{-1}	$0.49 \cdot 10^{-3}$ y^{-1}
d	4.0	2.3
S(0)/N(0)	0.08	0.06
R(0)/N(0)	0.92	0.95

Supplementary material

As this method is still relatively new, we briefly summarize heuristics that were more and less useful for fitting. For each of the models with and without cross-immunity, we first performed a sweep of approximately one million points in parameter space, filtering once at each point with only a small number of particles. We then started two sets of larger populations (of initially 10^4 particles each) at the forty best points. Each set was assigned a different standard deviation in their random walks (standard deviation of 0.05 or 0.1) and high between-iteration variance (variance factor = 1.3) in attempt to find a compromise between speed and accuracy. In rugged areas, populations with a standard deviation of 0.1 could actually lose information and begin declining in likelihood. In smoother areas, these populations were able to climb dramatically faster than populations with a random walk of 0.05. However, since many of the populations' trajectories pass through rugged areas, the best long-term strategy is probably to allow populations to climb slowly with a small standard deviation. The density of the particle population is also critically important and interacts with the standard deviation of the random walk. Information is more easily lost when Monte Carlo error (from demographic stochasticity of the particles) is high. Some of the effects of large standard deviation can thus be ameliorated by substantially increasing the population size. Developing an algorithm that incorporates an adaptive standard deviation and/or particle density might be a useful means to increase efficiency.

We allowed populations to climb without cooling for 300-400 iterations and then slowly cooled for 200-250 iterations with a lower between-iteration variance (cooling parameter = 0.995, variance factor = 1.1). Beyond using multiple standard deviations, we found no advantage to replicating the iterations, as populations' trajectories through parameter space were similar. However, all trajectories had not converged by the end of our procedure, demonstrating that our MLEs are effectively local and that our heuristics can be refined. Especially for the model with cross-immunity, 10^4 particles is probably too few. While this density was sufficient in some parts of parameter space, the large Monte Carlo error in others probably distorted its trajectory. Future work will focus on fitting with larger particle densities (30,000 and higher) and small-deviation random walks (0.05 and below). In addition, it is probably advantageous to restrict the flexibility

of the measurement model, specifically by bounding the dispersion parameter. Final confirmation of maxima will of course require extensive likelihood profiling.

Table 3.S1. Values of influenza's intrinsic reproduction number, R_0, and effective reproduction number, R_p, inferred by other studies. R_0 measures the expected number of secondary cases in an entirely susceptible population. R_p measures the expected number of secondary cases at the beginning of an epidemic, assuming some level of immunity in the population. If the strains are "mixed," then the study did not infer quantitative, type- or subtype-specific estimates of R_0 or R_p. ILI = outpatient visits with influenza-like illness; P&I = pneumonia and influenza.

R_0 (R_p)	Strain(s)	Time	Location	Data	Reference
Interpandemic influenza					
(1.3)	Mixed	1972-2002	United States	P&I and influenza-specific mortality	Chowell et al. (2008)
(1.3)		1972-1997	France		
(1.2, 1.3)		1972-1997	Australia		
(2.0)	H1N1	1951	Large cities in England	Influenza-specific mortality	Viboud et al. (2006b)
(2.2)			Liverpool		
(2.1)			Canada	Influenza-specific mortality and ILI	
(1.2-1.8)	H1N1 and B	Seven severe seasons between 1921 and 1944	England and Wales	Influenza-specific mortality	
1.4-1.7	Mixed	1985-2006	France	ILI	Cauchemez et al. (2008)
(1.5)	H3N2	1984-1985	France	ILI	Flahault et al. (1988)
Pandemic influenza					
2.9-3.9 (2-3)	H1N1	1918	45 U.S. cities	P&I mortality	Mills et al. (2004)
1.4-2.8	H1N1	1918	23 U.S. cities	P&I mortality	Bootsma & Ferguson (2007)
(2.0-5.4)	H1N1	1918 (summer wave)	Copenhagan Gothenberg, Oslo, and Stockholm	ILI, influenza and total hospitalizations	Andreasen et al. (2008)
(1.2-1.8)		1918 (fall wave)	Copenhagan	ILI, influenza and total hospitalizations, excess respiratory and all-cause deaths	
1.5	H1N1	1918 (summer wave)	Geneva	Hospitalizations with flu-like illnesses	Chowell et al. (2006)
(3.8)		1918 (fall wave)			

Table 3.S1. (continued)

R_0 (R_p)	Strain(s)	Time	Location	Data	Reference
(2.1)	H1N1	1918	England and Wales	Influenza-specific mortality	Viboud et al. (2006a)
(1.5)	H2N2	1957			
(1.8)	H3N2	1968			
2.0	H1N1	1918 (spring wave)	England and Wales	Clinical and serological attack rates	Gani et al. (2005)
1.6		1918 (fall wave)			
1.7		1918 (winter wave)			
1.7	H2N2	1957			
2.2	H3N2	1968			

Figure 3.S1. Hospitalizations confirmed influenza, by host age.

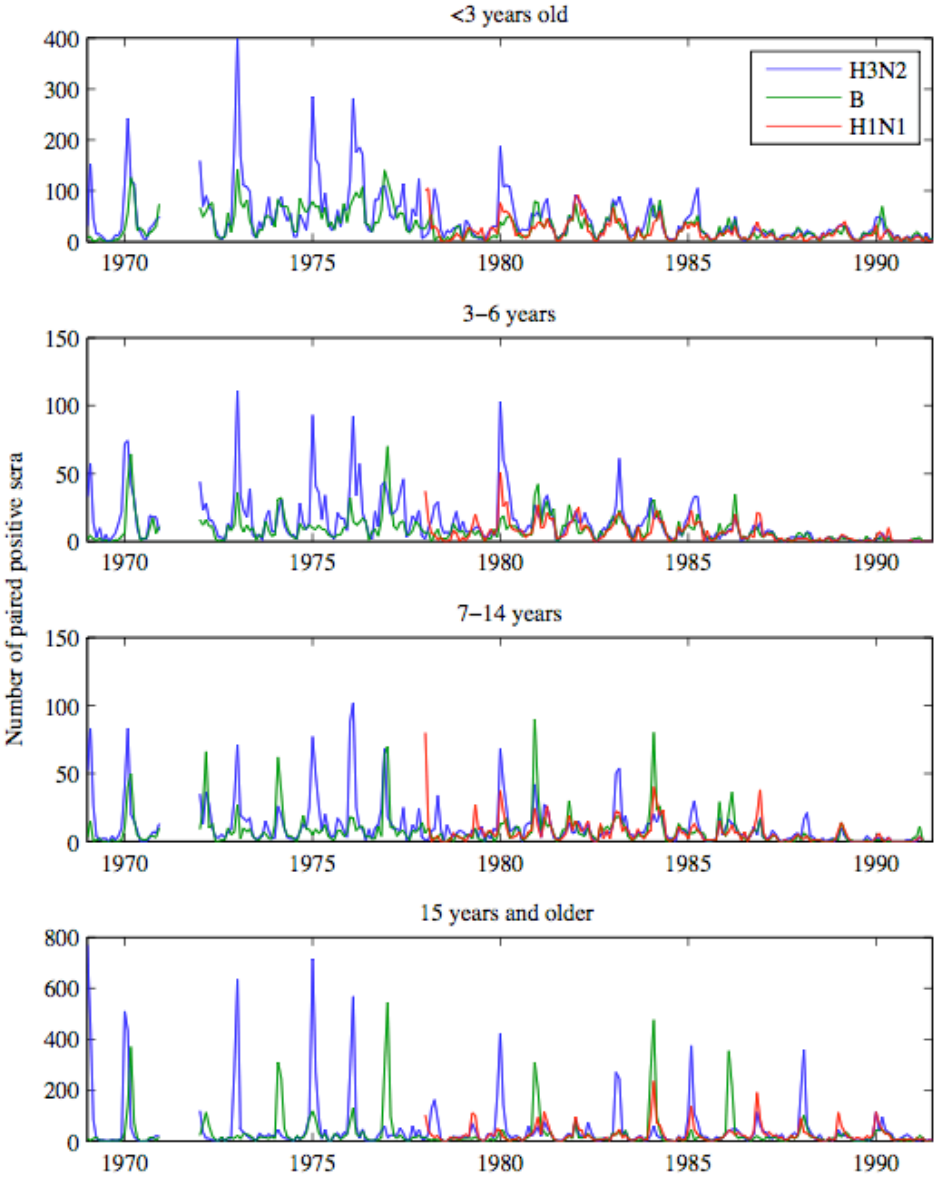

References

Andreasen, V., Viboud, C. & Simonsen, L. 2008 Epidemiologic characterization of the 1918 influenza pandemic summer wave in Copenhagen: Implications for pandemic control strategies. *Journal of Infectious Diseases* **197**, 270-278.

Benton, K. A., Misplon, J. A., Lo, C. Y., Brutkiewicz, R. R., Prasad, S. A. & Epstein, S. L. 2001 Heterosubtypic immunity to influenza A virus in mice lacking IgA, all Ig, NKT cells, or gamma delta T cells. *Journal of Immunology* **166**, 7437-7445.

Boon, A. C. M., de Mutsert, G., van Baarle, D., Smith, D. J., Lapedes, A. S., Fouchier, R. A. M., Sintnicolaas, K., Osterhaus, A. D. M. E. & Rimmelzwaan, G. F. 2004 Recognition of homo- and heterosubtypic variants of influenza A viruses by human CD8(+) T lymphocytes. *Journal of Immunology* **172**, 2453-2460.

Bootsma, M. C. J. & Ferguson, N. M. 2007 The effect of public health measures on the 1918 influenza pandemic in US cities. *Proceedings of the National Academy of Sciences of the United States of America* **104**, 7588-7593.

Carrat, F., Vergu, E., Ferguson, N. M., Lemaitre, M., Cauchemez, S., Leach, S. & Valleron, A. J. 2008 Time lines of infection and disease in human influenza: A review of volunteer challenge studies. *American Journal of Epidemiology* **167**, 775-785.

Cauchemez, S., Valleron, A. J., Boelle, P. Y., Flahault, A. & Ferguson, N. M. 2008 Estimating the impact of school closure on influenza transmission from Sentinel data. *Nature* **452**, 750-U6.

Chen, R. B. & Holmes, E. C. 2008 The evolutionary dynamics of human influenza B virus. *Journal of Molecular Evolution* **66**, 655-663.

Chowell, G., Ammon, C. E., Hengartner, N. W. & Hyman, J. M. 2006 Transmission dynamics of the great influenza pandemic of 1918 in Geneva, Switzerland: Assessing the effects of hypothetical interventions. *Journal of Theoretical Biology* **241**, 193-204.

Chowell, G., Miller, M. A. & Viboud, C. 2008 Seasonal influenza in the United States, France, and Australia: transmission and prospects for control. *Epidemiology and Infection* **136**, 852-864.

Cobey, S. & Koelle, K. 2008 Capturing escape in infectious disease dynamics. *Trends in Ecology & Evolution* **23**, 572-577.

Earn, D. J. D., Dushoff, J. & Levin, S. A. 2002 Ecology and evolution of the flu. *Trends in Ecology & Evolution* **17**, 334-340.

Epstein, S. L. 2006 Prior H1N1 influenza infection and susceptibility of Cleveland Family Study participants during the H2N2 pandemic of 1957: An experiment of nature. *Journal of Infectious Diseases* **193**, 49-53.

Ferguson, N. M., Galvani, A. P. & Bush, R. M. 2003 Ecological and immunological determinants of influenza evolution. *Nature* **422**, 428-433.

Fiore, A. E., Shay, D. K., Broder, K., Iskander, J. K., Uyeki, T. M., Mootrey, G., Bresee, J. S. & Cox, N. J. 2008 Prevention and control of influenza: Recommendations of the advisory committee on immunization practices (ACIP), 2008. *Morbidity and Mortality Weekly Report* **57**, 1-60.

Flahault, A., Letrait, S., Blin, P., Hazout, S., Menares, J. & Valleron, A. J. 1988 Modeling the 1985 Influenza Epidemic in France. *Statistics in Medicine* **7**, 1147-1155.

Gani, R., Hughes, H., Fleming, D., Griffin, T., Medlock, J. & Leach, S. 2005 Potential impact of antiviral drug use during influenza pandemic. *Emerging Infectious Diseases* **11**, 1355-1362.

Gog, J. R. & Swinton, J. 2002 A status-based approach to multiple strain dynamics. *Journal of Mathematical Biology* **44**, 169-184.

Greene, S. K., Ionides, E. L. & Wilson, M. L. 2006 Patterns of influenza-associated mortality among US elderly by geographic region and virus subtype, 1968-1998. *American Journal of Epidemiology* **163**, 316-326.

Heinen, P. P., de Boer-Luijtze, E. A. & Bianchi, A. T. J. 2001 Respiratory and systemic humoral and cellular immune responses of pigs to a heterosubtypic influenza A virus infection. *Journal of General Virology* **82**, 2697-2707.

Ionides, E. L., Breto, C. & King, A. A. 2006 Inference for nonlinear dynamical systems. *Proceedings of the National Academy of Sciences of the United States of America* **103**, 18438-18443.

Karpova, L. S. 2004 Social and ecological aspects of the epidemiological dynamics of influenza and advanced respiratory diseases in children (in Russian). In *Research Institute of Influenza*, vol. Ph.D., pp. 46. Saint Petersburg: Russian Academy of Medicine.

Karpova, L. S., Marinich, I. G. & Krainova, T. I. 2006 Etiology of influenza according to the data of serological diagnostics in hospital patients in St. Petersburg at the period of 1968-2000. *Zhurnal Mikrobiologii Epidemiologii i Immunobiologii*, 41-45.

Kendal, A. P., Joseph, J. M., Kobayashi, G., Nelson, D., Reyes, C. R., Ross, M. R., Sarandria, J. L., White, R., Woodall, D. F., Noble, G. R. & Dowdle, W. R. 1979 Laboratory-Based Surveillance of Influenza-Virus in the United-States During the Winter of 1977-1978 .1. Periods of Prevalence of H1n1 and H3n2 Influenza-a Strains, Their Relative Rates of Isolation in Different Age-Groups, and Detection of Antigenic Variantso. *American Journal of Epidemiology* **110**, 449-461.

King, A. A., Ionides, E. L., Pascual, M. & Bouma, M. J. 2008 Inapparent infections and cholera dynamics. *Nature* **454**, 877-880.

Koelle, K., Cobey, S., Grenfell, B. & Pascual, M. 2006 Epochal evolution shapes the phylodynamics of interpandemic influenza. *Science* **314**, 1898-1903.

Koelle, K., Kamradt, M. & Pascual, M. 2009 Understanding the dynamics of rapidly evolving pathogens through modeling the tempo of antigenic change: Influenza as a case study. *Epidemics* **1**, 129-137.

Kurimura, T., Hirano, A. & Okuno, Y. 1973 Cross immune reactions between A(H1N1) and A(H2N2) influenza viruses. *Biken journal* **16**, 51-56.

Liang, S. H., Mozdzanowska, K., Palladino, G. & Gerhard, W. 1994 Heterosubtypic Immunity to Influenza Type-a Virus in Mice - Effector Mechanisms and Their Longevity. *Journal of Immunology* **152**, 1653-1661.

Mills, C. E., Robins, J. M. & Lipsitch, M. 2004 Transmissibility of 1918 pandemic influenza. *Nature* **432**, 904-906.

Monto, a. S. & Kendal, a. P. 1973 Effect of Neuraminidase Antibody on Hong-Kong Influenza. *Lancet* **1**, 623-625.

Nelson, M. I., Viboud, C., Simonsen, L., Bennett, R. T., Griesemer, S. B., George, K. S., Taylor, J., Spiro, D. J., Sengamalay, N. A., Ghedin, E., Taubenberger, J. K. & Holmes, E. C. 2008 Multiple reassortment events in the evolutionary history of H1N1 influenza A virus since 1918. *PLoS Pathogens* **4**, e1000012.

Nobusawa, E. & Sato, K. 2006 Comparison of the mutation rates of human influenza A and B viruses. *The Journal of Virology* **80**, 3675-3678.

Rambaut, A., Pybus, O. G., Nelson, M. I., Viboud, C., Taubenberger, J. K. & Holmes, E. C. 2008 The genomic and epidemiological dynamics of human influenza A virus. *Nature* **453**, 615-620.

Raymond, F. L., Caton, A. J., Cox, N. J., Kendal, A. P. & Brownlee, G. G. 1983 Antigenicity and Evolution Amongst Recent Influenza-Viruses of H1n1 Subtype. *Nucleic Acids Research* **11**, 7191-7203.

Russell, C. A., Jones, T. C., Barr, I. G., Cox, N. J., Garten, R. J., Gregory, V., Gust, I. D., Hampson, A. W., Hay, A. J., Hurt, A. C., de Jong, J. C., Kelso, A., Klimov, A. I., Kageyama, T., Komadina, N., Lapedes, A. S., Lin, Y. P., Mosterin, A., Obuchi, M., Odagiri, T., Osterhaus, A. D. M. E., Rimmelzwaan, G. F., Shaw, M. W., Skepner, E., Stohr, K., Tashiro, M., Fouchier, R. A. M. & Smith, D. J. 2008 The global circulation of seasonal influenza A (H3N2) viruses. *Science* **320**, 340-346.

Scholtissek, C., Vonhoyningen, V. & Rott, R. 1978 Genetic Relatedness between New 1977 Epidemic Strains (H1N1) of Influenza and Human Influenza Strains Isolated between 1947 and 1957 (H1N1). *Virology* **89**, 613-617.

Shen, J., Kirk, B. D., Ma, J. P. & Wang, Q. H. 2009 Diversifying Selective Pressure on Influenza B Virus Hemagglutinin. *Journal of Medical Virology* **81**, 114-124.

Smirnov, Y. a., Lipatov, A. S., Gitelman, A. K., Okuno, Y., Van Beek, R., Osterhaus, A. D. M. E. & Claas, E. C. J. 1999 An epitope shared by the hemagglutinins of H1, H2, H5, and H6 subtypes of influenza A virus. *Acta Virologica* **43**, 237-244.

Smith, D. J., Lapedes, A. S., de Jong, J. C., Bestebroer, T. M., Rimmelzwaan, G. F., Osterhaus, A. D. M. E. & Fouchier, R. A. M. 2004 Mapping the antigenic and genetic evolution of influenza virus. *Science* **305**, 371-376.

Underwood, P. A. 1980 Serology and Energetics of Cross-Reactions among the H-3 Antigens of Influenza-Viruses. *Infection and Immunity* **27**, 397-404.

Van Reeth, K., Brown, I., Essen, S. & Pensaert, M. 2004 Genetic relationships, serological cross-reaction and cross-protection between H1N2 and other influenza - A virus subtypes endemic in European pigs. *Virus Research* **103**, 115-124.

Viboud, C., Tam, T., Fleming, D., Handel, A., Miller, M. A. & Simonsen, L. 2006a Transmissibility and mortality impact of epidemic and pandemic influenza, with emphasis on the unusually deadly 1951 epidemic. *Vaccine* **24**, 6701-6707.

Viboud, C., Tam, T., Fleming, D., Miller, M. A. & Simonsen, L. 2006b 1951 influenza epidemic, England and Wales, Canada, and the United States. *Emerging Infectious Diseases* **12**, 661-668.

Webster, R. G., Bean, W. J., Gorman, O. T., Chambers, T. M. & Kawaoka, Y. 1992 Evolution and Ecology of Influenza-A Viruses. *Microbiological Reviews* **56**, 152-179.

Wolf, Y. I., Viboud, C., Holmes, E. C., Koonin, E. V. & Lipman, D. J. 2006 Long intervals of stasis punctuated by bursts of positive selection in the seasonal evolution of influenza A virus. *Biology Direct* **1**, -.

Yu, X. C., Tsibane, T., McGraw, P. A., House, F. S., Keefer, C. J., Hicar, M. D., Tumpey, T. M., Pappas, C., Perrone, L. A., Martinez, O., Stevens, J., Wilson, I. A., Aguilar, P. V., Altschuler, E. L., Basler, C. F. & Crowe, J. E. 2008 Neutralizing antibodies derived from the B cells of 1918 influenza pandemic survivors. *Nature* **455**, 532-536.

Chapter 4

Strain competition under a multidegenerate genotype-phenotype map

Introduction

The consequences of strain competition have major implications for vaccination strategies and assessments of epidemic risk. Models of strain competition often implicitly assume that cross-immunity between strains is invariant among hosts: If hosts have the same infection history or immune repertoire, they share the same probability of being infected or infectious upon challenge with a new strain. Cross-immunity under this assumption can yield complex dynamics determined by the intensity of competition (Gupta et al. 1998). For realistic ratios of infection times and host lifespans, three general outcomes are possible. Intense strain competition leads to minimal diversity: All strains die out except a subset of discordant phenotypes. At intermediate competition, groups of discordant strains undergo cyclical or chaotic dynamics, causing diversity to vary in time. When cross-immunity is low, strains can coexist at an endemic equilibrium. These outcomes imply dramatic differences in the number of circulating strains and how the pathogen population might respond to immigration or mutation.

Recent models of influenza's dynamics find that some level of cross-immunity between strains is essential to constrain diversity to observed levels. Several posit that a necessary element of strain competition is a many-to-one mapping between individual strains, defined by their amino acid sequences, and their antigenic phenotypes (Ferguson et al. 2003; Gog & Grenfell 2002; Gokaydin et al. 2007; Koelle et al. 2006; Tria et al. 2005). These models assume to varying degrees that the cross-immunity between any two strains is static. There are reasons why this assumption might not hold in nature,

however. Several biologically plausible mechanisms exist that might allow a genotype to map to more than one phenotype, producing a multidegenerate genotype-phenotype map. Put simply, hosts with the same infection history or immune repertoire could then perceive genetically identical strains differently.

This study is an initial foray into the consequences of competition between strains when their phenotypes can vary among hosts. We begin by reviewing evidence for various mechanisms of heterogeneity in host responses, with an emphasis on influenza. We then present our model, which incorporates only the simplest level of heterogeneity. Our general result is that coexistence of strains is easier when responses at the individual level are narrow, and when responses at the population level are very diverse or homogeneous. It will thus be important to show that models of strain extinction through immune-mediated competition are either robust to this heterogeneity, that these differences disappear with further incorporation of biological detail, or that typical immune responses are quite broad. Our conclusions suggest there might be general differences in the competitive regimes faced by strains under selection from cellular versus antibody-mediated immunity.

Diversity in host responses

Different immune responses have been observed in humans infected with the same strains of influenza. Nakajima et al. (2000) found age-related patterns in the acute phase and convalescent sera of nine people infected with H3N2 during the 1990-1991 season. The sera of the three and four year old children had antibodies only to site B1, and all the older children and the one adult had antibodies binding to sites A, B1, B2, C, and C/E. In a follow-up study, Sato et al. (2004) examined the sera of 35 people who had been infected with a strain of the SY97 cluster and found that almost all young children developed antibodies to B1 and many to A. Older children and adults developed unique polyclonal responses involving several antibodies, often reacting more strongly to epitopes other than B1.

These patterns might arise from differences in past infection history, with polyclonal responses becoming more common as antibodies to formerly encountered

epitopes accumulate. There are several lines of evidence suggesting that additional dynamics might be involved. Hosts that have encountered the same sets of strains can respond differently depending on the order in which strains were encountered, a phenomenon known as original antigenic sin (OAS) (Francis 1960; Hoskins et al. 1979; Smith et al. 1999) (figure 4.1a). If strains *x*, *y*, and *z* are arranged consecutively along linear antigenic space, a host with immunity to strain *x* might reuse its antibodies to *x* when exposed to strain *y* (thereby avoiding infection or reducing infectiousness with *y*) and then be relatively defenseless upon encountering strain *z*. A host that encounters strain *y* first could, in contrast, be partially protected against both *x* and *z*.

Another source of differences can arise from variable immunodominance, which might operate alone or with OAS. The study by Sato et al. (2004) found that while two epitopes seemed especially immunogenic (attractive to antibodies) in children, the relative strengths of their antibodies to each epitope could be very different. Children with a stronger response to epitope B1 might thus react differently to future strains than children with a stronger response to epitope A. These differences might simply reflect the signature of OAS—B1 may be immunodominant, but some children had encountered epitope A before—but differences might arise even if the subjects' immune repertoires are identical. Experimental infections of influenza in naïve animals have shown that hosts can vary in which epitopes they target, and that when targeting the same epitopes, hosts often have quantitatively different responses (Cleveland et al. 1997; Laver et al. 1976), though some strains and/or host genotypes might generate more uniform responses (Lambkin & Dimmock 1995). Differences in host responses might be random, perhaps dependent on which B cells (which generate antibodies) and helper T cells (which stimulate select B cells) encounter epitopes first, or which B cells have the highest avidity for their epitope (figure 4.1b). These differences might on some level be predetermined. An individual's MHC alleles determine which T-cell epitopes (including those of helper T cells and CD8+ cells, which underlie cellular immunity) are recognized by the immune system. T-cell immunodominance hierarchies further appear to depend in a nontrivial way on the identities of other MHC alleles in individual hosts (Boon et al. 2004) and in some cases on which other T-cell epitopes are present (Jenkins et al. 2006). It might be possible that MHC class-II alleles, which are essential for B cell selection, could

predispose hosts for particular humoral responses (Crowe et al. 2006). Thus, hosts might fall into groups depending on which epitopes they are genetically predisposed to recognize (figure 4.1c).

Still other differences in host response are possible. For example, two hosts reacting to the same antigen can form antibodies with different potentials for cross-reactivity (Fleury et al. 2000). Strain dynamics might be further complicated by asymmetry in cross-immunity: Antibodies against x may be more effective against y than antibodies to y are against x (Underwood 1980). The strength of immune responses to particular epitopes might decay in time (Nowak et al. 1995).

This analysis ignores these possibilities and begins with a population of intrinsically identical hosts. Our only assumption is that epitopes compete for immunodominance. Not all hosts infected with the same strain will recover with antibodies to every epitope, but which epitope(s) a host develops immunity to is randomly determined.

Model

We begin by describing a general model of strain competition by Gupta et al. (1998) and then introduce our adaptation for heterogeneous host responses.

Strains have n loci, each defined by m possible alleles (Gupta et al. 1998). Each locus corresponds to an epitope, and each allele a possible phenotype of the epitope. Cross-immunity is set by γ, which gives the reduction in transmission probability conferred by previous infection with one strain; $(0 \leq \gamma \leq 1)$. Without heterogeneous immune responses, the fraction immune to a strain i from infection with i, z_i, changes as

$$\frac{dz_i}{dt} = (1 - z_i)\lambda_i - \mu z_i, \tag{5.1}$$

where λ_i is the force of infection of strain i (the per capita rate of rate of acquiring infection, which is linearly proportional to the number of infectious individuals), μ is the

birth and death rate, and $(1 - z_i)$ is the fraction of the population not immune to strain i from infection with i. An assumption of this model is that immunity to i is conferred immediately upon infection with strain i. Variable z_i thus represents cumulative incidence of i: it increases from direct infections with i and decreases only through mortality.

Compartment w_i represents hosts immune to all strains j that share alleles with i, including i itself:

$$\frac{dw_i}{dt} = (1 - w_i)\sum_{j \sim i} \lambda_j - \mu w_i, \tag{5.2}$$

The expression $j \sim i$ refers to all strains j sharing alleles with i, and $(1 - w_i)$ is the fraction of the population that has never been infected with a strain that shares alleles with i. The difference between z_i and w_i is that the former acquired immunity to i from infection with i, and the latter acquired immunity to i via infection with strain j that shares alleles with i. Thus, z_i is a subset of w_i. The w_i compartment thus tracks cumulative immunity to i, including in individuals currently infectious with i and in individuals who were never infected with i but who attained immunity through infection with j.

The population of individuals infectious with strain i, y_i, changes as:

$$\frac{dy_i}{dt} = [(1 - w_i) + (1 - \gamma)(w_i - z_i)]\lambda_i - \sigma y_i, \tag{5.3}$$

where σ is the rate of recovery. The quantity $(w_i - z_i)$ is individuals who acquired immunity to i through infection with a different strain. Equations 5.2 and 5.3 show that cross-immunity in this model acts through a reduction in infectiousness: fraction γ of individuals who are immune to i from infection with a different strain, $\gamma (w_i - z_i)$, cannot become infectious with i (though these individuals still become infected as z_i). The remaining fraction, $(1 - \gamma)(w_i - z_i)$, can become infectious with i, as can those individuals who have never been infected with a strain sharing alleles with i, $(1 - w_i)$. Thus, y_i is a subset of w_i and z_i.

To incorporate host heterogeneity into this formalism, we account for the possibility that hosts might not identify shared epitopes between strains due to immunodominance. In other words, infection with strain j will not automatically confer immunity to strain i simply because the two strains share common epitopes. An additional requirement must be met, which is that the shared epitope must have triggered a strong immune response during infection with strain j. Let p_n be the probability that individuals develop an antibody to epitope n; p_n thus measures the epitope's immunodominance. Initially, we assume all responses are on average monoclonal to one epitope, so that $\Sigma\, p_n = 1$. Equation 5.1 does not change: all people infected with strain i will mount a specific response to one of its epitopes and will not transmit i in the future. But now not all hosts with immunity to strain j, which shares epitopes with i, will have immunity to i. Only the fraction of hosts infected with j that mount antibodies to epitopes shared with i will then be immune to i. Let S_{ij} be the set of shared epitopes between strains i and j: $S_{ij} \equiv i \cap j$. The probability r_{ij} of developing antibodies to i if infected with j is

$$r_{ij} = \sum_{n \in S_{ij}} p_n, \tag{5.4}$$

Thus equation 5.2 becomes

$$\frac{dw_i}{dt} = (1 - w_i) \sum_j \lambda_j r_{ij} - \mu w_i, \tag{5.5}$$

We retain the assumption that there can be reduction in infectiousness γ between immune responses to i and j. Equation 5.3 thus remains the same.

Our analysis focuses on the effects of changing epitopes' immunodominance. Values of p_n are drawn from a normalized negative binomial distribution, which can allow every epitope to have the same immunodominance or for the probabilities to be highly skewed (supplementary material): skewed distributions correspond to less diverse immune responses at the population level and even distributions to more diverse responses. We initially assume that hosts retain immunity on average to only one epitope

(figure 4.2). Mathematically, this is equivalent to $\Sigma p_n = 1$. We then allow polyclonal responses ($\Sigma p_n > 1$) to the limit where infected hosts always develop immune responses to all epitopes, $\Sigma p_n = n$. To increase the breadth of the antibody response, we multiply each response p_n by a "polyclonality" factor c, which ranges from 1 to n, and further require $p_n \leq 1$. The ordinary differential equations were simulated numerically for the three locus ($n = 3$), two allele ($m = 2$) case (supplementary material).

Results

With a monoclonal response, the interesting dynamical regimes disappear (figure 4.3a). After initial oscillations, strains coexist at an endemic equilibrium, comparable in prevalence to the regime of low cross-immunity in the original model (figure 4.3b). This pattern results regardless of the relative immunodominance of the different epitopes.

When hosts recognize more epitopes ($c > 1$), the complex dynamical behavior at high levels of cross-immunity returns. When hosts recognize on average half the epitopes ($c = 1.5$), increasing the cross-immunity above approximately 0.7 (at $b = 0$, where all epitopes have equal probability of dominating) results in the onset of chaotic dynamics, followed by (from approximately $0.9 < \gamma \leq 1$) a regime of competitive exclusion and the dominance of one antigenically discordant set (figure 4.4). As the immunodominance distribution becomes more skewed ($b = 1/3$, $b = 2/3$), the chaotic dynamics expand to slightly higher γ and are preceded by a growing region of limit cycles. Extreme limit cycles also appear for high γ after the chaotic region for $b = 2/3$. Thus, increasing the skewness of the immunodominance distribution (but with $b < 1$) generally increases the region of cyclic and chaotic behavior.

Previous analyses have found a boundary between discrete strain structure, in which one discordant set dominates, and regimes of no, chaotic, or cyclic strain structure (Gupta et al. 1998; Recker & Gupta 2005). Increasing the breadth of the immune response even further ($c > 1.5$) expands the regions of cyclic, chaotic, and competitively exclusive behavior; all start at lower γ (figure 4.5 and figure 4.S1). The effects of changing the skewness, b, do not qualitatively differ as immune responses broaden from

$c = 1.5$ to $c = 3$. Since the dynamics analyzed in the original model (Gupta et al., 1998), correspond to the case where $c = 3$ and $b = 0$, our results show that reducing the breadth of the immune response ($c < 3$) increases the minimum cross-immunity required for the onset of competitive exclusion. When responses are monoclonal ($b = 1$), all strains coexist.

Discussion

Experiments with influenza in several host species suggest that hosts that have been exposed to the same strains will not necessarily develop the same immune repertoires, and hosts with identical immune repertoires will not necessarily respond identically upon infection with the same challenge strain. Understanding the outcome of strain competition is the motivation for many models of infectious disease, and yet the majority of models are grounded on simple and largely unquestioned assumptions about the nature of cross-immunity [cf. Kryazhimskiy et al. (2007)]. The aim of this study was to minimally relax a common assumption. We found that when hosts randomly varied in which epitopes they developed immunity to, coexistence among strains was more common. In particular, narrow immune responses that were focused on one epitope on average weakened competition so much that strains could coexist for any level of cross-immunity and any amount of diversity in the host population. As the breadth of the immune response increased, competition intensified. Limit cycles, chaos, and competitive exclusion then became possible at high levels of cross-immunity.

Other models have explored the consequences of heterogeneous host immune responses for strain competition and obtained complementary results. Gupta and Galvani (1999) considered a population of two host genotypes. Genotype "A" followed the dynamics outlined in the original model (equations 5.1-5.3) and genotype "B" recognized a locus common to all strains (i.e., perceived all strains as identical). Increasing the proportion of genotype B hosts gradually reduced the threshold level of cross-immunity γ required for strain structure to appear and increased the period of oscillations of discordant antigenic sets. In populations comprised solely of genotype B hosts, oscillations disappeared, and the strain with the highest R_0 dominated. Thus, increasing

the intensity of strain-transcendent competition (the fraction of genotype B hosts) reduced strain diversity, and the presence of hosts capable of strain-specific responses increased diversity. This result is consistent with the effects of generalized immunity, a transient strain-transcendent immunity that was found to dampen diversity in simulations (Ferguson et al. 2003).

The assumptions of a model by Recker and Gupta (2005) are closer to the ones here. Rather than assuming that the degree of cross-immunity between two strains was independent of the number of shared epitopes (assuming the strains share at least one), they introduced another class of individuals immune to any strain k that shares more than one allele with strain i. Individuals immune to i via prior infection with k have a greater reduction in infectiousness (higher cross-immunity, γ_2) than individuals immune to i via prior infection with strains sharing only one allele with i (with cross-immunity from the latter given by γ_1, and $\gamma_1 < \gamma_2$). A high degree of cross-immunity between more closely related strains, γ_2, could precipitate the onset of the transition to discrete strain structure even when γ_1 was relatively low. In other words, including some immunological precision about the extent of phenotypic similarity could restrict diversity further over the original model.

Several caveats are required to place this work in theoretical context. Our model suggests that such restrictions found by Recker and Gupta (2005) depend on the breadth and diversity of the immune response. Dynamically, changing c, the breadth of the immune response, appears to have similar effects on dynamics to changing the number of immunodominant epitopes, n (Gupta et al. 1998). Our model is also convergently similar in structure to models based on polarized immunity (Gog & Swinton 2002): Rather than cross-immunity acting through a partial reduction in infectiousness or susceptibility in all immune hosts, strain competition is effected when some fraction σ_{ij} of hosts infected with j develops immediate immunity to i. If $\gamma = 1$, we obtain a model of polarized immunity with $\sigma_{ij} = r_{ij}$, the effective similarity of the strains' phenotypes. When $\gamma < 1$, our model effectively allows cross-immunity to epitopes shared by strains i and j to be imperfect. To our knowledge, the status-based approach has not previously been described or applied in the context of immunodominance and natural heterogeneity in host responses.

Careful investigations are warranted in translating these results to practical biology. The summaries here are of equilibrium conditions, deterministically obtained, and ignore extinctions that would result from demographic stochasticity. Less obviously, our model, like models of polarized immunity, assumes it can represent the effects of many probabilistic outcomes (response versus non-response to epitopes by individual hosts) as average rates. Our model should thus contain less variance in host immunity than one might observe in an agent-based representation of this system. Such differences might be dwarfed by inclusion of more realistic mechanisms, such as the degree to which individuals may be genetically predisposed to respond to particular epitopes. Another potential area for investigation is whether differences arise in primary versus secondary responses (Crowe et al. 2003; Lambkin & Dimmock 1996).

Our findings underscore that research into the specificity, dynamics, and especially breadth and diversity of human immune responses to influenza will be important for developing accurate models. Since T-cell epitopes are recognized by a limited set of MHC alleles, whereas B cell adaptation is relatively unrestricted, we might expect greater coexistence of antigenically diverse strains in pathogen populations that compete mainly against hosts' cellular immunity. As pathogens are under selective pressure to minimize their numbers of immunogenic, neutralizing epitopes, the potential breadth of immune responses might also change in time. Understanding the breadth of immune responses will also be important to understand how mutants appear and spread. Nakajima et al. (2000) and Sato et al. (2004) posit that antigenic drift results from serial adaptation to monoclonally-responding subpopulations. For example, variants first escape site B1 and then sites targeted by others. Cleveland et al. (1997) recalled that major drift variants tend to have at least four amino acid substitutions in two epitopes (Wilson & Cox 1990). They predicted the existence of four different "human genetic groupings" with consistent, nonoverlapping epitope biases. Viruses drift as they move from group to group, acquiring a critical amino acid change in each, and become double escape mutants. In contrast to Sato et al. (2004), they argue that polyclonal responses can select for drift mutants under particular conditions. Other models in mice and ferrets suggest that mutants can arise from polyclonal responses as long as they could escape a predominant antibody [reviewed in (Nakajima et al. 2000)].

This work shows how consumer-resource dynamics can be qualitatively affected by the phenotypic resolution of one of the parties (here, the pathogen consumers). Dynamics may be more interesting still if the phenotypic resolution depends specifically on intrinsic properties of the resource, as when pathogens compete against MHC-restricted T-cell epitopes. We have highlighted several hypotheses of strain competition relevant to influenza, and which deserve further analytic and empirical investigation. Accurately predicting the outcome of strain dynamics will require choosing carefully among the assumptions.

Figure 4.1. Three possible mechanisms of heterogeneity in hosts' immune responses. Hosts are immunologically naïve before the first challenge. Each shape/location in a strain corresponds to an epitope/locus; each color corresponds to a different phenotype/allele at that epitope/locus. Symbols crossed in red represent specific adaptive immune responses (e.g., antibodies or T cells) to that particular phenotype/allele. (a) Original antigenic sin (OAS). OAS posits that strains that are closely antigenically related may not inspire novel immune responses. Thus, hosts exposed to the same strains but in different sequences will accumulate different immune repertoires and can respond differently upon infection with the same challenge strain. This example shows OAS with a multilocus and polyclonal response; it can also operate for a single locus and monoclonal response. (b) Random immunodominance. This mechanism, the basis of the model explored in this paper, assumes that hosts usually only perceive or develop a strong response to a subset (here, one) of available epitopes. Epitopes have certain probabilities of being immunodominant, and these probabilities do not vary among hosts. (c) Predetermined immunodominance. Hosts intrinsically vary in their propensities to mount immune responses to different epitopes. Host A recognizes only the first locus, and host B only the third. Host A thus perceives three distinct strains and host B two distinct strains.

Figure 4.1

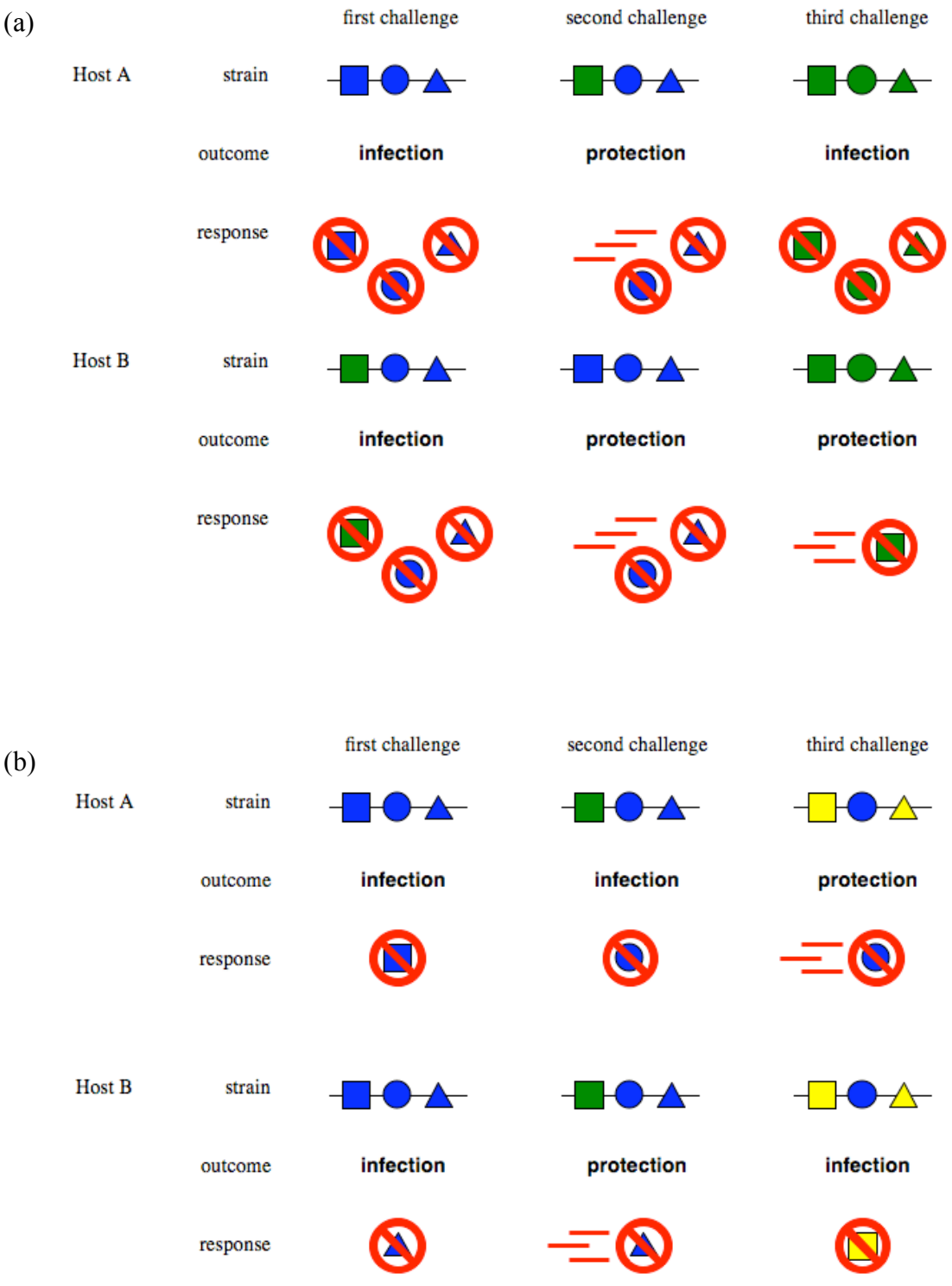
(a)
first challenge
second challenge
third challenge
Host A
strain
outcome
infection
protection
infection
response
Host B
strain
outcome
infection
protection
protection
response
(b)
first challenge
second challenge
third challenge
Host A
strain
outcome
infection
infection
protection
response
Host B
strain
outcome
infection
protection
infection
response

Figure 4.1 (continued)

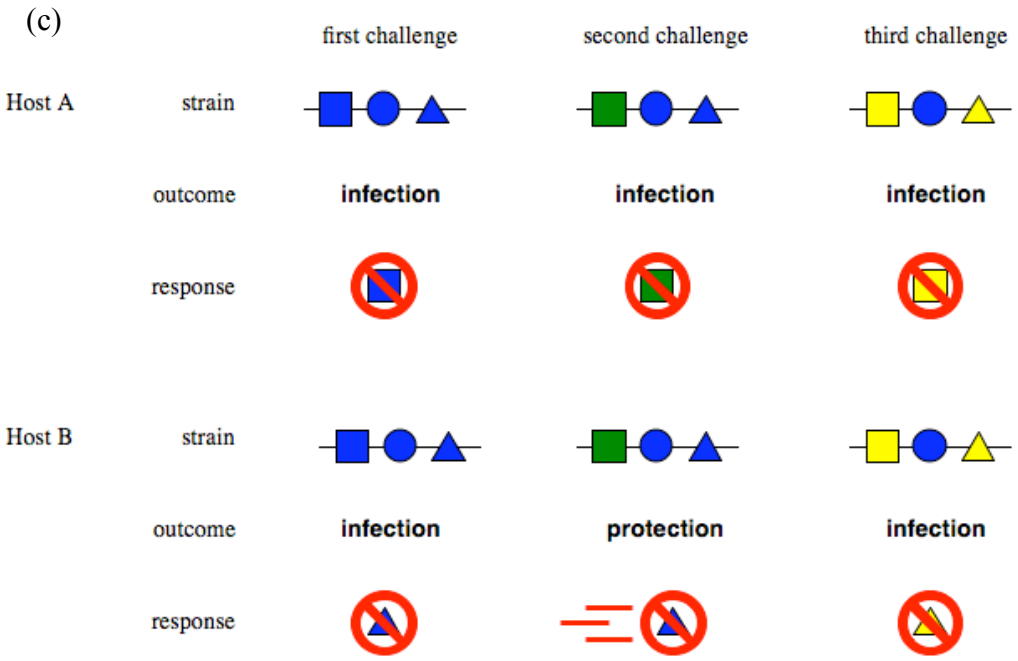

Figure 4.2. Distributions for p_n, the probability of developing an immunodominant response to epitope n, for the model where $n = 3$. Parameter c gives the breadth of the response: $c = 1$ corresponds to a monoclonal response and $c = n$ the maximum polyclonal response. Parameter b gives the skewness: $b \rightarrow 0$ yields equal p_n, and $b \rightarrow 1$ yields $p_1 \rightarrow 1$ and $p_{n\neq 1} \rightarrow 0$.

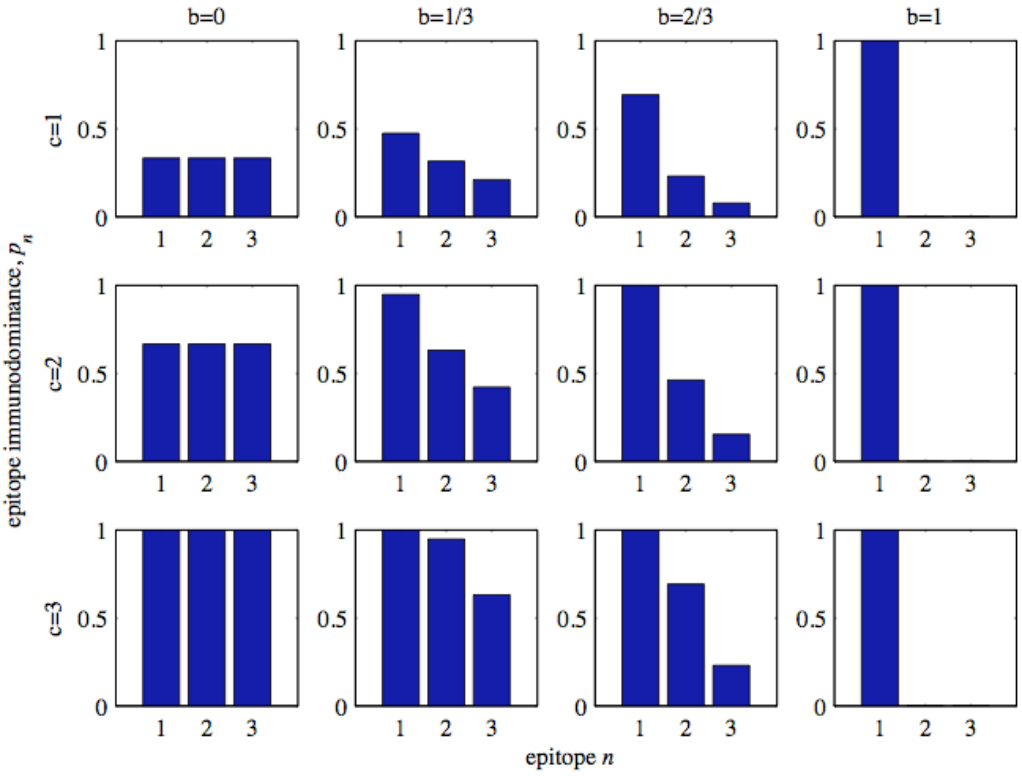

Figure 4.3. Dynamics with monoclonal immune responses ($c = 1$). (a) Equilibrium strain dynamics. (b) Sample time series showing transients of z_i, w_i, and y_i with $\gamma = 0.75$ and $b = 1/3$. Each color corresponds to a different strain. Note differences in the ranges of the y-axes between plots.

(a)

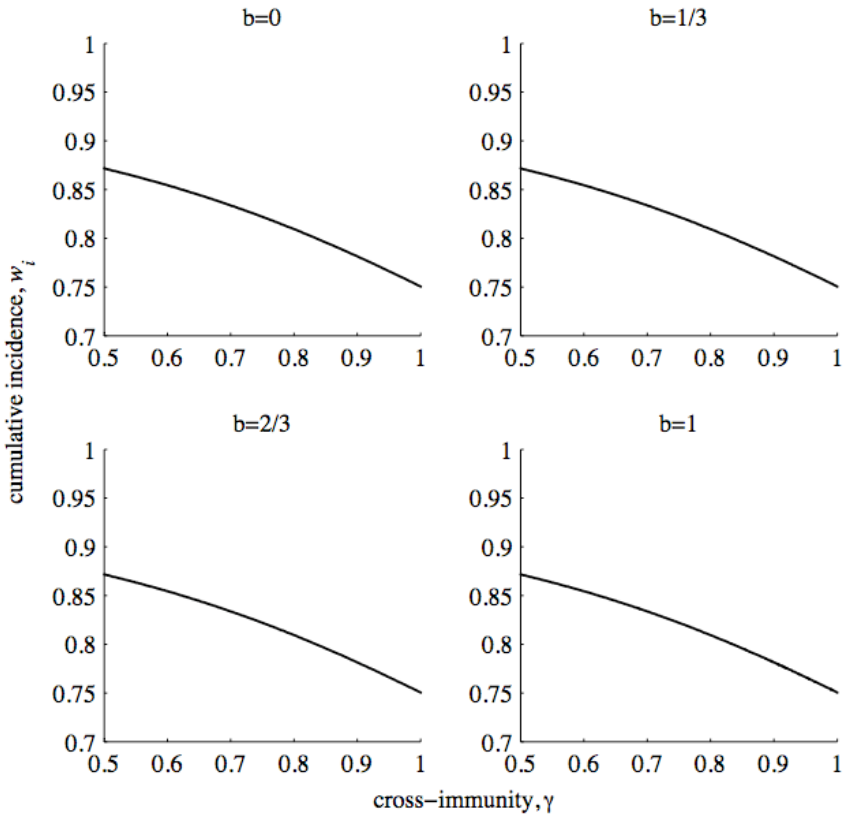

Figure 4.3 (continued)

(b)

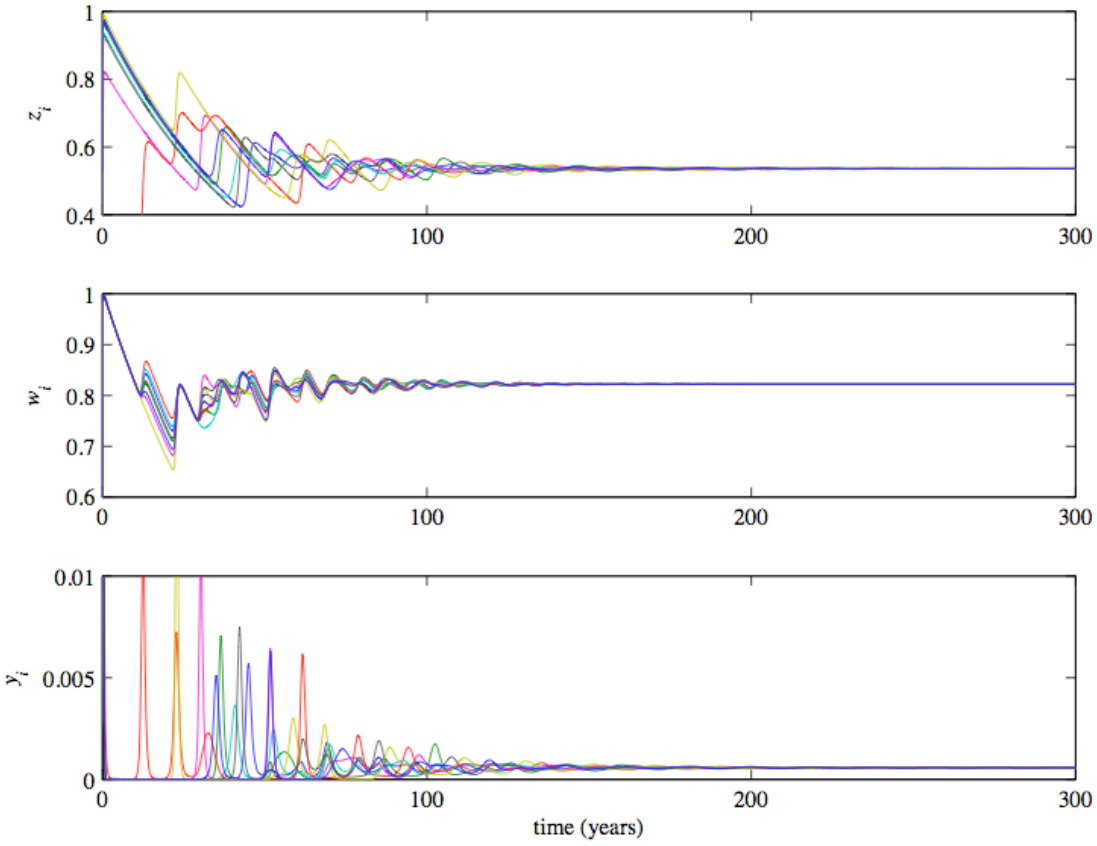

Figure 4.4. Dynamics under incomplete polyclonal immune responses ($c = 1.5$). (a) Equilibrium strain dynamics. Diagram for $b = 1$ is identical to figure 4.3a. (b) Sample time series showing transients of z_i for different values of γ; $b = 1/3$ or $b = 2/3$. Each color corresponds to a different strain. Note differences in the ranges of the y-axes between plots.

(a)

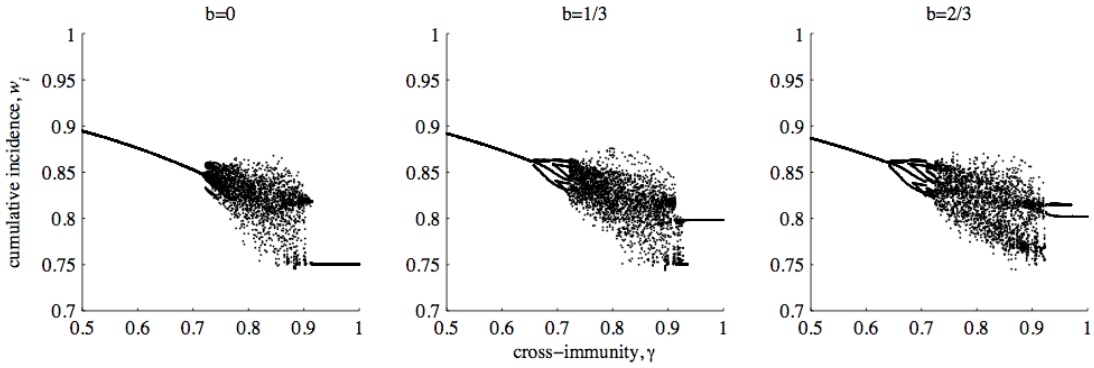

Figure 4.4 (continued)

(b)

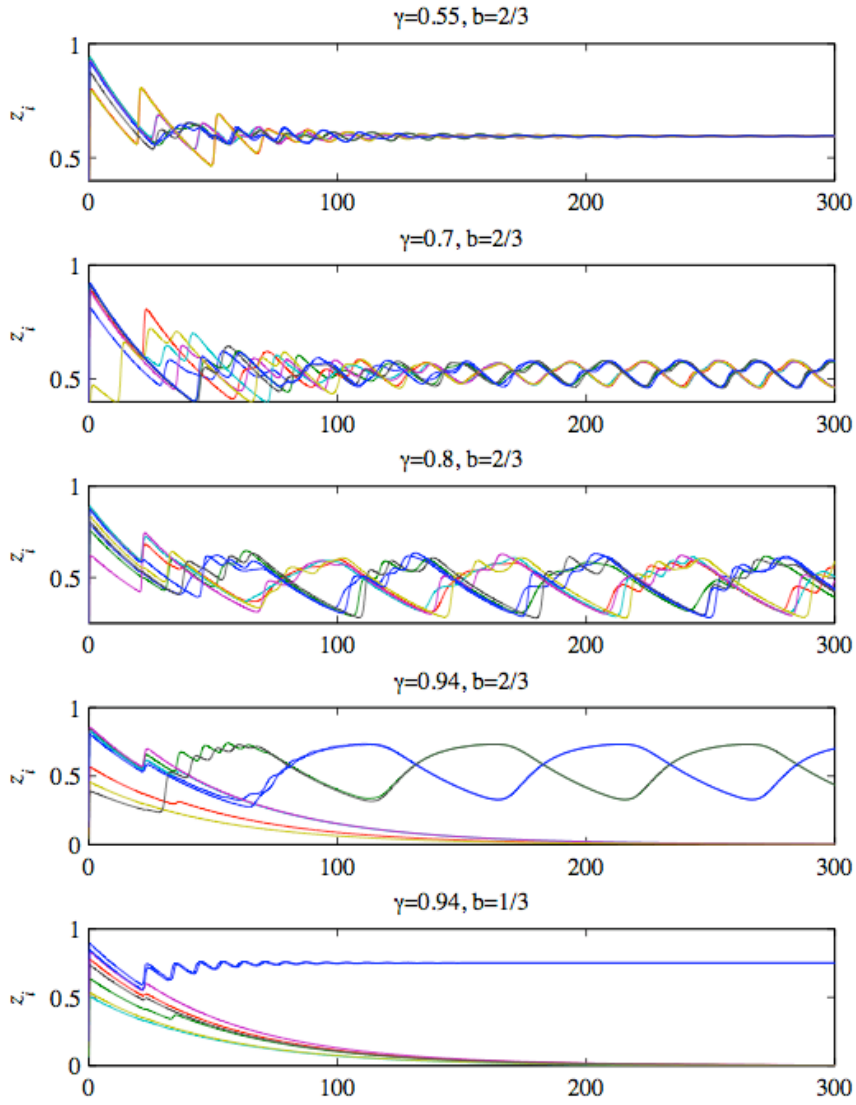

Figure 4.5. Dynamics under full polyclonal immune responses ($c = n = 3$). (a) Equilibrium strain dynamics. Diagram for $b = 1$ is identical to figure 4.3a. (b) Sample time series showing transients of z_i for different values of γ, $b = 1/3$ or $b = 2/3$. Though not clear, dynamics of z_i at $\gamma = 0.5$, $b = 1/3$, are damped, low-amplitude oscillations to the endemic equilibrium.

(a)

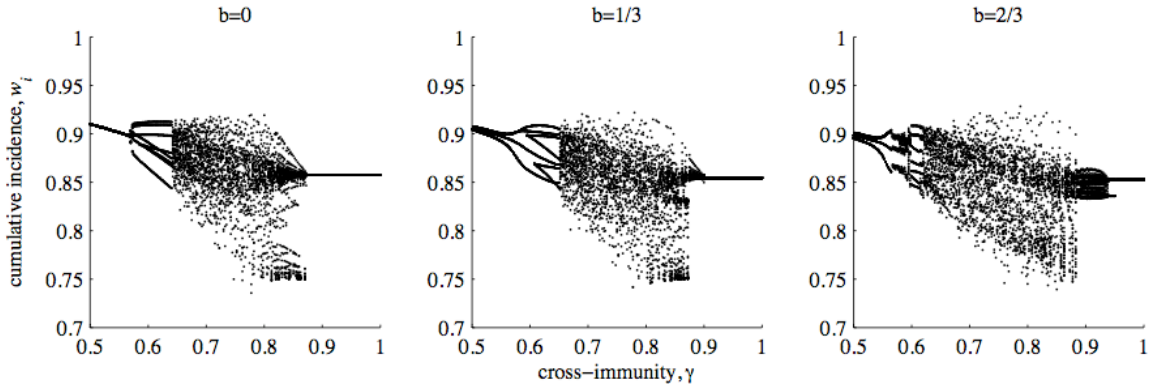

Figure 4.5 (continued)

(b)

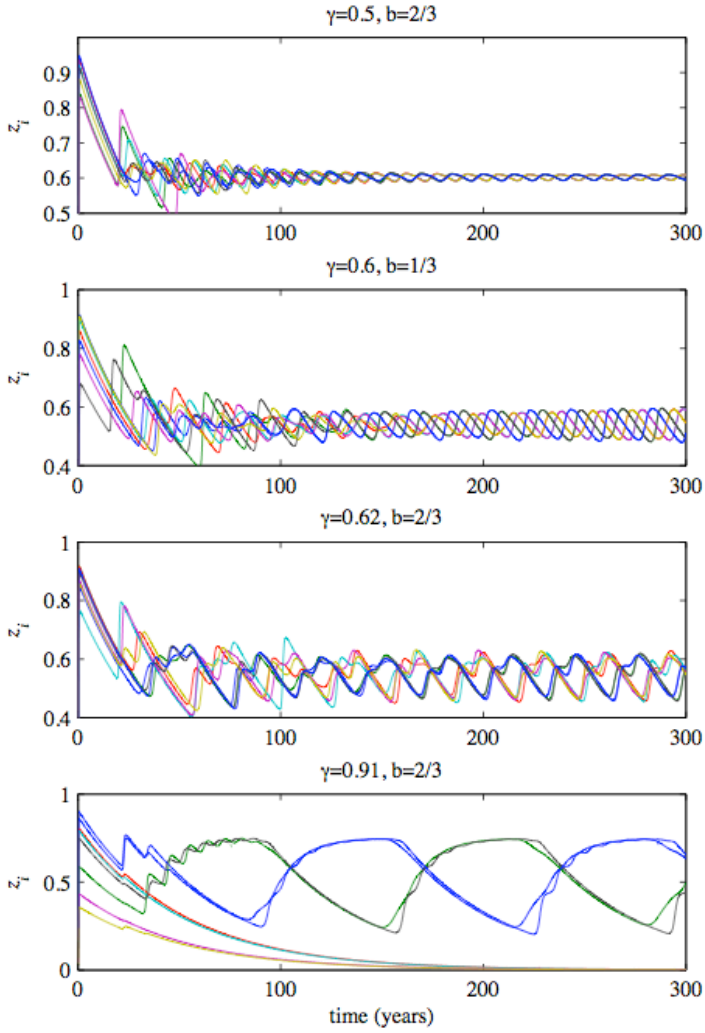

Supplementary material

Immunodominance distributions

The negative binomial distribution is typically written as

$$f(k;r,p) = \binom{k+r-1}{r-1} p^r (1-p)^k, \tag{5.S1}$$

where $0 < p < 1$ and $r > 0$. To avoid confusion with epitope immunodominance, we refer to p above as b. We set $r = 1$. The per epitope immunodominance p_k is

$$p_k = \min\left(1, \frac{cf(k;r,b)}{\sum_{k=1}^{n} f(k;r,b)}\right), \tag{5.S2}$$

where k refers to the epitope ($k \in \{1,\ldots,n\}$) and c is the degree of polyclonality (main text). To accommodate $b = 0$ and $b = 1$, we approximate completely flat and skewed distributions with $b = 10^{-10}$ and $b = 1-10^{-10}$, respectively.

Parameters

All rate parameters are the same as those used in Gupta et al. (1998): birth and death, μ = 1/50 y^{-1}; recovery, σ = 10 y^{-1}; $R_0 = 4$. Values of $y_i(0)$ were drawn from a uniform random interval over (0, 0.25], and $y_i(0) = z_i(0) = w_i(0)$. These random starting conditions were used for each of the sample time series shown in figures 5.3b, 5.4b, and 5.5b and also for each bifurcation diagram at $\gamma = 0.5$. For subsequent values of γ in the bifurcation diagrams, initial values were copied from the final values simulated for the previous value of γ.

Numerical solution of the ordinary differential equations

We used a fourth- and fifth-order Runge-Kutta solver implemented in Matlab (function ode45) with absolute and relative error tolerances of 10^{-6}. Simulations were run for 5000 years and then sampled for the next 1000 years. The diagrams show all maxima and minima over the sampling period. These inflection points were obtained using Matlab's findpeaks function, which returns every point that is greater than both its neighbors.

Figure 4.S1. Equilibrium dynamics under incomplete polyclonal immune responses (c = 2). The diagram for b = 1 is identical to that shown in figure 4.2.

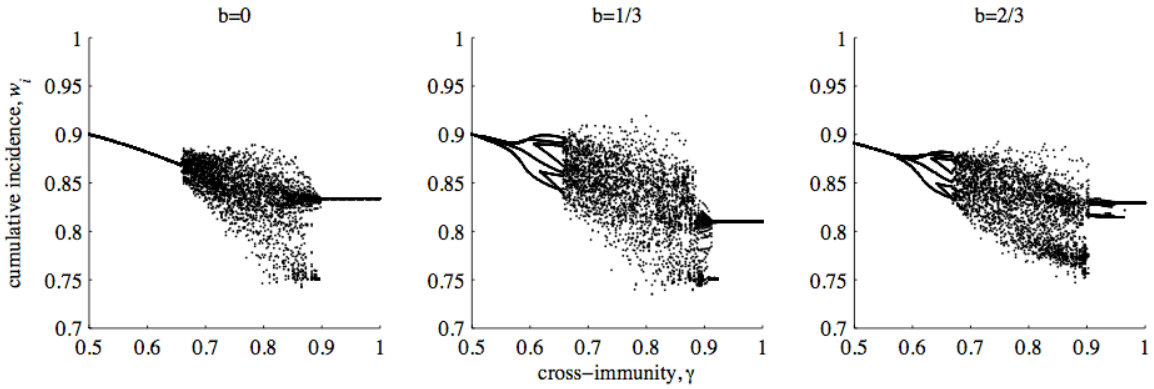

References

Boon, A. C. M., de Mutsert, G., van Baarle, D., Smith, D. J., Lapedes, A. S., Fouchier, R. A. M., Sintnicolaas, K., Osterhaus, A. D. M. E. & Rimmelzwaan, G. F. 2004 Recognition of homo- and heterosubtypic variants of influenza A viruses by human CD8(+) T lymphocytes. *Journal of Immunology* **172**, 2453-2460.

Cleveland, S. M., Taylor, H. P. & Dimmock, N. J. 1997 Selection of neutralizing antibody escape mutants with type A influenza virus HA-specific polyclonal antisera: Possible significance for antigenic drift. *Epidemiology and Infection* **118**, 149-154.

Crowe, S. R., Miller, S. C., Brown, D. M., Adams, P. S., Dutton, R. W., Harmsen, A. G., Lund, F. E., Randall, T. D., Swain, S. L. & Woodland, D. L. 2006 Uneven distribution of MHC class II epitopes within the influenza virus. *Vaccine* **24**, 457-467.

Crowe, S. R., Turner, S. J., Miller, S. C., Roberts, A. D., Rappolo, R. A., Doherty, P. C., Ely, K. H. & Woodland, D. L. 2003 Differential antigen presentation regulates the changing patterns of CD8(+) T cell immunodominance in primary and secondary influenza virus infections. *Journal of Experimental Medicine* **198**, 399-410.

Ferguson, N. M., Galvani, A. P. & Bush, R. M. 2003 Ecological and immunological determinants of influenza evolution. *Nature* **422**, 428-433.

Fleury, D., Daniels, R. S., Skehel, J. J., Knossow, M. & Bizebard, T. 2000 Structural evidence for recognition of a single epitope by two distinct antibodies. *Proteins-Structure Function and Genetics* **40**, 572-578.

Francis, T. 1960 On the doctrine of original antigenic sin. *Proceedings of the American Philosophical Society* **104**, 572-578.

Gog, J. R. & Grenfell, B. T. 2002 Dynamics and selection of many-strain pathogens. *Proceedings of the National Academy of Sciences of the United States of America* **99**, 17209-17214.

Gog, J. R. & Swinton, J. 2002 A status-based approach to multiple strain dynamics. *Journal of Mathematical Biology* **44**, 169-184.

Gokaydin, D., Oliveira-Martins, J. B., Gordo, I. & Gomes, M. G. M. 2007 The reinfection threshold regulates pathogen diversity: the case of influenza. *Journal of the Royal Society Interface* **4**, 137-142.

Gupta, S., Ferguson, N. M. & Anderson, R. M. 1998 Chaos, persistence, and evolution of strain structure in antigenically diverse infectious agents. *Science* **280**, 912-915.

Gupta, S. & Galvani, A. 1999 The effects of host heterogeneity on pathogen population structure. *Philosophical Transactions of the Royal Society of London Series B-Biological Sciences* **354**, 711-719.

Hoskins, T. W., Davis, J. R., Smith, A. J., Miller, C. L. & Allchin, A. 1979 Assessment of inactivated influenza A vaccine after three outbreaks of influenza A at Christ's Hospital. *Lancet* **i**, 33-35.

Jenkins, M. R., Webby, R., Doherty, P. C. & Turner, S. J. 2006 Addition of a prominent epitope affects influenza A virus-specific CD8+ T cell immunodominance hierarchies when antigen is limiting. *Journal of Immunology* **177**, 2917-2925.

Koelle, K., Cobey, S., Grenfell, B. & Pascual, M. 2006 Epochal evolution shapes the phylodynamics of interpandemic influenza. *Science* **314**, 1898-1903.

Kryazhimskiy, S., Dieckmann, U., Levin, S. A. & Dushoff, J. 2007 On state-space reduction in multi-strain pathogen models, with an application to antigenic drift in influenza A. *Plos Computational Biology* **3**, 1513-1525.

Lambkin, R. & Dimmock, N. J. 1995 All Rabbits Immunized with Type-a Influenza Virions Have a Serum Hemagglutination-Inhibition Antibody-Response Biased to a Single Epitope in Antigenic Site-B. *Journal of General Virology* **76**, 889-897.

Lambkin, R. & Dimmock, N. J. 1996 Longitudinal study of an epitope-biased serum haemigglutination-inhibition antibody response in rabbits immunized with type A influenza virions. *Vaccine* **14**, 212-218.

Laver, W. G., Downie, J. C. & Webster, R. G. 1976 Diversity of Antibody-Response to Different Antigenic Determinants on Hemagglutinin Subunits of Influenza-Viruses. *Journal of Immunology* **116**, 336-341.

Nakajima, S., Nobusawa, E. & Nakajima, K. 2000 Variation in response among individuals to antigenic sites on the HA protein of human influenza virus may be responsible for the emergence of drift strains in the human population. *Virology* **274**, 220-231.

Nowak, M. A., May, R. M. & Sigmund, K. 1995 Immune responses against multiple epitopes. *Journal of Theoretical Biology* **175**, 325-353.

Recker, M. & Gupta, S. 2005 A model for pathogen population structure with cross-protection depending on the extent of overlap in antigenic variant repertoires. *Journal of Theoretical Biology* **232**, 363-373.

Sato, K., Morishita, T., Nobusawa, E., Tonegawa, K., Sakae, K., Nakajima, S. & Nakajima, K. 2004 Amino-acid change on the antigenic region B1 of H3 haemagglutinin may be a trigger for the emergence of drift strain of influenza A virus. *Epidemiology and Infection* **132**, 399-406.

Smith, D. J., Forrest, S., Ackley, D. H. & Perelson, A. S. 1999 Variable efficacy of repeated annual influenza vaccination. *Proceedings of the National Academy of Sciences of the United States of America* **96**, 14001-14006.

Tria, F., Lassig, M., Peliti, L. & Franz, S. 2005 A minimal stochastic model for influenza evolution. *Journal of Statistical Mechanics-Theory and Experiment*, P07008.

Underwood, P. A. 1980 Serology and Energetics of Cross-Reactions among the H-3 Antigens of Influenza-Viruses. *Infection and Immunity* **27**, 397-404.

Wilson, I. a. & Cox, N. J. 1990 Structural Basis of Immune Recognition of Influenza-Virus Hemagglutinin. *Annual Review of Immunology* **8**, 737-771.

Chapter 5

Ecological factors driving the long-term evolution of influenza's host range

Introduction

Several challenges complicate the task of predicting evolution. One is the presence of evolutionary constraints: It might not be possible to optimize two phenotypic traits simultaneously, because a high value in one trait rules out high values in the other. Another problem concerns attainability: Evolutionary pathways may lead through regions of low fitness or, if mutations interact epistatically, may be difficult to map. Yet another class of problems arises from the environment or ecology in which evolution occurs: The fitness of a trait may be frequency-dependent, being determined by the phenotypes of other individuals. Fitness can also be affected by population size, spatial interactions, and extrinsic factors, and these relationships can be nonlinear and dynamic.

Predicting evolution of host ranges in pathogens requires confronting several of these problems at once. Many pathogens show adaptation to specific host or tissue types and are unable to infect other hosts or tissues without undergoing extensive adaptation (Baranowski et al. 2001; Webby et al. 2004). Such adaptation often comes at the expense of the ability to infect an original host type, and thus presents an evolutionary constraint in the form of a tradeoff. Pathogens tend to undergo extreme changes in population size during the same period in which rapid evolution occurs. Host immunity furthermore often imposes frequency-dependent selection.

Given this complexity, it is not surprising that there is little overarching theory for understanding the evolution of host ranges in pathogens. This is unfortunate, considering the ubiquity of zoonoses: Most pathogens of humans infect at least one other species

(Woolhouse & Gowtage-Sequeria 2005). Existing models address host range indirectly. For example, Parker (2003) used optimization principles to show how parasitic helminthes might expand their host range through trophic transmission to acquire complex life cycles. Gandon (2004) developed predictions for the evolution of virulence and transmission in a multihost environment. Some insights might also be gained by interpreting host range as a resource-choice problem for pathogens. In Levins's (1962) classic approach, consumers are predicted to specialize under strong tradeoffs and to adopt generalist strategies when tradeoffs are weak. His model, like Parker's, assumes that the optimal strategy will prevail. When selection is frequency-dependent, however, optimization principles are likely to give qualitatively incorrect predictions (Dieckmann et al. 2002; Egas et al. 2004; Koelle et al. 2005).

Our goal in this study is to develop basic predictions for the evolution of influenza's host range, though the methods of analysis are general and might be of interest also with regard to many other pathogens. Host range here refers to the specificity and diversity of pathogens in the community. Our analysis focuses on how a tradeoff in tissue specialization and host ecology may influence evolutionary outcomes in the long run. We do not consider the mechanistic details of evolutionary attainability here, since the genotype-to-phenotype maps relevant to influenza's host range are still only poorly known (Baigent & McCauley 2003). Like Levins's approach, ours ignores environmental variation, such as seasonality, and assumes that viral population dynamics are at equilibrium.

These simplifications allow us to obtain general results about the structure of host ranges in a heterogeneous host environment, when adaptation is restricted by a single evolutionary constraint. We find that specialists are favored for a broad range of weak and strong tradeoffs. It turns out that the ability of a second specialist to invade is very sensitive to interspecific transmission rates and host population sizes, but these dependencies are only weakly affected by tradeoff strength.

Background

The host range of many viruses is constrained by cell recognition (Baranowski et al. 2001). Influenza viruses all bind to cell surface oligosaccharides with a terminal sialic acids. Sialic acids fall into one of two general types of conformations: the Neu5Acα(2,3)-Gal linkage or the Neu5Acα(2,6)-Gal linkage. The intestinal and/or respiratory epithelia of waterfowl, horses, and dogs contain mainly cells with α2,3-linked sialic acids, whereas the upper respiratory epithelia of cats and humans are dominated by α2,6-linked sialic acid receptors (Baigent & McCauley 2003). Pigs, the alleged "mixing vessels" of influenza viruses (Webster et al. 1992), contain both types of receptors in their respiratory tracts (Scholtissek et al. 1998). Chickens also possess both types of receptors (Gambaryan et al. 2002). Experiments have shown that most viruses cannot replicate in host tissue of dissimilar receptor type, and viruses preferring one receptor type can usually sustain some replication in any host possessing that type, even if they are adapted to another species (Gambaryan et al. 2002; Ito & Kawaoka 2000; Ito et al. 1999; Kida et al. 1994; Lee et al. 2005). Thus, the chemistry of receptor binding creates a tradeoff between the ability to invade cells of one type or the other. No influenza A virus studied thus far appears able to bind both receptor conformations well simultaneously, though the tradeoffs may be more severe for some subtypes than for others (Harvey et al. 2004; Matrosovich et al. 2000; Matrosovich et al. 2001).

The distribution of α2,3- and α2,6-linked receptors in the host community presents an interesting evolutionary challenge: In a population of diverse potential hosts, under what circumstances will viruses evolve new receptor preferences? The emergence of avian influenza subtype H5N1 in humans has been ascribed to high interspecific mixing in backyard farms, high population densities in the expanding commercial poultry industry, and the presence of intermediate hosts, pigs or chickens, that serve as ecological and evolutionary bridges between waterfowl and humans (Bulaga et al. 2003; Liu et al. 2003; Webster 2004; Webster & Hulse 2004). How easily could α2,6-adapted mutant viruses invade in these different environments, and would they be able to coexist in the long run with α2,3-adapted resident viruses?

Here, we first ask how the host range of influenza changes with tradeoff strength in a neutral ecological model—except for differences in their receptors, host species are identical. We then adopt more realistic assumptions and explore how evolutionary dynamics are modulated by two major components of influenza's ecology, interspecific contact rates and the relative abundances of different host species.

Methods

Epidemiological dynamics

We consider a community with three host populations. One population, with density N_r, represents the waterfowl reservoir and has only α2,3-receptors. Another population, with density N_t, represents the "target" population (e.g., cats or humans) and has only α2,6-receptors. The third population, with density N_m, represents intermediate hosts such as pigs and chickens that possess both receptor types. We assume there are contacts between the reservoir and intermediate host (N_r and N_m) and between the intermediate and target hosts (N_m and N_t), but not between the reservoir and target host (figure 5.1a).

Epidemiological dynamics follow the susceptible-infected-recovered-susceptible (SIRS) model. The transition from recovered to susceptible indirectly captures two processes: the replenishment of susceptibles via birth and death processes and loss of immunity in recovered individuals due to antigenic evolution by the pathogen. Because our analysis considers only equilibrium numbers of susceptibles, infecteds, and recovereds, the SIRS model can represent the general features of a disease in a host population, such as a high level of immunity and low prevalence, or a high growth rate of the pathogen.

We initially assume that contact rates are frequency-dependent, with the interspecific transmission coefficient from host species j to species i, β_{ij}, equaling the average of the two corresponding intraspecific transmission coefficients scaled by a parameter c (Dobson 2004),

$$\beta_{ij} = \beta_{ji} = c\,\frac{\beta_{ii} + \beta_{jj}}{2}\ . \tag{2.1}$$

Whether a contact results in transmission depends on the host's receptor type and the virus's receptor preference p. We define p as the probability of infecting via an α2,6-receptor; a perfect α2,6-specialist thus has $p = P(\alpha 2,6) = 1$. The probability of infecting via an α2,3 receptor, $P(\alpha 2,3)$, is related to $P(\alpha 2,6)$ through a tradeoff with strength s (Egas et al. 2004),

$$P(\alpha 2,3)^{1/s} + P(\alpha 2,6)^{1/s} = 1\ . \tag{2.2}$$

The tradeoff can be tuned to be weak ($s < 1$) or strong ($s > 1$). For later reference, we introduce three broad categories of viral phenotypes: α2,6 specialists, α2,3 specialists, and generalists. We further classify specialization as "low" or "high." We consider an α2,6-specialist to have a low degree of specialization if $0.5 < P(\alpha 2,6) - P(\alpha 2,3) < 0.8$ and a high degree of specialization if $P(\alpha 2,6) - P(\alpha 2,3) \geq 0.8$. The criteria for α2,3-specialization are analogous. A virus is considered adapted to a receptor if it is specialized to that receptor. Generalist preferences comprise the remaining cases, $|P(\alpha 2,6) - P(\alpha 2,3)| \leq 0.5$ (figure 5.1b).

Epidemiological dynamics in our model are represented by six ordinary differential equations. These equations follow from the rates $\mathrm{d}S/\mathrm{d}t$ and $\mathrm{d}I/\mathrm{d}t$ at which the number of susceptible and infected hosts change in each of the three host species. Since we assume constant population sizes, the rates $\mathrm{d}R/\mathrm{d}t$ at which the number of recovered hosts changes in each of the three host species follow from those equations. For each host i = r, m, t, the rate of susceptible replenishment is given by γ_i, the rate of infection by λ_i, and the rate of recovery by ν_i. Below we explicitly show the equations for each state of the intermediate host,

$$\frac{dS_m}{dt} = \gamma_m R_m - \lambda_m S_m, \tag{2.3a}$$

$$\frac{dI_m}{dt} = \lambda_m S_m - \nu_m I_m, \tag{2.3b}$$

$$\frac{dR_m}{dt} = \nu_m I_m - \gamma_m R_m, \tag{2.3c}$$

and with the force of infection, λ_m, given by

$$\lambda_m = \max[P(\alpha 2,3), P(\alpha 2,6)] \left(\frac{\beta_{mr} I_r}{N_r + cN_m} + \frac{\beta_{mm} I_m}{cN_r + N_m + cN_t} + \frac{\beta_{mt} I_t}{cN_m + N_t} \right). \tag{2.3d}$$

Parameter c performs the same function as before, scaling the relative frequency of susceptibles of other species i perceived by an infected of species j (as $c \to 0$, all transmission becomes intraspecific). In equation 2.1, parameter c describes how interspecific contact rates relate to intraspecific contact rates, which there scale only with the densities of susceptible and infected individuals. To obtain the force of infection with frequency dependent transmission, the same parameter is used again to scale the total population sizes of the other species.

Equations for the other hosts are analogous (supplementary material). As equation 2.3d illustrates, in our model, infection of the intermediate host occurs via the receptor type to which the infecting virus is better adapted.

Evolutionary dynamics

To model the evolution of host range, we test the ability of a mutant virus with receptor preference p_1 to invade a system of hosts infected with a resident virus of preference p_2. To constrain the problem, we assume that, in each host class, the resident virus has reached the endemic equilibrium, and that the ability of the mutant to invade the resident is given by its instantaneous growth rate when rare in the environment determined by the resident. This growth rate, which is also known as the mutant's invasion fitness in the resident's environment (Metz et al. 1992), is given by the dominant eigenvalue of the Jacobian of the rare mutant's epidemiological dynamics (supplementary material).

Entries (i,j) of this matrix describe the rate per mutant-infected host in class j at which the abundance of mutant-infected hosts in class i grows through transmission from those in class j when mutant-infected hosts are rare. The endemic equilibrium and the dominant eigenvalue were calculated numerically (since both are determined by polynomial equations with orders in excess of four).

By solving for the growth rate of every possible mutant phenotype against every possible resident phenotype, we can obtain pairwise invasibility plots (PIPs). PIPs show which phenotypes are uninvasible once reached and which phenotypes can be reached through the succession of small and advantageous mutational steps. The former phenotypes are called evolutionarily stable, the latter convergence stable. Our assumptions and approach are an application of the theory of adaptive dynamics (Dieckmann & Law 1996; Geritz et al. 1998; Metz et al. 1996).

Results

Effects of tradeoff strength in a neutral ecology

We first examine how host range evolves when the host populations are identical in every respect but their receptors: hosts share the same population sizes and rates of birth, death, transmission, recovery, and susceptible replenishment, but their receptors vary (figure 5.1a). For simplicity, we assume interspecific transmission rates equal intraspecific transmission rates ($c = 1$).

For very weak tradeoffs (in figure 5.2a, $s = 0.05$, $s = 0.25$, and $s = 0.5$), a complicated dynamic emerges. The pairwise invasibility plots show two strategies that are both evolutionarily and convergence stable, but only locally. Which strategies are realized depends on the phenotype of the initial resident and the mutational step size. For $s = 0.5$, starting from a perfect $\alpha 2,3$ specialist (resident $p = 0$), mutants that are, relative to the resident, slightly better adapted to the target host can invade up to $p \approx 0.23$ (at this point, $P(\alpha 2,3) \approx 0.97$). If mutations are always small, this resident, which shows a low degree of $\alpha 2,3$ specialization, will persist indefinitely. However, there is evidence that in at least some subtypes, single mutations can effect large changes in receptor-binding properties (Matrosovich et al. 2000; Tumpey et al. 2007). If mutations are large, mutants

with p higher than ≈ 0.7 can still invade. Invasions by mutants with successively higher p could push the resident strategy to $p \approx 0.97$ (where $P(\alpha 2,3) \approx 0.23$, corresponding to low $\alpha 2,6$ specialization). This other attractor is also locally evolutionarily and convergence stable.

As the tradeoff strengthens, the two local attractors disappear, and only the repellor previously separating them remains. The two perfect specialists ($p = 0$ and $p = 1$) become evolutionary end points. If mutational step sizes are small, only one perfect specialist will arise from a given starting condition. For example, if $s = 0.75$, a resident starting at $p = 0.5$ can be progressively invaded by mutants with slightly smaller p until arriving at perfect $\alpha 2,3$ specialization. As before, which specialist appears depends on the phenotype of the initial resident. The plot also shows that if mutational step sizes are large, a mutant better adapted to $\alpha 2,6$-receptors (i.e., with $P(\alpha 2,6)$ above ≈ 0.7) could invade against a perfect $\alpha 2,3$ resident and evolve increasing $\alpha 2,6$ specialization, and vice-versa.

Assuming that large mutations can occur and that multiple specialists are able to arise, will they coexist? Reflecting the plots across the main diagonal reveals areas of mutual invasibility, or coexistence: both the mutant and the resident have positive fitness in the background of the other type. Evaluating the selection gradient in the regions of coexistence shows whether this coexistence is transient or evolutionarily stable. When the tradeoff is very weak ($s = 0.05$, 0.25, and 0.5), we see the basins of attraction for the equilibria described previously (figure 5.2b). In addition, in the middle of the region of coexistence, we find a third attractor that is also locally evolutionarily stable. This kind of attractor is also known as a singular coalition (Geritz et al. 1998) [for a casual introduction, see Brännström and Festenberg (undated)]. At $s = 0.5$, this attractor occurs where one resident is highly $\alpha 2,6$-specialized and the other is highly $\alpha 2,3$ specialized. For stronger tradeoffs ($s = 0.75$ and above), this attractor is absent, and we find perfect specialists can coexist as evolutionary end points.

In summary, a neutral ecology almost always gives rise to pairs of specialists that are able to coexist in the long run; generalists only appear when the tradeoff is extremely weak ($s = 0.05$). These results appear robust for reasonable ecological parameters (figures

5.S1 and 2.S2). Our analysis up to this point reveals several further features of the evolution of host range in this system. First, PIPs are not anti-symmetric, that is, they are not invariant under reflection about the main diagonal and the subsequent exchange of signs. This demonstrates that selection for receptor preference is frequency-dependent [PIPs under frequency-independent selection are always anti-symmetric; Meszéna et al. (2001)]. Second, evolutionary branching, i.e., the endogenous generation of two different phenotypes from a single phenotype through frequency-dependent disruptive selection (Metz et al. 1992; Geritz et al. 1998), cannot occur in this system for a wide range of plausible ecological parameters (supplementary material). In other words, when a phenotype in our system is convergence stable, it will always experience stabilizing selection. Third, we find that once the tradeoff increases so that perfect specialists are evolutionary end points, further increases in tradeoff strength have virtually no effect on the invasion potential of strong α2,6-specialists. When perfect α2,3-specialists are endemic, approximately the same phenotypic threshold ($P(\alpha 2,6) \approx 0.7$) governs invasions by α2,6-specialists.

Effects of host ecology

We explored how our results might be affected by ecological features that are relevant to influenza. First, we allow hosts to vary in their rates of transmission, recovery, and loss of infectiousness. Next, we introduce a modified version of the model that might better capture the dynamics of fecal-oral and confined aerosol transmission between and within the reservoir and intermediate host. We then examine the effects of two possible long-term intervention strategies: changing the densities of intermediate and target hosts and the rates of mixing between different host species.

Differences in host demography and epidemiology

Natural host populations of influenza differ markedly in their quality, determined not only by their receptors but also demographic and epidemiologic rates. We consider two main features of host populations, the rate of susceptible replenishment γ and the intrinsic reproductive rate of the pathogen, R_0, that each population allows.

Parameter γ in equations 2.3a and 2.3c traditionally represents replenishment of the susceptible population through loss of immunity. It can also be used to regulate the densities of S^*, I^*, and R^* at equilibrium, and thereby approximate the effects of birth, death, immigration, and emigration. We choose a relatively high value of γ (1/3 and 1/6 months^{-1}) for the reservoir and intermediate host, respectively, essentially claiming that a recovered individual will, on average, be replaced every three or six months by a susceptible. In the intermediate host, replacement mainly occurs through culling or sale. In waterfowl, it occurs mainly through loss of immunity and migration (Kida et al. 1980). We initially assume that γ is approximately fourfold smaller in the target host (i.e., 1/2 y^{-1}). This choice reflects the characteristic temporal scale of influenza's antigenic evolution in humans, the longer life span of the target population, and a high rate of immigration and emigration events.

Better estimates are available of epidemiologic rates of transmission and recovery among influenza's different hosts (supplementary material). A measure of a pathogen's fitness in a population is the intrinsic reproductive number, R_0, which equals the total number of secondary infections caused by the index case in a susceptible population. For the intermediate host, the total number of secondary cases (in all species) is

$$R_0 = \frac{\beta_{wm} + \beta_{mm} + \beta_{tm}}{\nu_m}. \qquad (2.4)$$

The intraspecific R_0, or total number of secondary cases in the intermediate host population, is β_{mm}/ν_m. Our parameters yield the maximum possible intraspecific R_0 in the reservoir ($R_0 = 4$ for a perfect α2,3 specialist), lowest in the target host ($R_0 = 1.5$ for a perfect α2,6 specialist) and an intermediate R_0 in the intermediate host ($R_0 = 1.75$ for either perfect specialist). These choices of R_0 and γ allow the highest prevalences (I^*) to be reached in the reservoir, and the highest levels of immunity (R^*) in the target host.

Changing the quality of the different host patches predictably breaks the symmetry in evolutionary outcomes. In general, if interspecific transmission rates equal intraspecific rates ($c = 1$) and the tradeoff is not especially weak (not $s = 0.05$ or 0.25) or

strong (s = 1.5), perfect α2,3 specialists will tend to dominate: they are the evolutionary end point from the majority of starting strategies, assuming small mutational step sizes (figures 5.S3-2.S5). Even if large mutations were possible, α2,6 specialists often cannot invade α2,3 residents, or invasion is allowed for only perfect or nearly perfect α2,6 specialists. This restriction on α2,6-specialist invasion is influenced more by hosts' differences in maximum possible growth rates (R_0) than rates of susceptible replenishment, γ. If all host species have the same R_0, poor α2,6 specialists can invade against a background of perfect α2,3 specialists even when susceptible replenishment in the target population is extremely slow (e.g., $\gamma_t = 1/20\ y^{-1}$) relative to the reservoir ($\gamma_r = 1/90\ d^{-1}$) (figure 5.S3c,d). The two specialists will furthermore coexist evolutionarily. Increasing the maximum potential fitness of viruses in the reservoir eliminates this possibility (figure 5.S5).

Density dependent transmission

Influenza viruses appear to be transmitted predominantly by the fecal-oral route in wild waterfowl via contamination of shared water sources (Webster et al. 1992). Water is presumably the route by which they infect domesticated animals, including pigs and chickens. Pigs and chickens in confined feeding operations, whether commercial or family-owned, crowd at high densities and permit aerosol transmission (Alexander 2000; Brown 2000; Ly et al. 2007). We assume that rates of waterborne and aerosol transmission in confined areas scale more closely with the densities of infected individuals than the frequencies of infecteds in the population. This assumption corresponds to density-dependent transmission. Aerosol transmission by the potential target hosts is better represented by frequency dependence, as rates of contact between target and intermediate hosts are a saturating function [effectively, predation events; Ly et al. (2007) and Thiry et al. (2007)].

Our modified model thus assumes density-dependent transmission within and between the reservoir and intermediate host and frequency-dependent transmission in the target host and between the target and intermediate host. For further analysis, we decouple the relative interspecific transmission parameter into c_I for transmission

between the reservoir and intermediate host and c_2 for transmission between the intermediate and target hosts.

The force of infection perceived by the intermediate host, analogous to equation 2.3d above, becomes:

$$\lambda_m = \max[P(\alpha 2,3), P(\alpha 2,6)]\left(\beta_{mr} I_r + \beta_{mm} I_m + \frac{\beta_{mt} I_t}{c_2 N_m + N_t}\right). \quad (2.5)$$

The shift from frequency dependent to density dependent transmission requires a change in the value and dimensions of β_{ij} for $[i,j] \in \{\mathrm{m,r}\}$. We choose β_{ij} so that the initial growth rates in each host are identical to the frequency dependent case with $N_\mathrm{r} = N_\mathrm{m} = 100$. We let the density dependent interspecific transmission rates scale with the intraspecific transmission rates of the infecting species:

$$\beta_{rm} = c_1 \beta_{mm} \quad (2.6a)$$

$$\beta_{mr} = c_1 \beta_{rr} \quad (2.6b)$$

$$\beta_{mt} = \beta_{tm} = c_2 \beta_{tt} \quad (2.6c)$$

A complete analytic description of the model is in equations 2.S3-2.S5 (supplementary material). The consequences of this form of transmission will be explored in the context of possible intervention strategies.

Intermediate and target host densities

The densities of the intermediate and target hosts have nonlinear effects on the ability of α2,6 specialists to invade perfect α2,3 specialists. In general, increasing the density of the intermediate host population diminishes the ability of α2,6 specialists to invade by large mutations when perfect α2,3 specialists are endemic. In contrast, increasing the density of the target host population improves the ability of α2,6-adapted viruses to

invade. These patterns hold for both frequency dependent and density dependent models, and in the neutral and non-neutral ecologies (figures 5.S6-2.S9).

There are nonetheless some notable quantitative differences in the evolutionary outcomes allowed by different models. Unsurprisingly, frequency-dependent transmission attenuates the effects of increasing densities. In otherwise neutral ecologies, even when the intermediate host is twice as large as the target host population, invasion by α2,6-adapted viruses with a low degree of specialization is still possible (figure 5.S6a); similarly, invasion by α2,6 specialists is still possible when the target host population is roughly a fifth as large as the other hosts (figure 5.S8). In an otherwise neutral ecology, density dependent transmission between the reservoir and intermediate host still permits α2,6-invasion when intermediate host density is quite large (figure 5.S6b). Incorporating species-specific differences in R_0 and susceptible replenishment greatly restricts the densities allowing α2,6-invasion (figures 5.S7 and 2.S9). For intermediate tradeoff strengths (e.g., $s = 0.75$ and $s = 1$), α2,6 specialists cannot invade and coexist if the target host density is lower than the densities of other species or if the intermediate host density exceeds that of the other species. Interestingly, the target and intermediate host densities that form the threshold for α2,6 specialist invasion do not vary substantially as tradeoff strength varies from $s = 0.25$ to $s = 1$ (figures 5.S7 and 2.S9). At a higher tradeoff strength ($s = 1.5$), both thresholds decrease.

Relative rates of interspecific transmission

The evolution of pathogens' host range is potentially affected not only by the qualities and sizes of different host patches but also by rates of contact between them. In particular, it is interesting to ask whether reducing the intermediate host's relative rate of contact with the reservoir population, c_1, has a greater effect on host range evolution than reducing rates of contact between the intermediate host and target population, c_2.

The ability of α2,6 specialists to invade and coexist with α2,3 residents increases as interspecific contact rates decline. This result holds when interspecific transmission rates are considered separately (as c_1 and c_2) in the density dependent case in both neutral and non-neutral ecologies (figures 5.S11 and 2.S12). It is also true in the frequency

dependent case when interspecific contact rates c_1 and c_2 are varied together as c (figure 5.S10). In neutral ecologies, the ability of α2,6 viruses to invade is slightly more sensitive to changes in interspecific contact between the target and intermediate hosts than between the reservoir and intermediate hosts (figures 5.S11a and 2.S12a). Nonetheless, a neutral ecology permits invasion of viruses with a low degree of α2,6 specialization even when interspecific contact rates are twice intraspecific rates. Under more realistic ecologies, opportunities are much more restricted (figures 5.S11b and 2.S12b). For all but the weakest tradeoffs, an increase in interspecific transmission c_1 between the intermediate host and reservoir will quickly limit the invasion potential of α2,6-adapted viruses. Between the intermediate and target hosts, a slightly greater increase in relative transmission c_2 is necessary to achieve the same effect.

Our findings show how the invasion potential of viral phenotypes is affected by tradeoff strength, target host density, and interspecific transmission. From this we can infer whether perfect α2,3- and α2,6-specialists can coexist in the absence of evolution. We find that, in general, coexistence is facilitated by low interspecific contact rates, a relatively low density of the intermediate host population, and a relatively high density of the target population (figure 5.3). In the frequency dependent model, such coexistence is stable even for high interspecific contact rates when the relative density of target hosts is high, and is stable even for low relative densities of target hosts when interspecific contact rates are low. Interestingly, these conditions appear relatively insensitive to tradeoff strength. Except at extremely weak tradeoffs ($s \approx 0.05$), ecological coexistence denotes evolutionary coexistence; if perfect specialists do not coexist in the long run, extremely well-adapted specialists do.

Discussion

We have shown how the evolution of host range, predicated on a single tradeoff, can be shaped by frequency-dependent selection, tradeoff strength, and host ecology. As expected, very weak tradeoffs favor generalist strategies. Unexpectedly, however, weak tradeoffs can promote the evolution and coexistence of viral phenotypes specialized on alternative receptor types, assuming large phenotypic mutations are possible. In that case,

both host ecology and tradeoff strength nonlinearly affect the ability of α2,6-adapted mutants to invade when α2,3-specialists are resident. The invasion of α2,6-adapted viruses is facilitated by low interspecific contact rates, small populations of intermediate hosts, and high densities of target hosts.

Tradeoff strength varies among influenza viruses. Viable intermediate phenotypes with dual receptor functionality have been reported for some subtypes and clades, but not for others. Matrosovich et al. (2001) identified a lineage of H9N2 from wild aquatic birds and poultry that retained relatively high binding affinity for both ovomucoid (α2,3-receptors) and pig macroglobulin (α2,6-receptors). Experimental mutation of H5N1 also yielded seemingly infectious viruses with intermediate binding affinities (Harvey et al. 2004). In contrast, strains of H1N1, H2N2, and H3N2 from humans and pigs showed only weak affinity for α2,3-sialosides, and a complete change in receptor preference resulting from only a few amino acid substitutions (Matrosovich et al. 2000; Tumpey et al. 2007). Our simple model predicts that subtypes with higher tradeoff strengths would more readily give rise to the long-term (evolutionary) coexistence of nearly perfect specialists. This pattern is in accordance with the observation that the subtypes that have circulated in humans (H1N1, H2N2, and H3N2) show evidence of affinity either to α2,3 or α2,6 receptors, but not both simultaneously.

Our results lend strong support to the idea that certain ecologies facilitate expansions of host range. We find that, fortunately, the coexistence of specialists is much more difficult in influenza's natural ecology than a neutral one. Assuming large mutations are possible, the invasion of α2,6-specialists is promoted by low interspecific contact rates, small intermediate host populations, and large target host populations. These changes increase the fraction of hosts that are susceptible to α2,6-mutants by limiting exposure to α2,3-viruses in the intermediate host. Low contact rates c_1 between the reservoir and intermediate host enable α2,6 invasion by preserving a larger fraction of susceptibles in the intermediate host population. Low interspecific contact rates c_2 reduce the fraction of target hosts' contacts to intermediate hosts, which are apt to be resistant to infection from exposure to α2,3-adapted viruses. This reduction opposes a potential "dilution effect" of wasting contacts on incompetent (here, immune) hosts (Schmidt &

Ostfeld 2001). While the effect of increasing the population of the target host is unsurprising, a less intuitive result is that large intermediate host populations, by supporting increased transmission of α2,3-adapted viruses with the reservoir, thereby reduce the fraction of hosts potentially susceptible to α2,6-adapted viruses. Of course, large populations of intermediate hosts in nature could pose an increased risk for emergence if host density correlates with increased genetic diversity of the pathogen, and thus provides more mutant phenotypes (of potentially larger phenotypic range) on which selection can act. This result nonetheless underscores the major roles of immunity in the intermediate host population and rates of contact between target and intermediate hosts.

Notably, the effects of interspecific contact rates and host densities are nonlinear, indicating that small changes in host ecology can induce major shifts in viral phenotypes. In an environment where avian-adapted influenza is endemic, random mixing ($c = 1$) of hosts provides a natural inoculum for the community that prevents α2,6-adapted viruses from invading. Invasion of α2,6 specialists is more efficiently obtained by reducing contact rates between the intermediate and target hosts than intermediate hosts and the reservoir. Increasing the density of the target host so that it is larger than the other populations, or decreasing the intermediate host population to roughly one-tenth its former size, also allows invasion by α2,6-adapted specialists.

Our model makes general predictions about the long term evolution of pathogens facing tradeoffs in simple ecologies, but further investigations into the nonequilibrium dynamics of emergence would be useful. Influenza is seasonal in most animals, and transmission rates are likely also seasonal (Brown 2000; Halvorson et al. 1985; Munster et al. 2007; Viboud et al. 2006). If the amplitude of oscillations in the actual disease dynamics is sufficiently high, equilibria of viral evolution can be different from those predicted here (White et al. 2006).

Increasing genetic detail on receptor specificity in different viruses will also help address questions of evolutionary accessibility; the tradeoff between α2,3- and α2,6-preference is only a first-order approximation of binding ability (Gambaryan et al. 2005), and receptor binding ability is one small, though critical, component of host range (Baigent & McCauley 2003). It might be feasible to model additional adaptations

indirectly as a change in the tradeoff strength, which we might expect to weaken over time (i.e., as increasingly better "molecular compromises" are found at the receptor-binding site and also in other genes). It is also important to recognize the fundamentally probabilistic nature of adaptation. Though we considered our threshold for invasion to be positive growth of the mutant when rare, negative growth rates in nature stochastically generate chains of transmission that can be long enough to allow significant adaptation and ultimately positive growth (Andre & Day 2005; Antia et al. 2003). In other words, it may be possible for α2,6-adapted viruses to gain a foothold outside the areas of positive growth in the plots presented here.

This work shows that the evolution of host range may be as sensitive to ecological considerations as the physiological details of adaptation. The long term diversity of influenza viruses, for all realistic tradeoffs, is highly sensitive to host contact rates and population sizes. Naturally or artificially acquired immunity in the intermediate host and diluting contacts among competent hosts are key to reducing the long-term ability of α2,6-adapted viruses to persist.

Figure 5.1. Contact network and tradeoff in receptor preference. (a) Contact network, showing receptor conformations in three classes of host population: reservoir hosts (waterfowl; r), intermediate hosts (pigs and chickens; m), and target hosts (humans; t). Total host densities in each class are denoted by N_i with i = r, m, t. (b) Tradeoff for receptor preference. The strength of the tradeoff is given by s, with $s < 1$ characterizing a weak tradeoff and $s > 1$ a strong tradeoff. Moving away from the origin, the curves correspond to s = 1.5, 1, 0.75, 0.5, 0.25, and 0.05. Colors show degree of specialization on the nearby receptor: red (high specialization), orange (low specialization), and blue (no specialization: generalist).

(a)

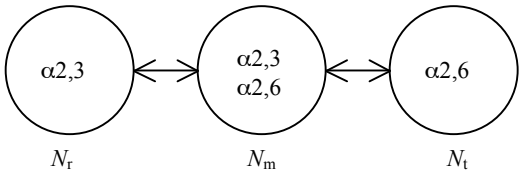

(b)

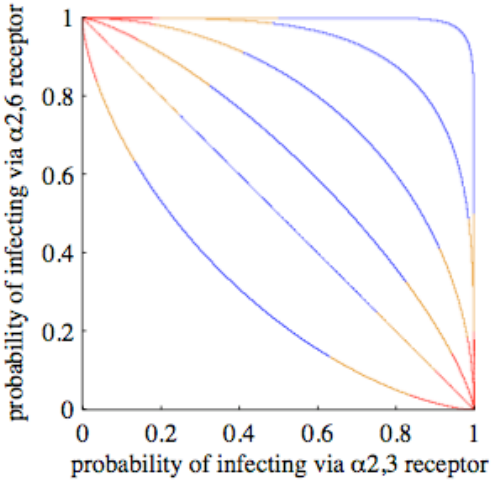

Figure 5.2. Evolutionary outcomes in a neutral ecology. (a) Pairwise invasibility plots for different tradeoff strengths s for $N_t = N_m = N_r$ and $c = 1.0$, $\beta_{rr} = \beta_{mm} = \beta_{tt} = 1/3$ days^{-1}, $\nu_r = \nu_m = \nu_t = 1/6$ days^{-1}, and $\gamma_r = \gamma_m = \gamma_t = 1/180$ days^{-1}. Black (white) areas indicate where the mutant has a positive (negative) growth rate in the endemic environment determined by the resident. Gray areas indicate regions in which the resident phenotype is not viable. (b) Trait evolution plots for the pairwise invasibility plots in (a). Gray areas indicate phenotype pairs that are mutually invasible. Black lines are isoclines and black circles correspond to evolutionary attractors if filled and repellors if open. Arrows show the direction at the quadrant level of selection pressure. For readability, they are shown here only for the largest bounded regions.

Figure 5.2

(a)

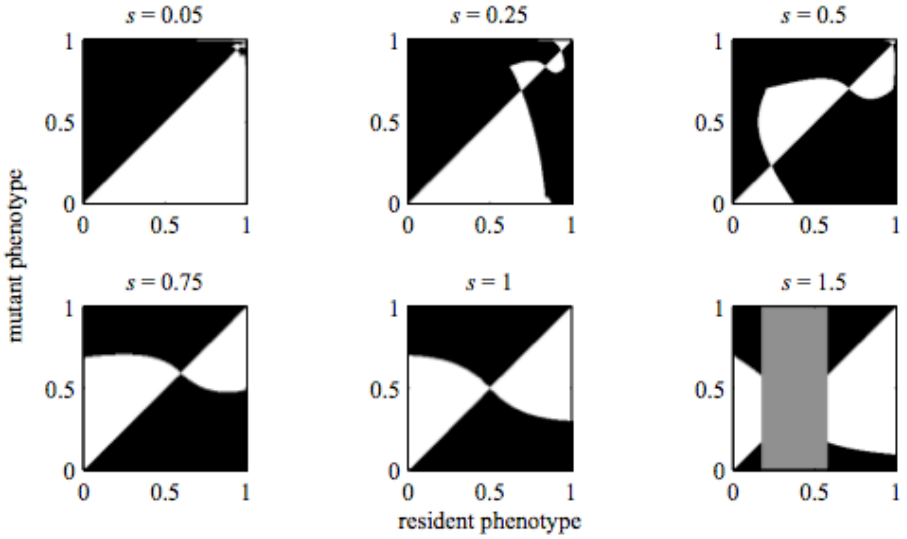
s = 0.05
s = 0.25
s = 0.5
s = 0.75
s = 1
s = 1.5
mutant phenotype
resident phenotype
0
0.5
1

(b)

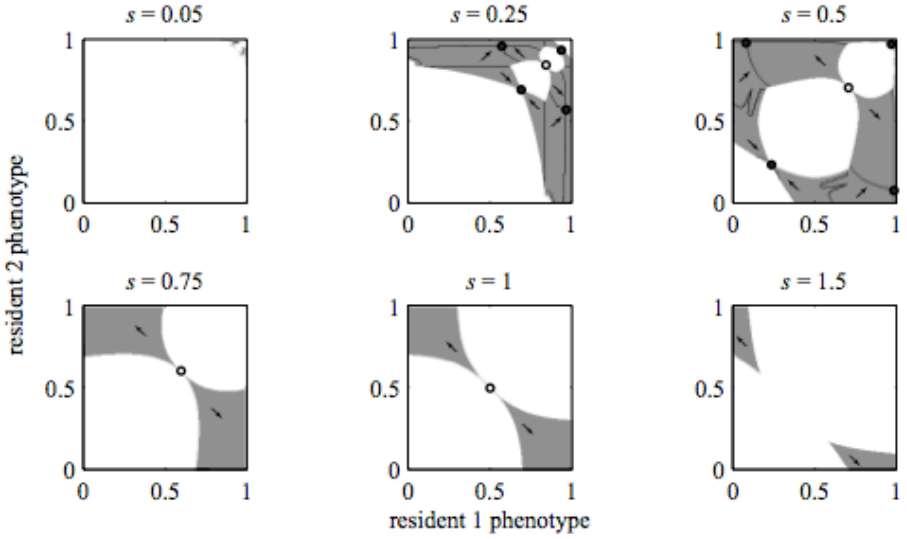
s = 0.05
s = 0.25
s = 0.5
s = 0.75
s = 1
s = 1.5
resident 2 phenotype
resident 1 phenotype
0
0.5
1

Figure 5.3. Conditions that permit the coexistence of perfect specialists. The model assumes frequency dependent transmission, realistic host ecological parameters (table 5.S1), and a neutral tradeoff ($s = 1$). The combinations that permit specialists' coexistence are in gray. Coexistence is evolutionarily stable for higher tradeoffs ($s = 0.75$ and above) but not the weaker tradeoffs; however, even at weaker tradeoffs extremely well adapted viruses are able to coexist (see text, fig. 2.2). (a) Intermediate host's relative population density N_m/N_r ($= N_m/N_t$) and relative rate of contact with the reservoir, c_1. (b) Target host's relative population density, N_t/N_r ($= N_t/N_m$), and relative rate of contact with the intermediate host, c_2.

(a)

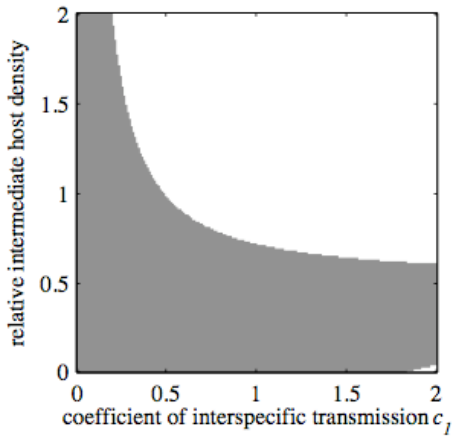

(b)

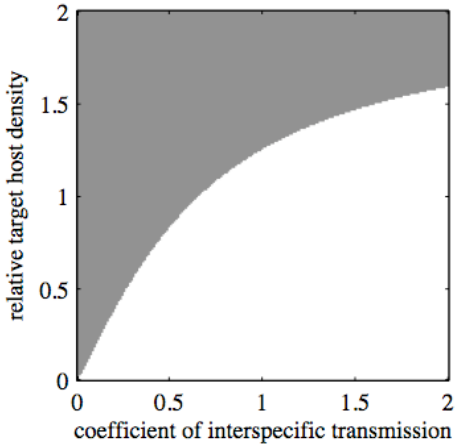

Supplementary material

SIRS equations for reservoir and target hosts

SIRS equations for the intermediate host are given in the main text (eqs. 2.3a-c). Corresponding equations for the reservoir are:

$$\frac{dS_r}{dt} = \gamma_r R_r - P(\alpha 2,3)\left(\frac{\beta_{rr} I_r}{N_r + cN_m} + \frac{\beta_{rm} I_m}{cN_r + N_m + cN_t}\right) S_r \tag{2.S1a}$$

$$\frac{dI_r}{dt} = P(\alpha 2,3)\left(\frac{\beta_{rr} I_r}{N_r + cN_m} + \frac{\beta_{rm} I_m}{cN_r + N_m + cN_t}\right) S_r - \nu_r I_r \tag{2.S1b}$$

$$\frac{dR_r}{dt} = \nu_r I_r - \gamma_r R_r \tag{2.S1c}$$

SIRS dynamics for the target host population are analogous:

$$\frac{dS_t}{dt} = \gamma_t R_t - P(\alpha 2,6)\left(\frac{\beta_{tt} I_t}{N_t + cN_m} + \frac{\beta_{tm} I_m}{cN_r + N_m + cN_t}\right) S_t \tag{2.S2a}$$

$$\frac{dI_t}{dt} = P(\alpha 2,6)\left(\frac{\beta_{tt} I_t}{N_t + cN_m} + \frac{\beta_{tm} I_m}{cN_r + N_m + cN_t}\right) S_t - \nu_t I_t \tag{2.S2b}$$

$$\frac{dR_t}{dt} = \nu_t I_t - \gamma_t R_t \tag{2.S2c}$$

Jacobian of system with frequency-dependent transmission

The Jacobian of this system shows the instantaneous rates of growth from an infected of class j to susceptibles of class i.

$$J = \begin{bmatrix} P_1(\alpha 2,3)\left(\frac{\beta_{rr} S_r^*}{N_r + cN_m}\right) - \nu_r & P_1(\alpha 2,3)\left(\frac{\beta_{rm} S_r^*}{cN_r + N_m + cN_t}\right) & 0 \\ \max[P_1(\alpha 2,3), P_1(\alpha 2,6)]\left(\frac{\beta_{mr} S_m^*}{N_r + cN_m}\right) & \max[P_1(\alpha 2,3), P_1(\alpha 2,6)]\left(\frac{\beta_{mm} S_m^*}{cN_r + N_m + cN_t}\right) - \nu_m & \max[P_1(\alpha 2,3), P_1(\alpha 2,6)]\left(\frac{\beta_{mt} S_m^*}{cN_m + N_t}\right) \\ 0 & P_1(\alpha 2,6)\left(\frac{\beta_{mm} S_t^*}{cN_r + N_m + cN_t}\right) & P_1(\alpha 2,6)\left(\frac{\beta_{mt} S_t^*}{cN_m + N_t}\right) - \nu_t \end{bmatrix}$$

P_1 refers to the phenotype of the mutant virus.

Description of parameter values

We chose parameters in keeping with general observations on the relative growth rates of different influenza subtypes in different hosts (Webster et al. 1992) (table 5.S1):

- The rates of loss of immunity, γ_i, are qualitative estimates based on several observations. Rates are highest in waterfowl, since they appear to have little long-term immunity to influenza. The intermediate hosts, as domesticated animals, also have relatively high turnover. Turnover rates in the target population are low due to longer host life spans and long-lasting immunity (whose loss is here a proxy for antigenic evolution). However, we assume they are offset by relatively high host mobility (migration).
- The assumption of frequent, regular contact (suitable for transmission) between intermediate hosts and a target host population such as humans in both rural and more industrial settings is supported by serological surveys of pigs (Brown et al. 1995; Olsen et al. 2000; Yu et al. 2007), asymptomatic pig farm workers (Campitelli et al. 1997; Halvorson et al. 1983; Karunakaran et al. 1983; Myers et al. 2006; Olsen et al. 2002; Sivanandan et al. 1991), and poultry workers (Koopmans et al. 2004).

SIRS equations for model with density-dependent transmission

All parameters and variables are as defined in the main text.

Reservoir, r

$$\frac{dS_r}{dt} = \gamma_r R_r - P(\alpha 2,3) S_r \left(\beta_{rr} I_r + \beta_{rm} I_m\right) \quad \text{(2.S3a)}$$

$$\frac{dI_r}{dt} = P(\alpha 2,3) S_r \left(\beta_{rr} I_r + \beta_{rm} I_m\right) - \nu_r I_r \quad \text{(2.S3b)}$$

$$\frac{dR_r}{dt} = \nu_r I_r - \gamma_r R_r \quad \text{(2.S3c)}$$

Intermediate host, m

$$\frac{dS_m}{dt} = \gamma_m R_m - \max[P(\alpha 2,3), P(\alpha 2,6)] S_m \left(\beta_{mr} I_r + \beta_{mm} I_m + \frac{\beta_{mt} I_t}{c_2 N_m + N_t} \right) \quad \text{(2.S4a)}$$

$$\frac{dI_m}{dt} = \max[P(\alpha 2,3), P(\alpha 2,6)] S_m \left(\beta_{mr} I_r + \beta_{mm} I_m + \frac{\beta_{mh} I_h}{c_2 N_m + N_t} \right) - \nu_m I_m \quad \text{(2.S4b)}$$

$$\frac{dR_m}{dt} = \nu_m I_m - \gamma_m R_m \quad \text{(2.S4c)}$$

Target host, t

$$\frac{dS_t}{dt} = \gamma_t R_t - P(\alpha 2,6) S_t \left(\frac{\beta_{mm} I_m}{c_2 N_t + N_m} + \frac{\beta_{tt} I_t}{N_t + c_2 N_m} \right) \quad \text{(2.S5a)}$$

$$\frac{dI_t}{dt} = P(\alpha 2,6) S_t \left(\frac{\beta_{mm} I_m}{c_2 N_t + N_m} + \frac{\beta_{tt} I_t}{N_t + c_2 N_m} \right) - \nu_t I_t \quad \text{(2.S5b)}$$

$$\frac{dR_t}{dt} = \nu_t I_t - \gamma_t R_t \quad \text{(2.S5c)}$$

Figure 5.S1. Evolutionary outcomes in a neutral ecology (intraspecific $R_0 = 1.5$). Pairwise invasibility (a) and trait evolution (b) plots for hosts that are identical except for their receptor preferences. Parameters are identical to figure 5.2, except $\nu_r = \nu_m = \nu_t = 1/4.5$ days^{-1}. Gray areas in (a) indicate regions where the resident is inviable, whereas in (b) they denote regions of coexistence. In the trait evolution plots, black lines are isoclines and black circles correspond to evolutionary attractors if filled and repellors if open. Arrows show the direction at the quadrant level of selection pressure. For clarity, they are sometimes shown extending outside the plot, though phenotypes are bounded by the axes.

Figure 5.S1

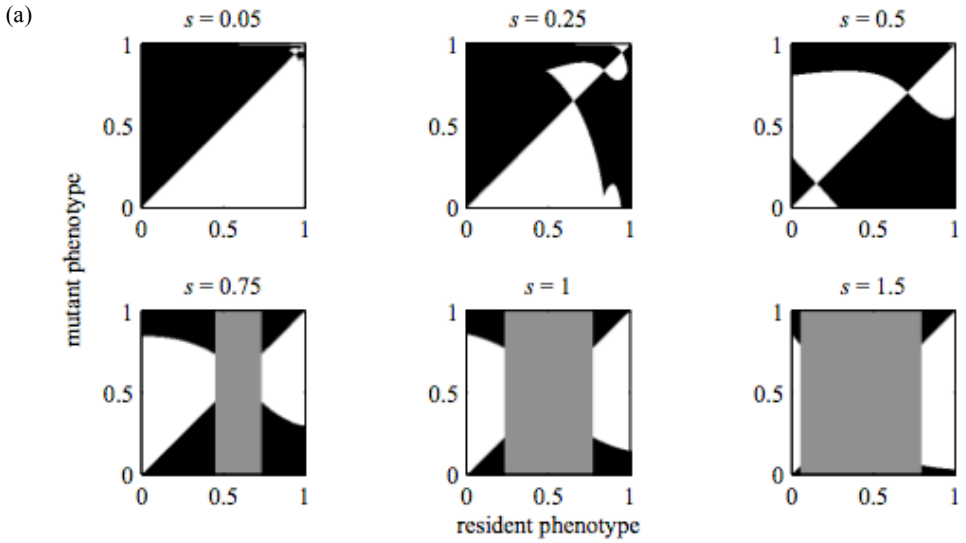
(a)
s = 0.05
s = 0.25
s = 0.5
s = 0.75
s = 1
s = 1.5
mutant phenotype
resident phenotype
0
0.5
1

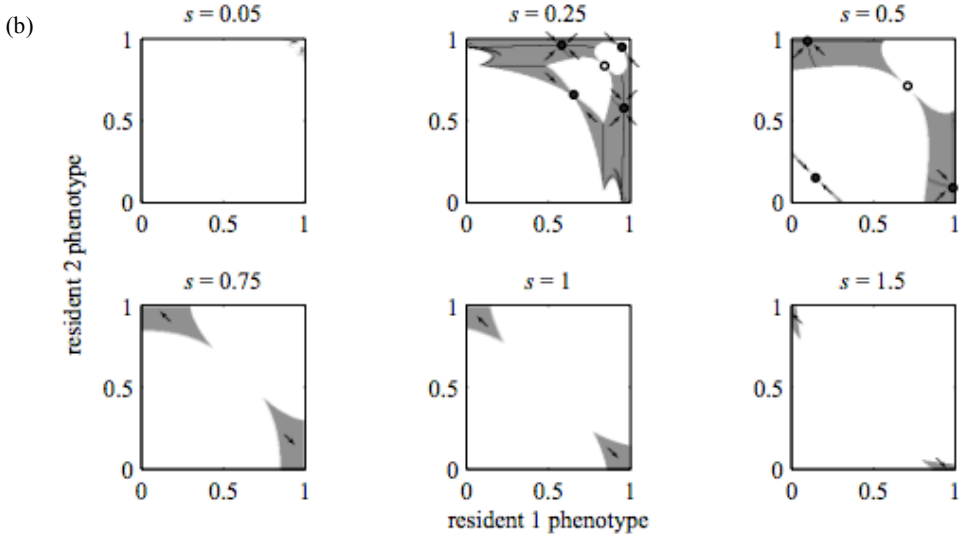
(b)
s = 0.05
s = 0.25
s = 0.5
s = 0.75
s = 1
s = 1.5
resident 2 phenotype
resident 1 phenotype
0
0.5
1

Figure 5.S2. Evolutionary outcomes in a neutral ecology (intraspecific $R_0 = 4$). Pairwise invasibility (a) and trait evolution (b) plots for hosts that are identical except for their receptor preferences. Parameters are identical to figure 5.2, except $\nu_r = \nu_m = \nu_t = 1/12$ days^{-1}. Gray areas in (b) denote regions of coexistence. In the trait evolution plots, black lines are isoclines and black circles correspond to evolutionary attractors if filled and repellors if open. Arrows show the direction at the quadrant level of selection pressure. For clarity, they are sometimes shown extending outside the plot, though phenotypes are bounded by the axes.

Figure 5.S2

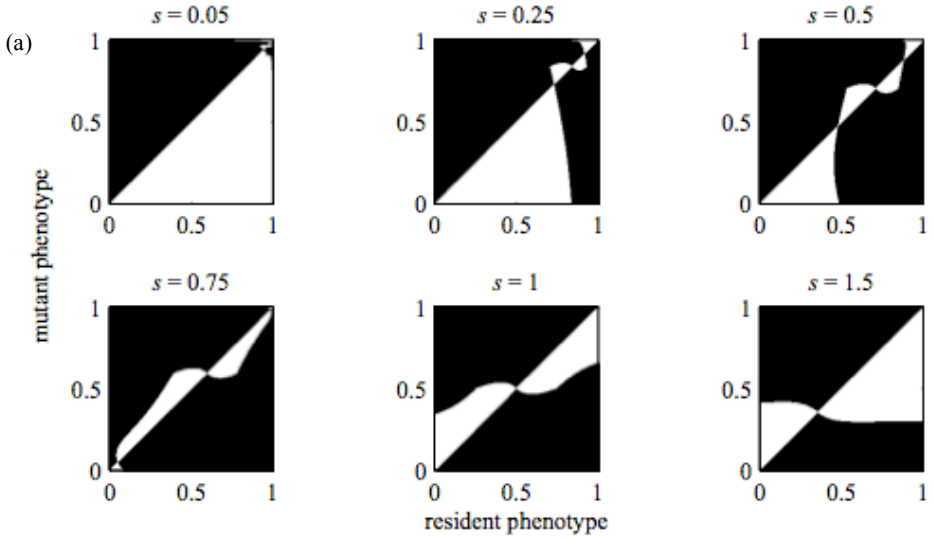
(a)
s = 0.05
s = 0.25
s = 0.5
s = 0.75
s = 1
s = 1.5
mutant phenotype
resident phenotype
0
0.5
1

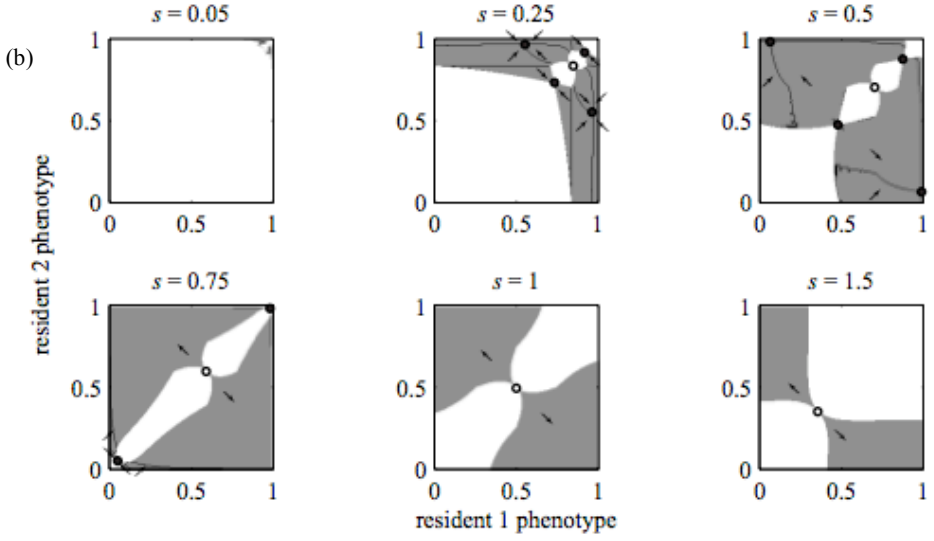
(b)
s = 0.05
s = 0.25
s = 0.5
s = 0.75
s = 1
s = 1.5
resident 2 phenotype
resident 1 phenotype
0
0.5
1

Figure 5.S3. Evolutionary outcomes when hosts differ in rates of susceptible replenishment. Pairwise invasibility (a, c) and trait evolution (b, d) plots for host populations differing in their rates of susceptible replenishment, γ but not R_0. In all plots, $\gamma_r = 1/90$ days^{-1} and $\gamma_m = 1/180$ days^{-1}. The intraspecific R_0 for all hosts is 2 ($\beta_{rr} = \beta_{mm} = \beta_{tt} = 1/3$ days^{-1}, $\nu_r = \nu_m = \nu_t = 1/6$ days^{-1}). Hosts have equal population sizes, interspecific transmission rates equal intraspecific rates ($c = 1$), and transmission rates are frequency dependent. In (a) and (b), $\gamma_t = 1/730$ days^{-1}. In (c) and (d), $\gamma_t = 1/7300$ days^{-1}. Gray areas in (a) indicate regions where the resident is inviable, whereas in (b) they denote regions of coexistence. In the trait evolution plots, black lines are evolutionary isoclines and black circles correspond to evolutionary attractors if filled and repellors if open. Arrows show the direction at the quadrant level of selection pressure. For clarity, they are sometimes shown extending outside the plot, though phenotypes are bounded by the axes.

Figure 5.S3

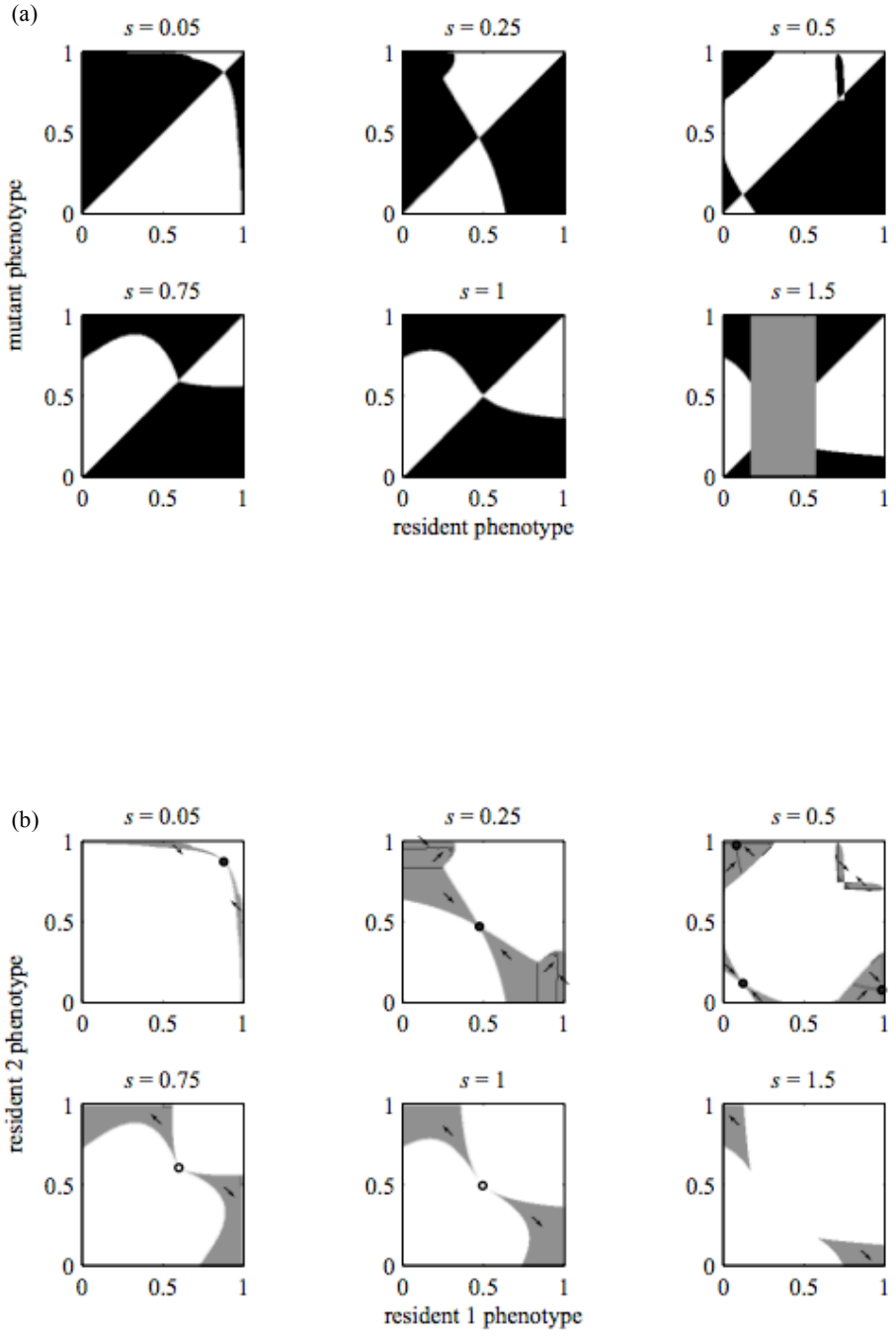
(a)
s = 0.05
s = 0.25
s = 0.5
s = 0.75
s = 1
s = 1.5
mutant phenotype
resident phenotype
(b)
s = 0.05
s = 0.25
s = 0.5
s = 0.75
s = 1
s = 1.5
resident 2 phenotype
resident 1 phenotype

Figure 5.S3 (continued)

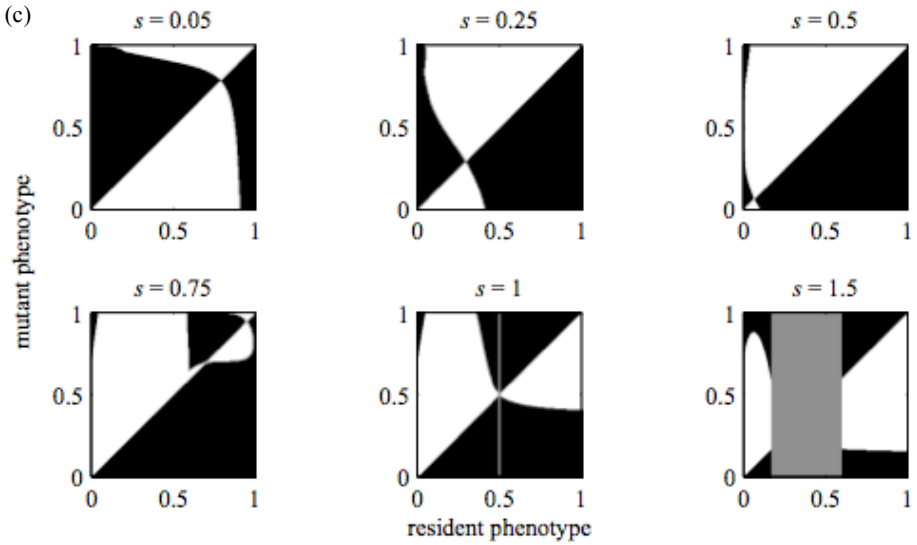

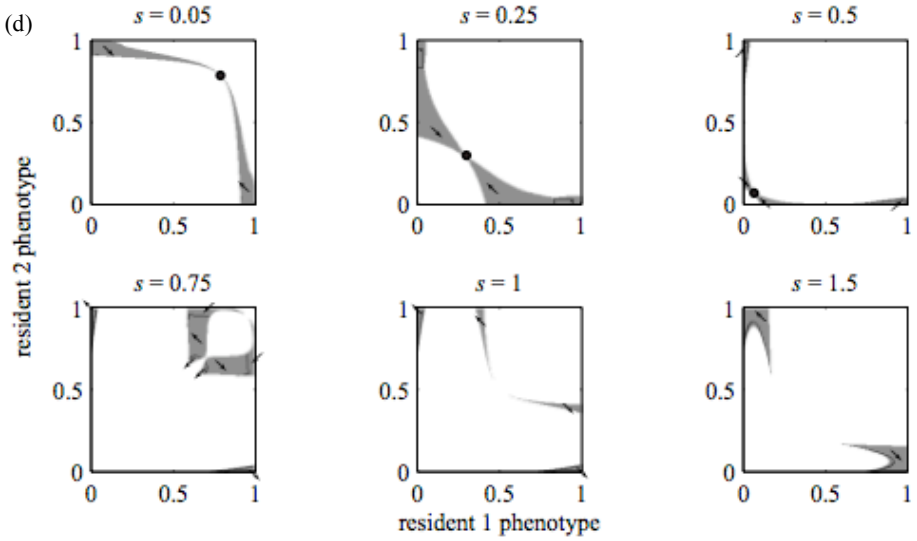

Figure 5.S4. Evolutionary outcomes when hosts differ in intraspecific R_0. Pairwise invasibility (a) and trait evolution (b) plots for host populations differing in their R_0 but not their rate of susceptible replenishment. Here, intraspecific R_0 is 4 in the reservoir (β_{rr} = 1/3 days^{-1}, ν_r = 1/12 days^{-1}), 1.75 in the intermediate host (β_{mm} = 1/4 days^{-1}, ν_m = 1/7 days^{-1}), and 1.5 in the target host (β_{tt} = 1/4 days^{-1}, ν_t = 1/6 days^{-1}), as in table 5.S1. Hosts have identical population sizes and rates of susceptible replenishment ($\gamma_r = \gamma_m = \gamma_t$ = 1/180 days^{-1}), interspecific transmission rates equal intraspecific rates (c = 1), and transmission rates are frequency dependent. Gray areas in (a) indicate regions where the resident is inviable, whereas in (b) they denote regions of coexistence. In the trait evolution plots, black lines are evolutionary isoclines and black circles correspond to evolutionary attractors if filled and repellors if open. Arrows show the direction at the quadrant level of selection pressure.

Figure 5.S4

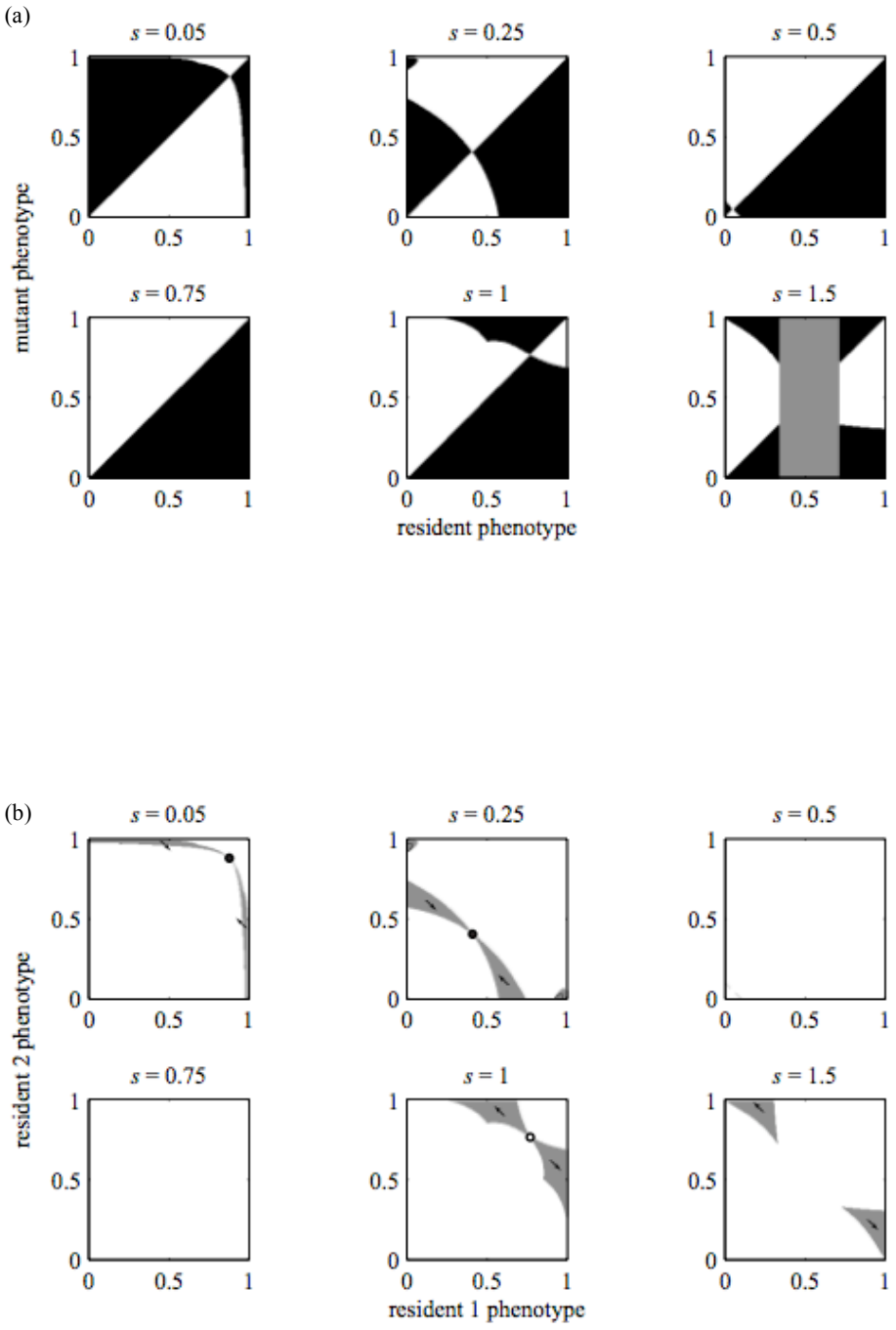
(a)
s = 0.05
s = 0.25
s = 0.5
s = 0.75
s = 1
s = 1.5
mutant phenotype
resident phenotype
(b)
s = 0.05
s = 0.25
s = 0.5
s = 0.75
s = 1
s = 1.5
resident 2 phenotype
resident 1 phenotype

Figure 5.S5. Evolutionary outcomes when hosts differ both in R_0 and rates of susceptible replenishment. Pairwise invasibility (a, c) and trait evolution (b, d) plots. Parameters are the same as those used for figure 5.S4, except where noted, and rates of susceptible replenishment are the same ones used for figure 5.S3 and listed in table 5.S1. For (c) and (d), intraspecific R_0 in the reservoir ($R_0 = 2$; $\nu_r = 1/6$ days^{-1}) is lower than in (a) and (b), though in both cases it is still higher than in the intermediate ($R_0 = 1.75$) and target hosts ($R_0 = 1.5$). Gray areas in (*a*) indicate regions where the resident is inviable, whereas in (b) they denote regions of coexistence. In the trait evolution plots, black lines are evolutionary isoclines and black circles correspond to evolutionary attractors if filled and repellors if open. Arrows show the direction at the quadrant level of selection pressure.

Figure 5.S5

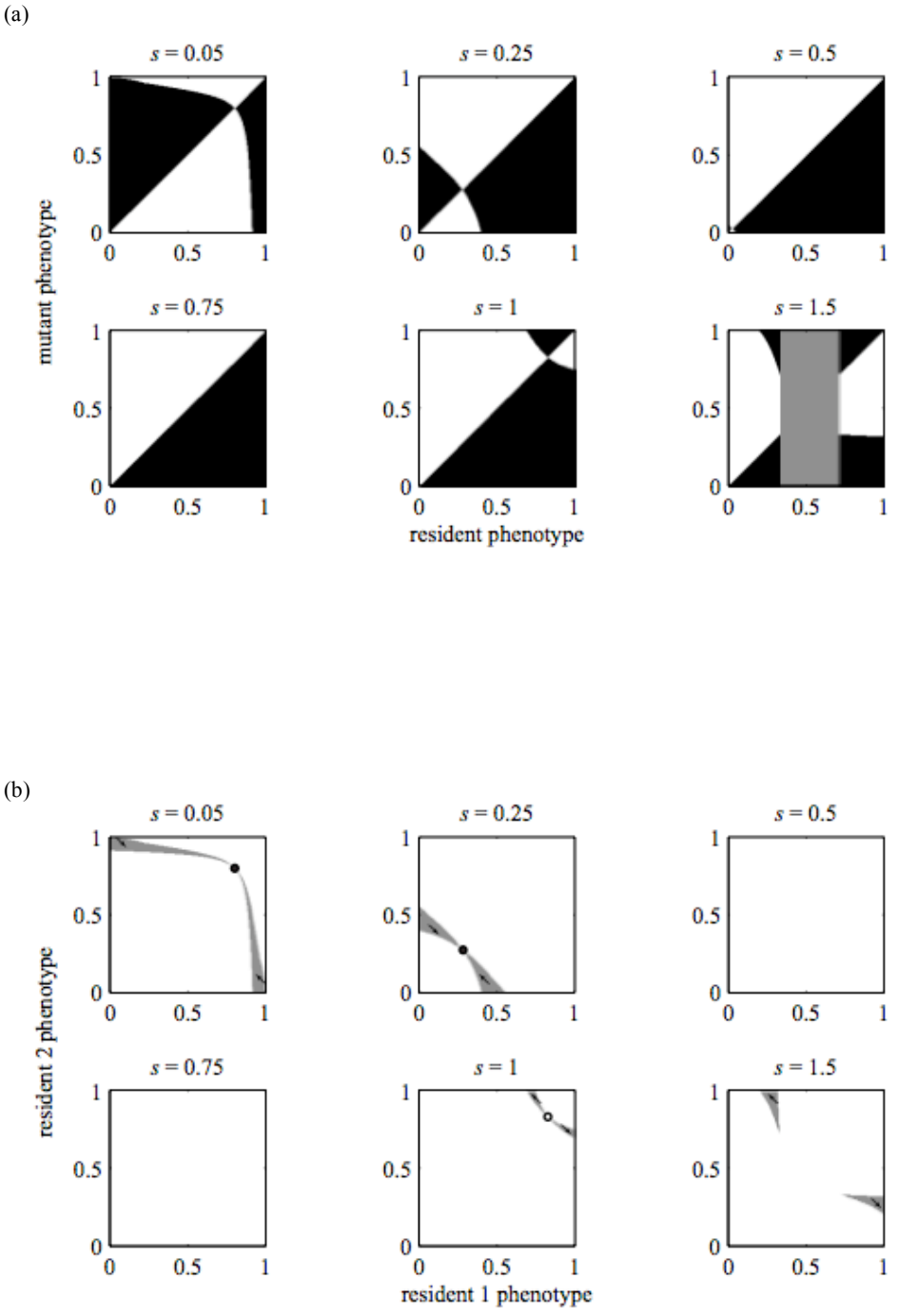
(a)
s = 0.05
s = 0.25
s = 0.5
s = 0.75
s = 1
s = 1.5
mutant phenotype
resident phenotype
(b)
s = 0.05
s = 0.25
s = 0.5
s = 0.75
s = 1
s = 1.5
resident 2 phenotype
resident 1 phenotype

Figure 5.S5 (continued)

(c)

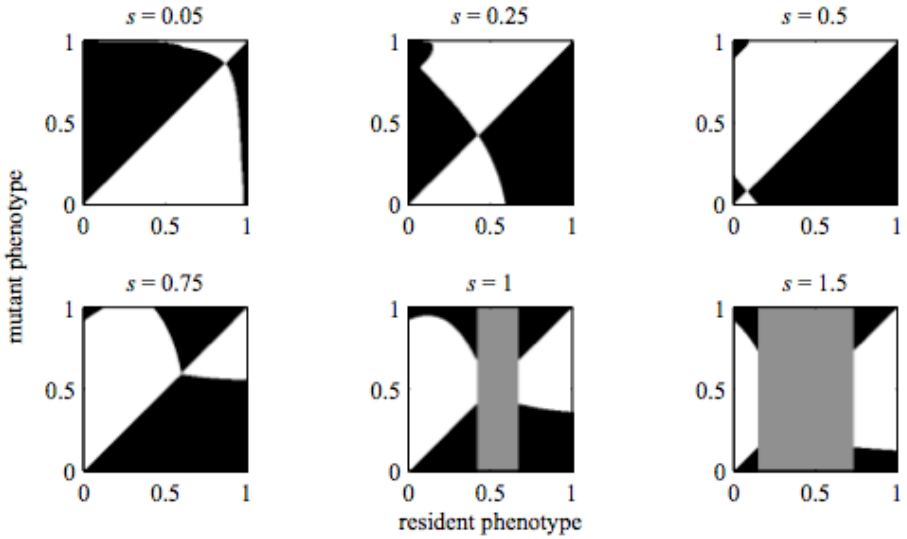

(d)

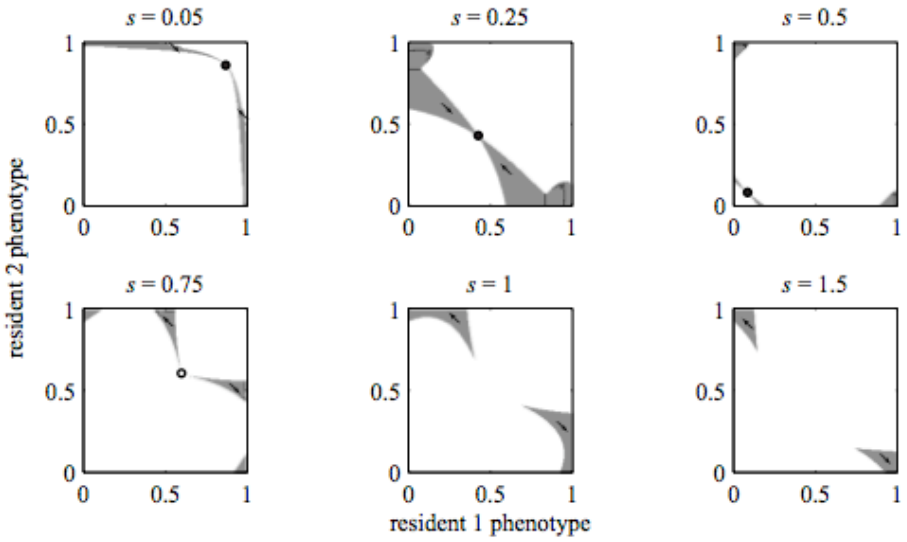

Figure 5.S6. Changing intermediate host density in a neutral ecology. Plots show (a) frequency dependent and (b) density dependent transmission. Ecological parameters are the same as those used in figure 5.2 (for all hosts, $R_0 = 2$ and $\gamma = 1/180$ days^{-1}). Pairwise invasibility and trait evolution plots corresponding to where $N_m = N_t = N_r$ with frequency dependent transmission are shown in figure 5.2. Plus signs indicate areas of coexistence, which correspond to the gray regions of trait evolution plots.

Figure 5.S6

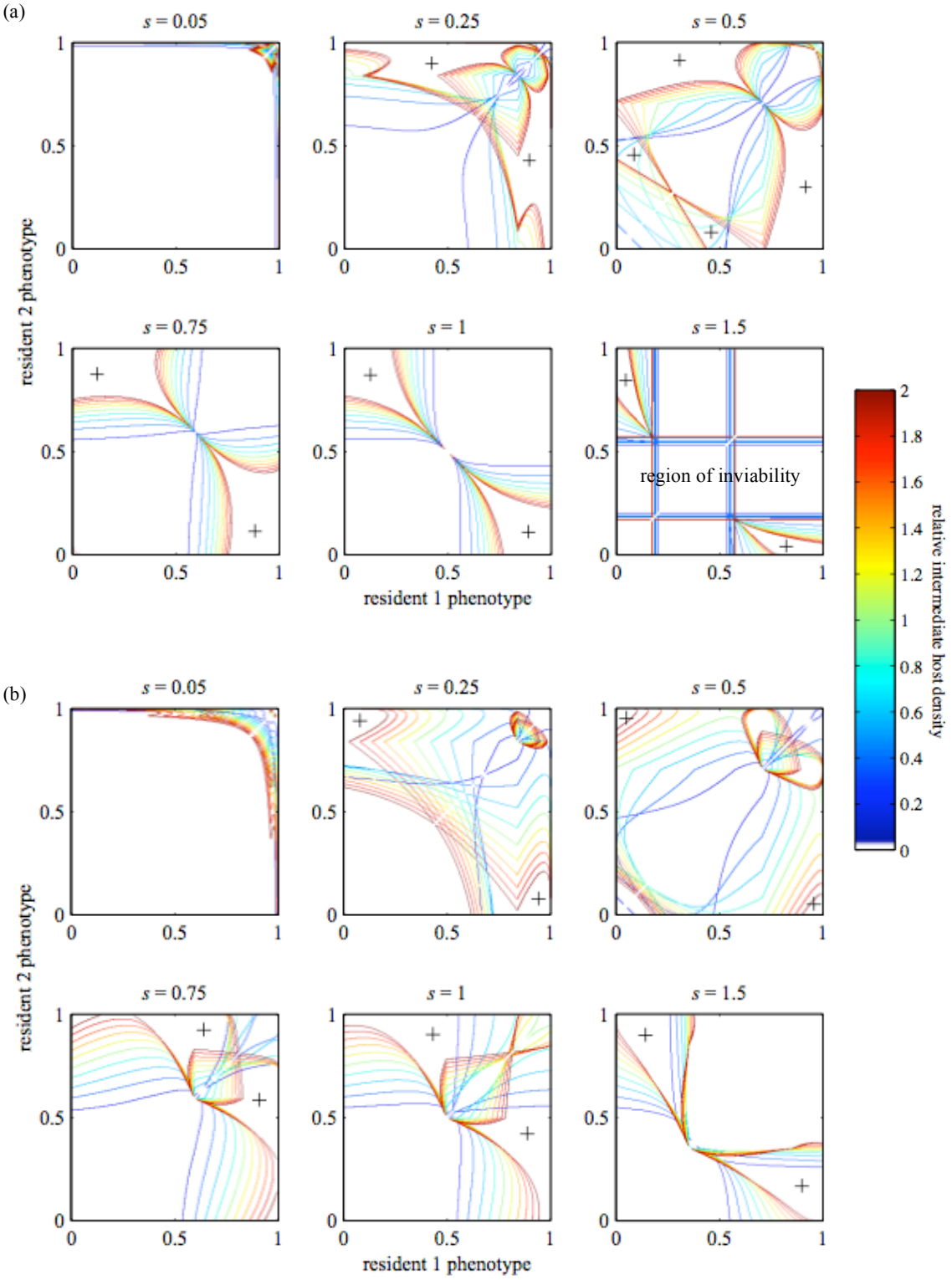
(a)
s = 0.05
s = 0.25
s = 0.5
s = 0.75
s = 1
s = 1.5
region of inviability
resident 2 phenotype
resident 1 phenotype
relative intermediate host density
(b)
s = 0.05
s = 0.25
s = 0.5
s = 0.75
s = 1
s = 1.5
resident 2 phenotype
resident 1 phenotype

Figure 5.S7. Changing intermediate host density in a non-neutral ecology. Plots show (a) frequency dependent and (b) density dependent transmission. Ecological parameters are the same as those used in table 5.S1. Pairwise invasibility and trait evolution plots corresponding to where $N_m = N_t = N_r$ with frequency dependent transmission are shown in figure 5.S5(a, b). Plus signs indicate areas of coexistence, which correspond to the gray regions of trait evolution plots.

Figure 5.S7

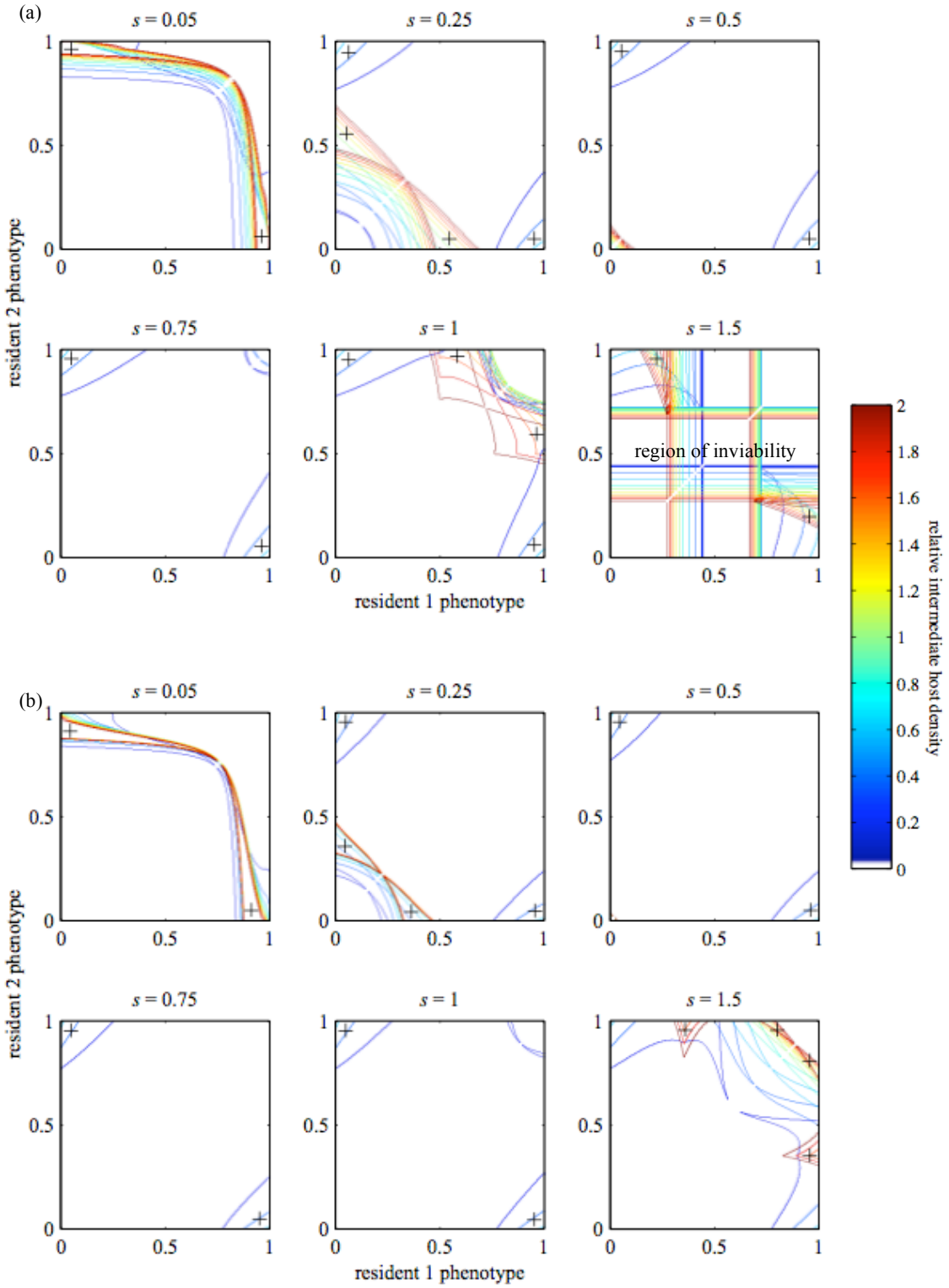
(a)
s = 0.05
s = 0.25
s = 0.5
s = 0.75
s = 1
s = 1.5
region of inviability
resident 2 phenotype
resident 1 phenotype
relative intermediate host density
(b)
s = 0.05
s = 0.25
s = 0.5
s = 0.75
s = 1
s = 1.5
resident 2 phenotype
resident 1 phenotype

Figure 5.S8. Changing target host density in a neutral ecology. Plots assume dependent transmission. Ecological parameters are the same as those used in figure 5.2 (for all hosts, $R_0 = 2$ and $\gamma = 1/180$ days^{-1}). Pairwise invasibility and trait evolution plots corresponding to where $N_t = N_m = N_r$ with frequency dependent transmission are shown in figure 5.2. Plus signs indicate areas of coexistence, which correspond to the gray regions of trait evolution plots.

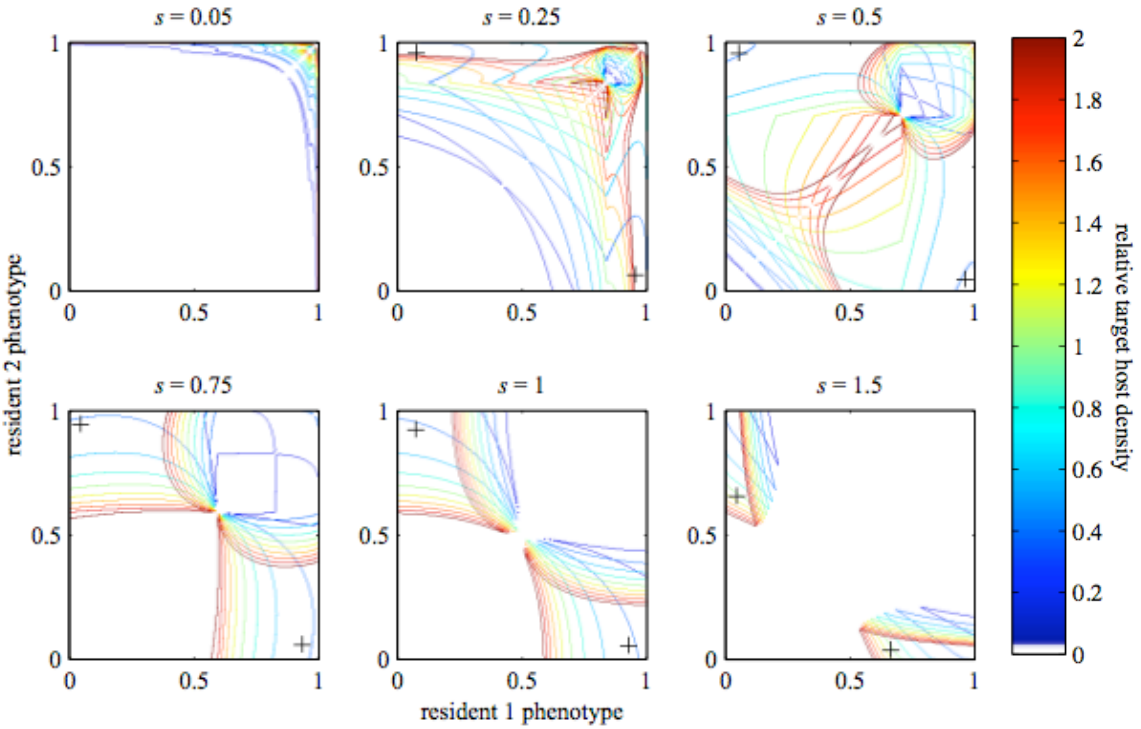

Figure 5.S9. Changing target host density in a non-neutral ecology. Plots assume frequency dependent transmission. Ecological parameters are the same as those used in table 5.S1. Pairwise invasibility and trait evolution plots corresponding to where $N_t = N_m = N_r$ with frequency dependent transmission are shown in figure 5.S5(a,b). Plus signs indicate areas of coexistence, which correspond to the gray regions of trait evolution plots.

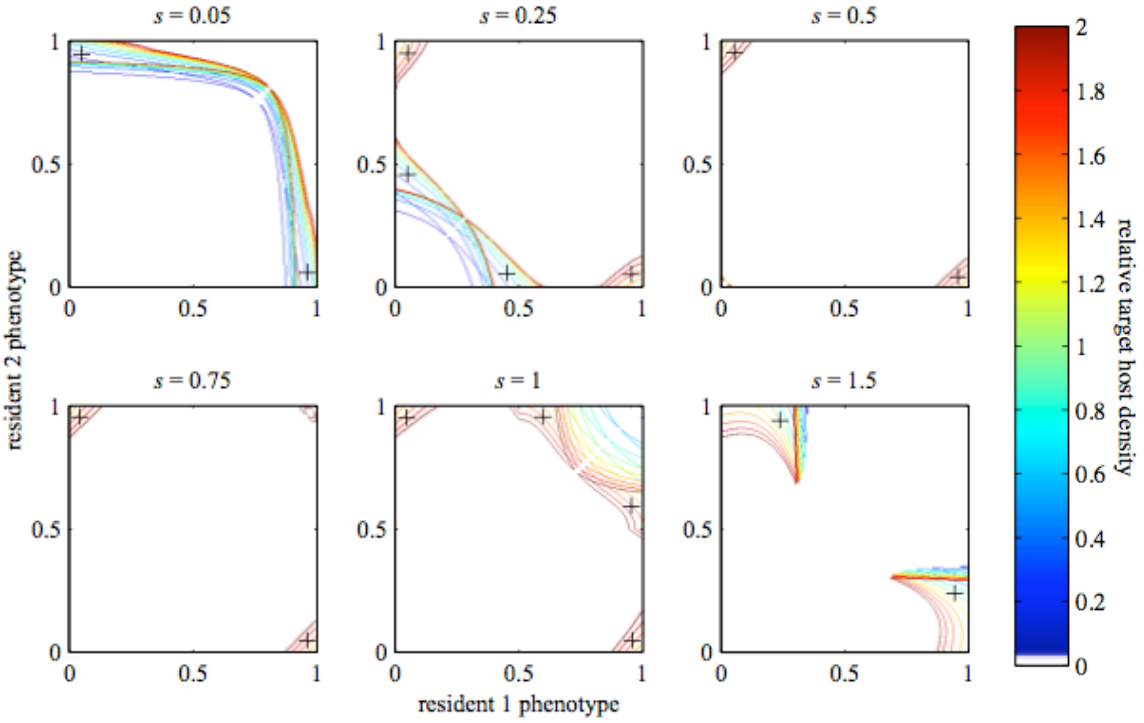

Figure 5.S10. Changing relative interspecific transmission rates identically ($c = c_1 = c_2$) when all transmission rates are frequency dependent. Coexistence plots are shown for (a) neutral and (b) non-neutral ecologies. Pairwise invasibility and trait evolution plots corresponding to the case where $c = 1$ are shown in figure 5.2 and figure 5.S5(a,b), respectively, assuming frequency dependent transmission. Plus signs indicate areas of coexistence, which correspond to the gray regions of trait evolution plots.

Figure 5.S10

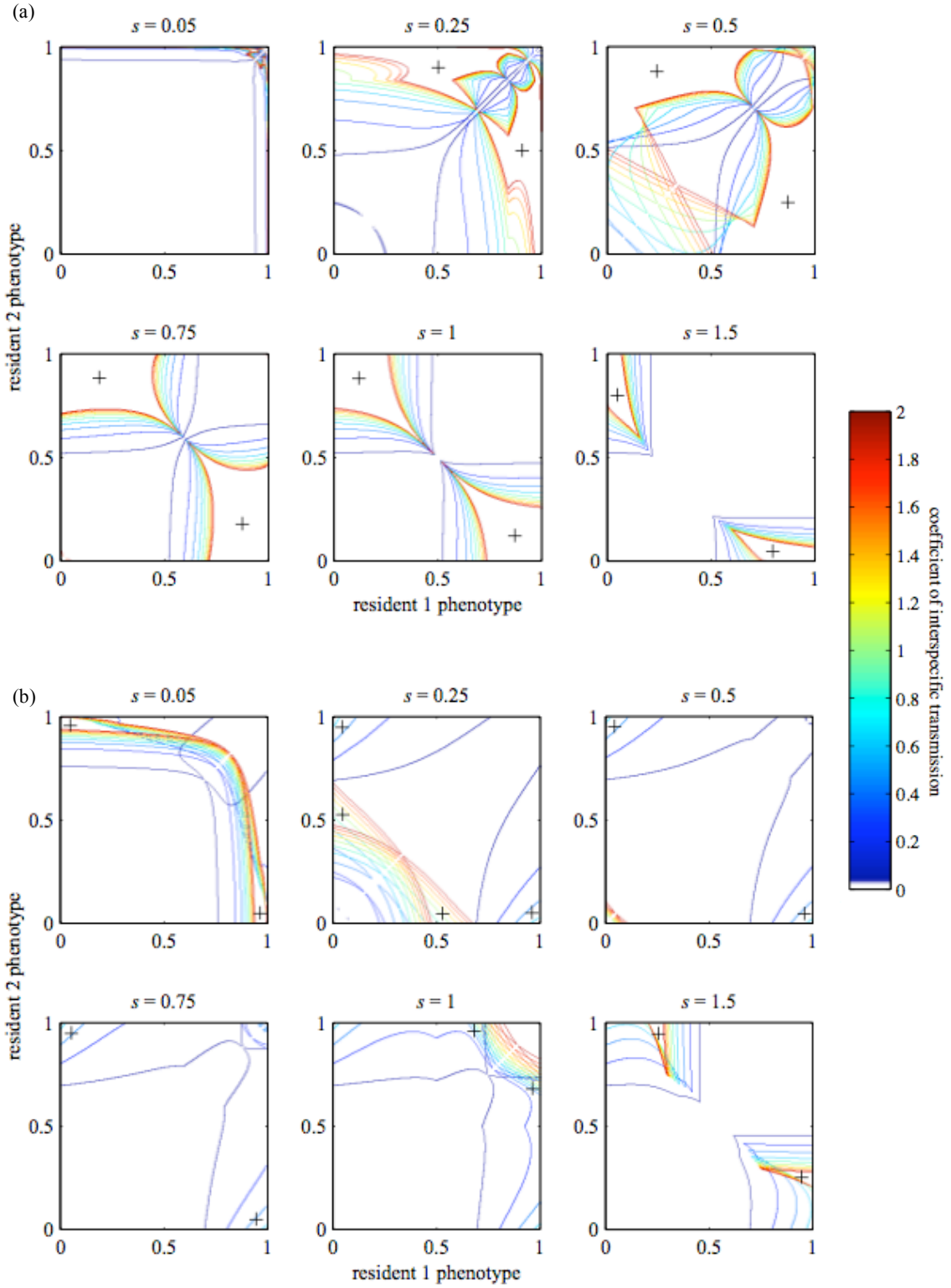
(a)
s = 0.05
s = 0.25
s = 0.5
s = 0.75
s = 1
s = 1.5
resident 2 phenotype
resident 1 phenotype
(b)
s = 0.05
s = 0.25
s = 0.5
s = 0.75
s = 1
s = 1.5
resident 2 phenotype
resident 1 phenotype
coefficient of interspecific transmission
0
0.2
0.4
0.6
0.8
1
1.2
1.4
1.6
1.8
2

Figure 5.S11. Changing c_1 only in (a) neutral and (b) non-neutral ecologies, assuming density-dependent transmission. Plus signs indicate areas of coexistence, which correspond to the gray regions of trait evolution plots.

Figure 5.S11

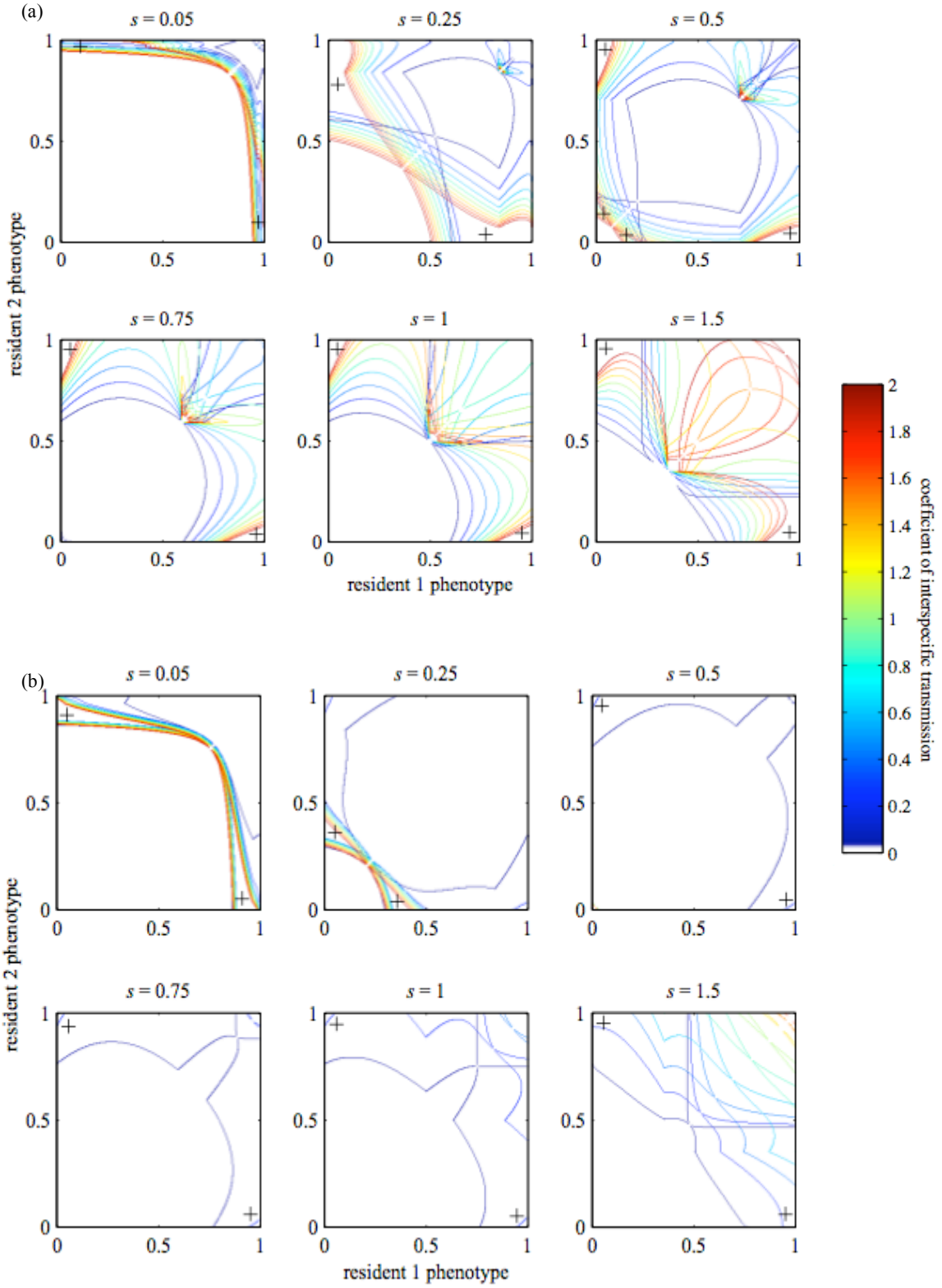
(a)
s = 0.05
s = 0.25
s = 0.5
s = 0.75
s = 1
s = 1.5
resident 2 phenotype
resident 1 phenotype
(b)
s = 0.05
s = 0.25
s = 0.5
s = 0.75
s = 1
s = 1.5
resident 2 phenotype
resident 1 phenotype
coefficient of interspecific transmission
0
0.2
0.4
0.6
0.8
1
1.2
1.4
1.6
1.8
2

Figure 5.S12. Changing c_2 only in (a) neutral and (b) non-neutral ecologies, assuming density-dependent transmission. Plus signs indicate areas of coexistence, which correspond to the gray regions of trait evolution plots.

Figure 5.S12

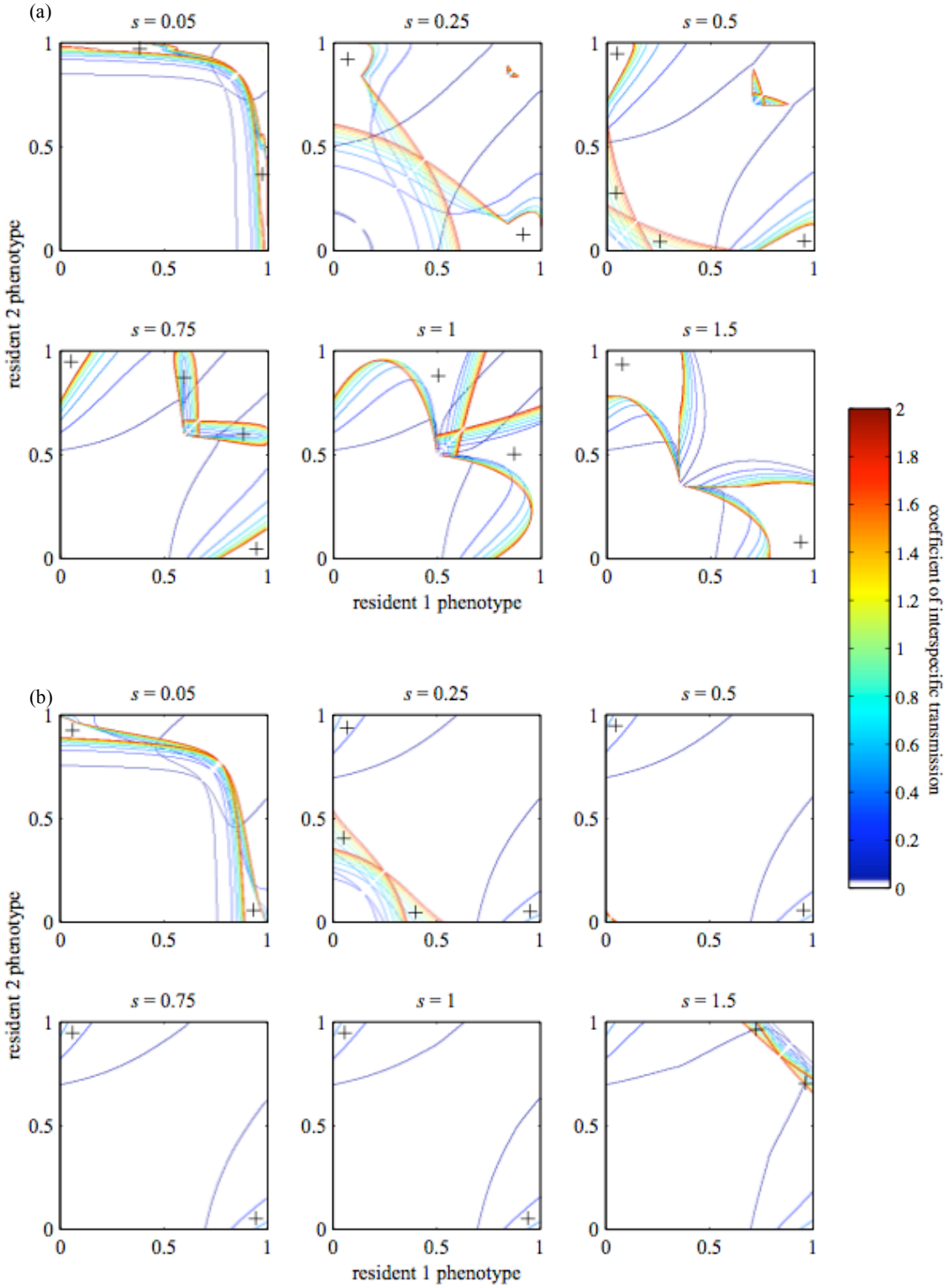
(a)
s = 0.05
s = 0.25
s = 0.5
s = 0.75
s = 1
s = 1.5
resident 2 phenotype
resident 1 phenotype
(b)
s = 0.05
s = 0.25
s = 0.5
s = 0.75
s = 1
s = 1.5
resident 2 phenotype
resident 1 phenotype
coefficient of interspecific transmission
0
0.2
0.4
0.6
0.8
1
1.2
1.4
1.6
1.8
2

Table 5.S1. Default parameter values used in non-neutral models

Symbol	Meaning	Value	References
ν_r	Rate of recovery in reservoir	1/(12 days)	Hulse-Post et al. (2005)
ν_m	Rate of recovery in intermediate host	1/(7 days)	Hinshaw et al. (1981), Brown (2000), Van der Groot et al. (2003)
ν_t	Rate of recovery in target population	1/(6 days)	Leekha et al. (2007), Carrat et al. (2008)
β_{rr}	Transmission coefficient in reservoir	(1 contact)/(3 days)	
β_{mm}	Transmission coefficient in intermediate host	(1 contact)/(4 days)	Saenz et al. (2006)
β_{tt}	Transmission coefficient in target population	(1 contact)/(4 days)	Saenz et al. (2006)
γ_r	Rate of susceptible replenishment in reservoir	1/(90 days)	Kida et al. (1980), Hulse-Post et al. (2005)
γ_m	Rate of susceptible replenishment in intermediate host	1/(180 days)	
γ_t	Rate of susceptible replenishment in target population	1/(730 days)	
c (c_1, c_2)	Scaling coefficient for interspecific contact rates (between reservoir and intermediate host, between intermediate and target host)	1.0 (except where explicitly varied)	

References

Alexander, D. J. 2000 A review of avian influenza in different bird species. *Veterinary Microbiology* **74**, 3-13.

Andre, J. B. & Day, T. 2005 The effect of disease life history on the evolutionary emergence of novel pathogens. *Proceedings of the Royal Society B-Biological Sciences* **272**, 1949-1956.

Antia, R., Regoes, R. R., Koella, J. C. & Bergstrom, C. T. 2003 The role of evolution in the emergence of infectious diseases. *Nature* **426**, 658-661.

Baigent, S. J. & McCauley, J. W. 2003 Influenza type A in humans, mammals and birds: determinants of virus virulence, host-range and interspecies transmission. *Bioessays* **25**, 657-671.

Baranowski, E., Ruiz-Jarabo, C. M. & Domingo, E. 2001 Evolution of cell recognition by viruses. *Science* **292**, 1102-1105.

Brown, I. H. 2000 The epidemiology and evolution of influenza viruses in pigs. *Veterinary Microbiology* **74**, 29-46.

Brown, I. H., Harris, P. A. & Alexander, D. J. 1995 Serological Studies of Influenza-Viruses in Pigs in Great-Britain 1991-2. *Epidemiology and Infection* **114**, 511-520.

Bulaga, L. L., Garber, L., Senne, D. A., Myers, T. J., Good, R., Wainwright, S., Trock, S. & Suarez, D. L. 2003 Epidemiologic and surveillance studies on avian influenza in live-bird markets in New York and New Jersey, 2001. *Avian Diseases* **47**, 996-1001.

Campitelli, L., Donatelli, I., Foni, E., Castrucci, M. R., Fabiani, C., Kawaoka, Y., Krauss, S. & Webster, R. G. 1997 Continued evolution of H1N1 and H3N2 influenza viruses in pigs in Italy. *Virology* **232**, 310-318.

Carrat, F., Vergu, E., Ferguson, N. M., Lemaitre, M., Cauchemez, S., Leach, S. & Valleron, A. J. 2008 Time lines of infection and disease in human influenza: A review of volunteer challenge studies. *American Journal of Epidemiology* **167**, 775-785.

Dieckmann, U. & Law, R. 1996 The dynamical theory of coevolution: A derivation from stochastic ecological processes. *Journal of Mathematical Biology* **34**, 579-612.

Dieckmann, U., Metz, J. A. J., Sabelis, M. W. & Sigmund, K. 2002 *Adaptive Dynamics of Infectious Diseases: In Pursuit of Virulence Management*. Cambridge Studies in Adaptive Dynamics. Cambridge, U.K.: Cambridge University Press.

Dobson, a. 2004 Population dynamics of pathogens with multiple host species. *American Naturalist* **164**, S64-S78.

Egas, M., Dieckmann, U. & Sabelis, M. W. 2004 Evolution restricts the coexistence of specialists and generalists: The role of trade-off structure. *American Naturalist* **163**, 518-531.

Gambaryan, A., Yamnikova, S., Lvov, D., Tuzikov, A., Chinarev, A., Pazynina, G., Webster, R., Matrosovich, M. & Bovin, N. 2005 Receptor specificity of influenza viruses from birds and mammals: New data on involvement of the inner fragments of the carbohydrate chain. *Virology* **334**, 276-283.

Gambaryan, A. S., Yamnikova, S. S., Lvov, D. K., Robertson, J. S., Webster, R. G. & Matrosovich, M. N. 2002 Differences in receptor specificity between the influenza viruses of duck, chicken, and human. *Molecular Biology* **36**, 429-435.

Gandon, S. 2004 Evolution of multihost parasites. *Evolution* **58**, 455-469.

Geritz, S. A. H., Kisdi, É., Meszéna, G. & Metz, J. A. J. 1998 Evolutionarily singular strategies and the adaptive growth and branching of the evolutionary tree. *Evolutionary Ecology* **12**, 35-57.

Halvorson, D., Karunakaran, D., Senne, D., Kelleher, C., Bailey, C., Abraham, a., Hinshaw, V. & Newman, J. 1983 Epizootiology of Avian Influenza - Simultaneous Monitoring of Sentinel Ducks and Turkeys in Minnesota. *Avian Diseases* **27**, 77-85.

Halvorson, D. A., Kelleher, C. J. & Senne, D. A. 1985 Epizootiology of Avian Influenza - Effect of Season on Incidence in Sentinel Ducks and Domestic Turkeys in Minnesota. *Applied and Environmental Microbiology* **49**, 914-919.

Harvey, R., Martin, A. C. R., Zambon, M. & Barclay, W. S. 2004 Restrictions to the adaptation of influenza A virus H5 hemagglutinin to the human host. *Journal of Virology* **78**, 502-507.

Hinshaw, V. S., Webster, R. G., Easterday, B. C. & Bean, W. J. 1981 Replication of Avian Influenza-a Viruses in Mammals. *Infection and Immunity* **34**, 354-361.

Hulse-Post, D. J., Sturm-Ramirez, K. M., Humberd, J., Seiler, J. P., Govorkova, E. A., Krauss, S., Scholtissek, C., Puthavathana, P., Buranathai, C., Nguyen, T. D., Long, H. T., Naipospos, T. S. P., Chen, H., Ellis, T. M., Guan, Y., Peiris, J. S. M. & Webster, R. G. 2005 Role of domestic ducks in the propagation and biological evolution of higthly pathogenic H5N1 influenza viruses in Asia. *Proceedings of the National Academy of Sciences of the United States of America* **102**, 10682-10687.

Ito, T. & Kawaoka, Y. 2000 Host-range barrier of influenza A viruses. *Veterinary Microbiology* **74**, 71-75.

Ito, T., Kawaoka, Y., Nomura, A. & Otsuki, K. 1999 Receptor specificity of influenza A viruses from sea mammals correlates with lung sialyloligosaccharides in these animals. *Journal of Veterinary Medical Science* **61**, 955-958.

Karunakaran, D., Hinshaw, V., Poss, P., Newman, J. & Halvorson, D. 1983 Influenza-a Outbreaks in Minnesota Turkeys Due to Subtype-H10N7 and Possible Transmission by Waterfowl. *Avian Diseases* **27**, 357-366.

Kida, H., Ito, T., Yasuda, J., Shimizu, Y., Itakura, C., Shortridge, K. F., Kawaoka, Y. & Webster, R. G. 1994 Potential for Transmission of Avian Influenza-Viruses to Pigs. *Journal of General Virology* **75**, 2183-2188.

Kida, H., Yanagawa, R. & Matsuoka, Y. 1980 Duck Influenza Lacking Evidence of Disease Signs and Immune-Response. *Infection and Immunity* **30**, 547-553.

Koelle, K., Pascual, M. & Yunus, M. 2005 Pathogen adaptation to seasonal forcing and climate change. *Proceedings of the Royal Society of London, Series B-Biological Sciences* **272**, 971-977.

Koopmans, M., Wilbrink, B., Conyn, M., Natrop, G., van der Nat, H., Vennema, H., Meijer, A., van Steenbergen, J., Fouchier, R., Osterhaus, A. & Bosman, A. 2004 Transmission of H7N7 avian influenza A virus to human beings during a large outbreak in commercial poultry farms in the Netherlands. *Lancet* **363**, 587-593.

Lee, C. W., Suarez, D. L., Tumpey, T. M., Sung, H. W., Kwon, Y. K., Lee, Y. J., Choi, J. G., Joh, S. J., Kim, M. C., Lee, E. K., Park, J. M., Lu, X. H., Katz, J. M., Spackman, E., Swayne, D. E. & Kim, J. H. 2005 Characterization of highly pathogenic H5N1 avian influenza A viruses isolated from South Korea. *Journal of Virology* **79**, 3692-3702.

Leekha, S., Zitterkopf, N. L., Espy, M. J., Smith, T. F., Thompson, R. L. & Sampathkumar, P. 2007 Duration of influenza a virus shedding in hospitalized patients and implications for infection control. *Infection Control and Hospital Epidemiology* **28**, 1071-1076.

Levins, R. 1962 Theory of fitness in a heterogeneous environment. I. The fitness set and adaptive function. *The American Naturalist* **96**, 361-373.

Liu, M., He, S. Q., Walker, D., Zhou, N. N., Perez, D. R., Mo, B., Li, F., Huang, X. T., Webster, R. G. & Webby, R. J. 2003 The influenza virus gene pool in a poultry market in South Central China. *Virology* **305**, 267-275.

Ly, S., Van Kerkhove, M. D., Holl, D., Froehlich, Y. & Vong, S. 2007 Interaction between humans and poultry, rural Cambodia. *Emerging Infectious Diseases* **13**, 130-132.

Matrosovich, M., Tuzikov, A., Bovin, N., Gambaryan, A., Klimov, A., Castrucci, M. R., Donatelli, I. & Kawaoka, Y. 2000 Early alterations of the receptor-binding properties of H1, H2, and H3 avian influenza virus hemagglutinins after their introduction into mammals. *Journal of Virology* **74**, 8502-8512.

Matrosovich, M. N., Krauss, S. & Webster, R. G. 2001 H9N2 influenza a viruses from poultry in Asia have human virus-like receptor specificity. *Virology* **281**, 156-162.

Meszéna, G., Kisdi, É., Dieckmann, U., Geritz, S. A. H. & Metz, J. A. J. 2001 Evolutionary optimization models and matrix games in the unified perspective of adaptive dynamics. *Selection 2* **2**, 193-210.

Metz, J. A. J., Geritz, S. A. H., Meszéna, G., Jacobs, F. J. A. & van Heerwaarden, J. S. 1996 Adaptive dynamics: a geometrical study of the consequencies of nearly faithful reproduction. In *Stochastic and Spatial Structures of Dynamical Systems* (ed. S. J. van Strien & S. M. Verduyn Lunel), pp. 183-231. Amsterdam: North Holland.

Metz, J. A. J., Nisbet, R. M. & Geritz, S. A. H. 1992 How Should We Define Fitness for General Ecological Scenarios. *Trends in Ecology & Evolution* **7**, 198-202.

Munster, V. J., Baas, C., Lexmond, P., Waldenstrom, J., Wallensten, A., Fransson, T., Rimmelzwaan, G. F., Beyer, W. E. P., Schutten, M., Olsen, B., Osterhaus, A. D. M. E. & Fouchier, R. A. M. 2007 Spatial, temporal, and species variation in prevalence of influenza A viruses in wild migratory birds. *Plos Pathogens* **3**, 630-638.

Myers, K. P., Olsen, C. W., Setterquist, S. F., Capuano, A. W., Donham, K. J., Thacker, E. L., Merchant, J. A. & Gray, G. C. 2006 Are swine workers in the United States at increased risk of infection with zoonotic influenza virus? *Clinical Infectious Diseases* **42**, 14-20.

Olsen, C. W., Brammer, L., Easterday, B. C., Arden, N., Belay, E., Baker, I. & Cox, N. J. 2002 Serologic evidence of H1 swine influenza virus infection in swine farm residents and employees. *Emerging Infectious Diseases* **8**, 814-819.

Olsen, C. W., Carey, S., Hinshaw, L. & Karasin, A. I. 2000 Virologic and serologic surveillance for human, swine and avian influenza virus infections among pigs in the north-central United States. *Archives of Virology* **145**, 1399-1419.

Parker, G. A., Chubb, J. C., Ball, M. A. & Roberts, G. N. 2003 Evolution of complex life cycles in helminth parasites. *Nature* **425**, 480-484.

Saenz, R. A., Hethcote, H. W. & Gray, G. C. 2006 Confined animal feeding operations as amplifiers of influenza. *Vector-Borne and Zoonotic Diseases* **6**, 338-346.

Schmidt, K. A. & Ostfeld, R. S. 2001 Biodiversity and the dilution effect in disease ecology. *Ecology* **82**, 609-619.

Scholtissek, C., Hinshaw, V. S. & Olsen, C. W. 1998 Influenza in Pigs and their Role as the Intermediate Host. In *Textbook of Influenza* (ed. K. G. Nicholson, R. G. Webster & A. J. Hay), pp. 137-145. Malden, MA: Blackwell Science.

Sivanandan, V., Halvorson, D. a., Laudert, E., Senne, D. a. & Kumar, M. C. 1991 Isolation of H13N2 Influenza-a Virus from Turkeys and Surface-Water. *Avian Diseases* **35**, 974-977.

Thiry, E., Zicola, A., Addie, D., Egberink, H., Hartmann, K., Lutz, H., Poulet, H. & Horzinek, M. C. 2007 Highly pathogenic avian influenza H5N1 virus in cats and other carnivores. *Veterinary Microbiology* **122**, 25-31.

Tumpey, T. M., Maines, T. R., Van Hoeven, N., Glaser, L., Solorzano, A., Pappas, C., Cox, N. J., Swayne, D. E., Palese, P., Katz, J. M. & Garcia-Sastre, A. 2007 A two-amino acid change in the hemagglutinin of the 1918 influenza virus abolishes transmission. *Science* **315**, 655-659.

Van der Goot, J. A., De Jong, M. C. M., Koch, G. & Van Boven, M. 2003 Comparison of the transmission characteristics of low and high pathogenicity avian influenza A virus (H5N2). *Epidemiology and Infection* **131**, 1003-1013.

Viboud, C., Alonso, W. J. & Simonsen, L. 2006 Influenza in tropical regions. *Plos Medicine* **3**, 468-471.

Webby, R., Hoffmann, E. & Webster, R. 2004 Molecular constraints to interspecies transmission of viral pathogens. *Nature Medicine* **10**, S77-S81.

Webster, R. G. 2004 Wet markets - a continuing source of severe acute respiratory syndrome and influenza? *Lancet* **363**, 234-236.

Webster, R. G., Bean, W. J., Gorman, O. T., Chambers, T. M. & Kawaoka, Y. 1992 Evolution and Ecology of Influenza-A Viruses. *Microbiological Reviews* **56**, 152-179.

Webster, R. G. & Hulse, D. J. 2004 Microbial adaptation and change: avian influenza. *Revue Scientifique Et Technique De L Office International Des Epizooties* **23**, 453-465.

White, A., Greenman, J. V., Benton, T. G. & Boots, M. 2006 Evolutionary behaviour in ecological systems with trade-offs and non-equilibrium population dynamics. *Evolutionary Ecology Research*, 387-398.

Woolhouse, M. E. J. & Gowtage-Sequeria, S. 2005 Host range and emerging and reemerging pathogens. *Emerging Infectious Diseases* **11**, 1842-1847.

Yu, H., Zhang, G. H., Hua, R. H., Zhang, Q., Liu, T. Q., Liao, M. & Tong, G. Z. 2007 Isolation and genetic analysis of human origin H1N1 and H3N2 influenza viruses from pigs in China. *Biochemical and Biophysical Research Communications* **356**, 91-96.

Zhou, T., Gu, W. J., Ma, J. M., Sun, X. & Lu, Z. H. 2005 Analysis of synonymous codon usage in H5N1 virus and other influenza A viruses. *Biosystems* **81**, 77-86.

Chapter 6

Conclusion

The conflation of ecological and evolutionary time scales, characteristic of host interactions with viral and bacterial pathogens, guarantees that emerging infectious diseases will remain a threat to human populations for the indefinite future. These host-pathogen interactions are also a wonderful frontier for science. Few other systems require integrating nonlinear dynamics across multiple scales and sifting through as many potential factors about host behavior, immune specificity, mechanisms of competition, and the pathogen's immediate evolutionary potential. Improved surveillance should enhance this picture in the coming years and reveal recurring themes. This dissertation presented several explanations and possibilities for how the interplay of ecological and evolutionary dynamics can regulate the diversity of influenza in different host populations over different time scales. Though the analyses weight the contribution of each dynamic differently, they all suggest that accurate predictions about influenza—and potentially other pathogens—will not be possible without a phylodynamic perspective.

Chapter 2 measured the strength of positive selection on H3N2 viruses circulating in humans to evaluate evidence for a model of epochal evolution. Understanding the strength and targets of selection is important not only for developing better vaccines but also for predicting when a large fraction of the population might lose immunity, e.g., due to a mutation or reassortment. Such events are accompanied by increases in seasonal incidence. We found evidence for episodically strong and otherwise weak, continuous positive selection on the HA and positive selection (of unknown tempo) on NA, NP, and M2. That some positive selection appears to occur continuously in HA implies that the susceptible population is regularly replenished not only from births but also from individuals losing immunity. This dynamic makes eradication more difficult.

Chapter 3 focused on identifying the ecological parameters associated with H3N2, H1N1, and influenza B in humans. The model implicitly included evolution in the loss of immunity. Improvements in the method of inference are required before conclusive results can be drawn. However, the fits reflect previously noted qualitative differences in the relative fitnesses of the different strains and suggest a possible role for cross-immunity. The punctuated nature of antigenic evolution in H3N2 is also suggested by patterns of infection by age.

Chapter 4 showed that the diversity of immune responses has major consequences for strain diversity. Extremely low and extremely high diversity in responses at the population level and narrow responses at the individual level allow strains to coexist more easily. Future vaccination strategies may benefit from considering the diversity of responses in a population and immunogenicity of current and potential epitopes.

Chapter 5 asked how host ecology could affect the long term evolution of influenza viruses' host range, assuming a tradeoff in the ability to infect different hosts. Surprisingly, the strength of the tradeoff generally had very little effect on the outcome: What mattered far more were the densities of different host populations and the rates at which they contacted one another. However, this analysis also assumed that ecological dynamics always reached equilibrium between mutations. Analysis of nonequilibrium dynamics and incorporating specific molecular detail will be critical in developing policies to prevent spillovers and adaptation.

Our current understanding of influenza allows only for simple predictions, and this dissertation demonstrates the kinds of factors likely influencing dynamics in different host populations and time periods. Below, I outline specific areas where progress could greatly improve understanding and management of influenza.

Future directions

Space

Until recently, a lack of influenza surveillance in the tropics limited hypotheses about the role of space in influenza's epidemiological and evolutionary dynamics. New observations of H3N2 show that strains in temperate latitudes frequently emigrate from East and Southeast Asia (Russell et al. 2008). Time series of viral isolations in E and SE Asia suggest that strains there go extinct locally (i.e., in individual cities) following epidemics, and the epidemics do not follow a clear seasonal pattern. The authors synthesized these observations in a verbal model, proposing that all meaningful evolution occurs in a network of populations in E and SE Asia, and that this network seeds annual epidemics in temperate latitudes. This has also been called the "source-sink" model (Rambaut et al. 2008).

Another interesting observation from the study of Russell et al. (2008) is that the antigenic evolution of all strains globally appears relatively smooth and continuous in time. Antigenic evolution in Asia especially appears continuous, and its range does not appear to change dramatically from year to year. Critically, the antigenic distance accumulated in just one to two years is ostensibly enough to escape prior immunity in once-challenged ferrets (D. Smith, pers. comm.). How might influenza's genetic and antigenic diversity be constrained in Asia over short time periods, e.g., within a single cluster?

Though selective sweeps precipitated by cluster transitions may not be the major constraint (or only major constraint) on influenza's evolution, that phenotypic jumps occur is still likely. The argument for the existence of antigenic clusters relied primarily on samples collected from temperate latitudes. If North America and Europe were indeed successfully seeded at annual intervals, sampling exclusively their isolates would make antigenic evolution appear more punctuated than if sampling included E and SE Asia. At the limit, one or two new clusters would then be reported every year, depending on the amount of sampling in each hemisphere. Instead, only eleven were identified over a 34-year period, despite regular sampling. This difference implies that sampling bias alone cannot account for the existence of the clusters identified in Smith et al. (2004).

Cluster transitions may not be the main mechanism by which influenza's diversity is restricted, however. Local extinctions followed by recolonization events—the latter brought about by spatial effects (e.g., differences in seasonal forcing and transmission rates between populations)—may be the essential factor in ensuring that roughly continuous antigenic evolution appears punctuated in any one location, allowing competitive exclusion of resident strains and antigenic drift at rates higher than permitted in the model of Koelle et al. (2006). It is hard to see how antigenic evolution could otherwise occur so rapidly in Asia from year to year without the rapid accumulation of antigenic or genetic diversity. In this model, abrupt phenotypic changes caused by cluster transitions can then augment strain displacement and would account for some of the interannual variation in antigenic diversity and attack rates; such transitions are not, however, dynamically essential to restrict diversity. It would be interesting to test whether a metapopulation model, where all populations are below the critical community size for endemic persistence, can produce realistic epidemiological and evolutionary dynamics with continuous antigenic evolution. It is possible that the relevant metapopulation for influenza's evolution is not the network of populations in E and SE Asia but also includes North America, Europe, and Oceania, which can occasionally contribute successful strains to Asia (T. Bedford, pers. comm.). Ecological dynamics in space, and not the particular topology of influenza's genotype-phenotype map, would then be the main shaper of influenza's evolution.

The complexity of immune-mediated interactions

Chapter 5 highlighted some of the uncertainties in modeling competition between influenza strains. Uncertainty over the specificity, dynamics, and nature (cellular versus humoral) of the immune response drives the pursuit of diverse strategies in preparing seasonal and pandemic vaccines (Carrat & Flahault 2007; Doherty & Turner 2009; Mintern et al. 2009). Several recent studies have generated excitement in the popular press by identifying an epitope common to multiple subtypes (Sui et al. 2009; Throsby et al. 2008; Yoshida et al. 2009). The studies and others hint that conserved epitopes on HA or other proteins might form the basis of a "universal" vaccine, a prospect that has

attracted media attention (Hellemans 2008; Pollack 2009). Human antibodies to a conserved HA epitope were found in a preexisting antibody library, suggesting that at least a fraction of the human population may be able to produce such highly cross-reactive antibodies to HA naturally (Sui et al. 2009). Another conserved epitope on M2 has successfully induced antibodies in clinical trials (Hellemans 2008).

If protection against a conserved epitope could be generated through vaccination, it would allow the strain or subtype with the highest R_0 to exclude other strains with that epitope; if vaccination rates were sufficiently high, extinction of all strains with the epitope could result. Unfortunately, influenza's high mutation rate might allow escape mutations at the epitope or nearby, potentially through the addition of glycosylation sites. An attempt by one study to select escape mutants at a conserved HA epitope was unsuccessful but also very limited (Sui et al. 2009).

A deeper potential obstacle for the design of universal vaccines is that the basis of B cell selection is binding affinity, not neutralization ability. The best epitopes to attack to neutralize the virus are not always the most immunogenic (Ndifon et al. 2009). Influenza viruses might be under selection to evolve highly immunogenic but weakly neutralizing epitopes, which could potentially interfere with preexisting antibodies to highly efficient neutralizing epitopes (such as those around the receptor binding site), e.g., from a vaccine. There is evidence that seasonal immune escape by H3N2 might involve manipulating steric inhibition between antibodies (Ndifon et al. 2009). This dynamic increases the number of ways a virus can escape immunity. A clearer picture of the breadth and composition of existing B cell repertoires, epitopes' relative immunogenicities, and opportunities for escape mutations should underlie future vaccine development.

Long term strategies to manage influenza evolution

Research on fundamental questions of influenza's evolution could lead to a broad and flexible array of tools for managing the disease over the long term. The high mutation rate of RNA viruses has been ascribed to life history pressures, such as the need to escape adaptive immunity, and to a tradeoff with replication speed (Belshaw et al. 2008). The

major cost of a high mutation rate is poor replicative fidelity, which results, at the extreme (borrowing a term from quasispecies models), in error catastrophe: the fittest sequence cannot, on average, perfectly replicate itself, leading to an accumulation of deleterious mutations and a gradual loss of fitness.

It seems reasonable to assume that influenza's high mutation rate is partly driven by strong, negative frequency dependent selection by host immunity, especially antibodies to HA. (It would be interesting to test this hypothesis by comparing influenza's substitution rates in different host species, whose populations will have different degrees of immune surveillance.) Strains with antigenically novel HA have a tremendous fitness advantage, but host immunity ensures that the advantage is only temporary. A strain with a temporarily superior fitness (due to mutations in HA) could also carry deleterious mutations on the HA and elsewhere. An interesting question is whether the intensity of negative frequency dependent selection could ever be so strong that over time, hitchhiking deleterious mutations cause a gradual decline in influenza's fitness. A means by which influenza viruses in nature could escape this decline in non-HA genes is through reassortment, the viral analogue of sex as a means to escape Muller's ratchet. Are reassortment rates high enough to guarantee rescue from the accumulation of deleterious mutations? Could vaccinations be manipulated to intensify frequency dependent selection beyond the threshold where reassortment can correct the deleterious mutations? Answering these questions might require detailed knowledge of the virus's genotype-phenotype map and the specificity of host immune responses.

One of the treatments for chronic infections with hepatitis C viruses is ribavirin, an antiviral mutagen that is thought to destroy viral fitness by inducing error catastrophe (Cuevas et al. 2009). The structure of influenza's genome suggests that it faces a delicate tradeoff between replication fidelity and replication speed. Its codon composition reflects evolved mutational robustness in conserved genes (Plotkin & Dushoff 2003), but it also contains overlapping reading frames, which increase sensitivity to random mutation in some parts of the genome. These relationships hint at potentially effective though theoretical interventions: forcing higher viral replication rates and focusing antiviral drugs and immune responses at proteins sharing overlapping reading frames (M1 and M2, NS1 and NS2) and other highly conserved areas.

The beautiful complexity of influenza's dynamics creates an ironic obstacle to understanding through intense competition among scientists and policymakers. There is an unfortunate though narrowing gap between the strength of theory related to the pathogen and quality of management and surveillance. Quarantines, antiviral stockpiling, and movement restrictions imposed by health departments around the world in response to the emergence of a new variant of H1N1 in the spring of 2009 do not appear to be scientifically motivated. The heuristics of seasonal vaccine selection, despite being organized by an international government agency, also remain inscrutable. Quantities of antigenic and genetic information on par with what is publicly available remain largely restricted to handfuls of cooperating labs. It is the obligation of researchers not only to develop models with some predictive ability but also to try to share their results promptly with nonscientists and especially one another. Though influenza is a global problem, policy should also be driven by more than a few centralized agencies.

Progress on pathogens such as influenza, HIV, parainfluenza, norovirus, *Staphylococcus*, *Streptococcus*, and many other bacteria and viruses will likely be synergistic. The dynamics of many are affected by interspecific transmission, seasonal forcing, serotype competition, heterogeneous immune responses, and rapid antigenic escape. Influenza's blazing success as a pathogen should make it a challenging yet fascinating subject that will drive research in this field for years to come.

References

Belshaw, R., Gardner, A., Rambaut, A. & Pybus, O. G. 2008 Pacing a small cage: mutation and RNA viruses. *Trends in Ecology & Evolution* **23**, 188-193.

Carrat, F. & Flahault, A. 2007 Influenza vaccine: The challenge of antigenic drift. *Vaccine* **25**, 6852-6862.

Cuevas, J. M., Gonzalez-Candelas, F., Moya, A. & Sanjuan, R. 2009 Effect of Ribavirin on the Mutation Rate and Spectrum of Hepatitis C Virus In Vivo. *Journal of Virology* **83**, 5760-5764.

Doherty, P. C. & Turner, S. J. 2009 Thinking About Broadly Cross-Reactive Vaccines. *Clinical Pharmacology & Therapeutics* **85**, 665-668.

Hellemans, A. 2008 Can this man beat the flu with a single universal vaccine? In *Scientific American*.

Koelle, K., Cobey, S., Grenfell, B. & Pascual, M. 2006 Epochal evolution shapes the phylodynamics of interpandemic influenza. *Science* **314**, 1898-1903.

Mintern, J. D., Bedoui, S., Davey, G. M., Moffat, J. M., Doherty, P. C. & Turner, S. J. 2009 Transience of MHC Class I-restricted antigen presentation after influenza A virus infection. *Proceedings of the National Academy of Sciences of the United States of America* **106**, 6724-6729.

Ndifon, W., Wingreen, N. S. & Levin, S. A. 2009 Differential neutralization efficiency of hemagglutinin epitopes, antibody interference, and the design of influenza vaccines. *Proceedings of the National Academy of Sciences of the United States of America* **106**, 8701-8706.

Plotkin, J. B. & Dushoff, J. 2003 Codon bias and frequency-dependent selection on the hemagglutinin epitopes of influenza A virus. *Proceedings of the National Academy of Sciences of the United States of America* **100**, 7152-7157.

Pollack, A. 2009 A long search for a universal flu vaccine. In *The New York Times*. New York.

Rambaut, A., Pybus, O. G., Nelson, M. I., Viboud, C., Taubenberger, J. K. & Holmes, E. C. 2008 The genomic and epidemiological dynamics of human influenza A virus. *Nature* **453**, 615-620.

Russell, C. A., Jones, T. C., Barr, I. G., Cox, N. J., Garten, R. J., Gregory, V., Gust, I. D., Hampson, A. W., Hay, A. J., Hurt, A. C., de Jong, J. C., Kelso, A., Klimov, A. I., Kageyama, T., Komadina, N., Lapedes, A. S., Lin, Y. P., Mosterin, A., Obuchi, M., Odagiri, T., Osterhaus, A. D. M. E., Rimmelzwaan, G. F., Shaw, M. W., Skepner, E., Stohr, K., Tashiro, M., Fouchier, R. A. M. & Smith, D. J. 2008 The global circulation of seasonal influenza A (H3N2) viruses. *Science* **320**, 340-346.

Smith, D. J., Lapedes, A. S., de Jong, J. C., Bestebroer, T. M., Rimmelzwaan, G. F., Osterhaus, A. D. M. E. & Fouchier, R. A. M. 2004 Mapping the antigenic and genetic evolution of influenza virus. *Science* **305**, 371-376.

Sui, J. H., Hwang, W. C., Perez, S., Wei, G., Aird, D., Chen, L. M., Santelli, E., Stec, B., Cadwell, G., Ali, M., Wan, H. Q., Murakami, A., Yammanuru, A., Han, T., Cox, N. J., Bankston, L. A., Donis, R. O., Liddington, R. C. & Marasco, W. A. 2009 Structural and functional bases for broad-spectrum neutralization of avian and human influenza A viruses. *Nature Structural & Molecular Biology* **16**, 265-273.

Throsby, M., van den Brink, E., Jongeneelen, M., Poon, L. L. M., Alard, P., Cornelissen, L., Bakker, A., Cox, F., van Deventer, E., Guan, Y., Cinatl, J., ter Meulen, J., Lasters, I., Carsetti, R., Peiris, M., de Kruif, J. & Goudsmit, J. 2008 Heterosubtypic neutralizing monoclonal antibodies cross-protective against H5N1 and H1N1 recovered from human IgM+ memory B cells. *PLoS One* **3**, e3942.

Yoshida, T., Igarashi, M., Ozaki, H., Kishida, N., Tomabechi, D., Kida, H., Ito, K. & Takada, A. 2009 Cross-protective potential of a novel monoclonal antibody directed against antigenic site B of the hemagglutinin of influenza A viruses. *PLoS Pathogens* **5**, e10000350.